# FRAME C:
# A Compact Procedure for
# Quantitative Energy-Dispersive
# Electron Probe X-ray Analysis

# NATIONAL BUREAU OF STANDARDS

The National Bureau of Standards[1] was established by an act of Congress on March 3, 1901. The Bureau's overall goal is to strengthen and advance the Nation's science and technology and facilitate their effective application for public benefit. To this end, the Bureau conducts research and provides: (1) a basis for the Nation's physical measurement system, (2) scientific and technological services for industry and government, (3) a technical basis for equity in trade, and (4) technical services to promote public safety. The Bureau's technical work is performed by the National Measurement Laboratory, the National Engineering Laboratory, and the Institute for Computer Sciences and Technology.

**THE NATIONAL MEASUREMENT LABORATORY** provides the national system of physical and chemical and materials measurement; coordinates the system with measurement systems of other nations and furnishes essential services leading to accurate and uniform physical and chemical measurement throughout the Nation's scientific community, industry, and commerce; conducts materials research leading to improved methods of measurement, standards, and data on the properties of materials needed by industry, commerce, educational institutions, and Government; provides advisory and research services to other Government agencies; develops, produces, and distributes Standard Reference Materials; and provides calibration services. The Laboratory consists of the following centers:

Absolute Physical Quantities[2] — Radiation Research — Thermodynamics and Molecular Science — Analytical Chemistry — Materials Science.

**THE NATIONAL ENGINEERING LABORATORY** provides technology and technical services to the public and private sectors to address national needs and to solve national problems; conducts research in engineering and applied science in support of these efforts; builds and maintains competence in the necessary disciplines required to carry out this research and technical service; develops engineering data and measurement capabilities; provides engineering measurement traceability services; develops test methods and proposes engineering standards and code changes; develops and proposes new engineering practices; and develops and improves mechanisms to transfer results of its research to the ultimate user. The Laboratory consists of the following centers:

Applied Mathematics — Electronics and Electrical Engineering[2] — Mechanical Engineering and Process Technology[2] — Building Technology — Fire Research — Consumer Product Technology — Field Methods.

**THE INSTITUTE FOR COMPUTER SCIENCES AND TECHNOLOGY** conducts research and provides scientific and technical services to aid Federal agencies in the selection, acquisition, application, and use of computer technology to improve effectiveness and economy in Government operations in accordance with Public Law 89-306 (40 U.S.C. 759), relevant Executive Orders, and other directives; carries out this mission by managing the Federal Information Processing Standards Program, developing Federal ADP standards guidelines, and managing Federal participation in ADP voluntary standardization activities; provides scientific and technological advisory services and assistance to Federal agencies; and provides the technical foundation for computer-related policies of the Federal Government. The Institute consists of the following centers:

Programming Science and Technology — Computer Systems Engineering.

# Frame C: A Compact Procedure for Quantitative Energy-Dispersive Electron Probe X-ray Analysis

R. L. Myklebust, C. E. Fiori, and
K. F. J. Heinrich

National Measurement Laboratory
National Bureau of Standards
Washington, DC 20234

National Bureau of Standards Technical Note 1106
Nat. Bur. Stand. (U.S.), Tech. Note 1106, 111 pages (Sept. 1979)
CODEN: NBTNAE

# Foreword

This publication was written in order to document a data evaluation procedure for quantitative energy-dispersive electron probe analysis. The procedure is imbedded in a program (FRAME C) written in BASIC, for on-line use with a small computer. A FORTRAN 4 version is available for use on a batch mode computer. After a general description of the procedure, results of analyses of materials of known composition are given, and a detailed example of execution of FRAME C is presented. In Appendix I, a previously published communication on Si(Li) detector artifacts is reproduced. This paper should be useful in acquainting the reader with some of the problems arising from the use of this detector, and give the rationale for some of the corrective procedures in FRAME C. Appendix II contains a list of the symbols used in the program, with their meaning. Appendix III is a listing of the program.

We hope that the reader will find this documentation to be complete and clear. Commentaries and criticisms, particularly from potential or actual users of the program, are welcomed.

R.L.M., C.E.F., and K.F.J.H.

# TABLE OF CONTENTS

# LIST OF TABLES

# LIST OF FIGURES

Frame C:   A Compact Procedure for Quantitative Energy-
Dispersive Electron Beam X-ray Analysis

R.L. Myklebust, C.E. Fiori, and K.F.J. Heinrich
Center for Analytical Chemistry
National Bureau of Standards
Washington, D.C. 20234

ABSTRACT

A data evaluation procedure (FRAME C) for carrying out
quantitative electron probe microanalysis with a lithium-
drifted silicon detector was developed for use with a small
computer.  The procedure consists of a background correction
calculated from two selected background regions of interest,
a simple method of resolving overlapping peaks, and the
matrix corrections for characteristic radiation (ZAF).  To
save computation time, small groups of adjacent channels
(regions of interest) in the multi-channel analyzer rather
than individual channels are used for the calculations.
The method for computing the overlap factors is described.
Examples of several types of analyses are presented.

# I. Introduction

The program FRAME on which FRAME C is based was written for use on small computers for routine quantitative electron probe microanalysis. The main consideration in its development was the need for accurate data reduction in an on-line operation. Results from the rigorous data reduction program COR [1][1] were used as a guideline in the adjustment of simplified expressions, and it was shown that the omission of the correction for continuum-induced x-ray fluorescence in FRAME has not introduced significant errors [2].

Earlier experience with MULTI 8 [3], a data reduction program requiring extensive manual input, had clearly indicated the need for internal generation of parameters such as the x-ray mass absorption coefficients. Such parameters can either be stored in memory or on tapes or discs, or be generated from fitting algorithms in subroutines. The FRAME C program was developed in our laboratory for the Tracor Northern[2] TN 1700 multi-channel analyzer (MCA) system (with 4096 channels). This system includes a Nova 2 computer which was expanded to a total memory of 24,000, 16 bit words, in order to handle FRAME C (which requires approximately 10,000, 16 bit, words). There is a nine-track tape system available which serves to store spectra for later reference as standards or evaluation in the MCA. However, no other external mass storage was available on our computer. For this reason most parameters used in the presently available version of FRAME (including the version of FRAME C given in

---

[1]Figures in brackets indicate the literature references at the end of this paper.

[2]In order to adequately describe materials and experimental procedures, it was occasionally necessary to identify commercial products by manufacturer's name or label. In no instance does such identification imply endorsement by the National Bureau of Standards nor does it imply that the particular products or equipment is necessarily the best available for that purpose.

Appendix III) are internally produced from algorithms. Considerable effort has been spent in ensuring the accuracy required for the specific purposes in the program. The reader should be warned, however, against using these algorithms for purposes other than intended, or outside the specified limits of wavelength or energy. We specifically decline responsibility for any error that may arise from improper use of these algorithms, as was attempted by some investigators (e.g., [4]). As external memory devices become available, some of these parameters (e.g., line and edge energies) will be stored in tables. The coefficients in the expressions for computing the energies of x-ray lines and absorption edges have been fitted in the energy range from 1 keV to 10 keV and should not be used outside of this range.

The new version, FRAME C, extends this on-line analysis to the evaluation of energy-dispersive spectra from a lithium-drifted silicon detector (Si(Li)). Some of the parameters involved (i.e., weights of lines, incomplete charge collection) are under study and improved values of these parameters will be incorporated as they become available. The main features of FRAME, which deal with the evaluation of relative x-ray intensities, remain unchanged. However, since the resolution of the Si(Li) detector is lower than that of wavelength dispersive spectrometers, the steps required to obtain the relative x-ray intensities from the energy spectra of specimen and standard are much more elaborate. In essence, what is required for each spectrum is to subtract the background due to continuum generation from the characteristic x-ray lines, and to resolve the line overlaps which occur frequently in energy spectra [5]. As in wavelength-dispersive spectrometry, one x-ray line per element is used in the correction scheme. However, lines which are not used in the correction calculations must also be considered as potential line interferences.

If in FRAME C, an x-ray line below 1 kV is selected,
the program will terminate. Also, for accurate analyses, the
overvoltage range should be 1.5 to 10 (overvoltage is defined
to be the energy of the electrons in the beam divided by the
critical excitation energy of the x-ray line of interest).
The dimensions in the program allow for analyses of up to ten
elements, with K$\alpha$, L$\alpha$, or M$\alpha$ x-ray lines. The full-width at
half-maximum (FWHM) obtained from a MnK$\alpha$ peak must be known,
and the region of interest for any x-ray peak must be exactly
the same on both the standard and unknown. The output of
results was limited to a simple teletype printout. Within
memory limitations, however, it was possible to include
variants such as the determination of elements by stoichio-
metry or difference.

The slow speed of small computers was an important
consideration in the development of the procedure. Energy
spectra are stored in a pulse-height analyzer, typically 1024
channels for each spectrum. Even simple operations, if they
must be performed at each channel, consume too much time to be
useful in on-line analysis. We therefore decided that only
the channels containing the characteristic x-ray lines would
be used, and that the contents of adjacent channels correspond-
ing to any one peak would be added, to form a "region of
interest" for this peak [6]. The problem to be resolved was
thus to determine the contribution of background and interfer-
ing x-ray lines to each region of interest.

The background prediction can be based either on the
use of a reference spectrum (such as that from carbon) with
subsequent calculation of the change in the continuum with
atomic number, as proposed by Smith et al., [7] or on the
reconstruction of the continuous spectrum from the x-ray
emissions of the same target at two or more regions of
interest which are free of lines. We chose this second
technique, which is a continuation of the previous work of
Ware and Reed [8] and of Lifshin [9]. The regions of

4

interest for the continuum need not be the same size and can be selected at will for each spectrum, so that the effects of line interference and incomplete charge collection can be minimized. The technique of background correction we have followed requires the knowledge of the detector efficiency function. The parameters needed to calculate this efficiency can be obtained by means of a simple calibration procedure which is repeated infrequently. The variation of the emitted continuum at the absorption edges of the target elements is calculated on the basis of the target composition. Therefore, this calculation is repeated after each of the iterations which are part of the matrix (ZAF) correction for characteristic x-ray line intensities [3] included in FRAME C.

The exact form of the absorption correction for the continuous radiation is still a subject of speculation. We assume at present in this program that the depth distribution of the continuum is identical with that of characteristic radiation [10,11]. The algorithm can be changed as more evidence is forthcoming. At the present time we have been unable to obtain experimental proof of systematic error in applying the algorithm which was proposed for characteristic radiation in reference [10].

With the use of regions of interest, the problem of line interferences is reduced to obtaining overlap factors which determine the fraction of the signal emitted by a line that falls within the region of interest of another line. The fact that the shapes of x-ray lines observed in the energy spectrum are virtually Gaussian is very helpful and once the apparent width of one line is measured, those of other lines can be accurately predicted.

The problem of line interference can be resolved if the count rate produced by the interfering element within the region of interest of the element to be measured can be determined. This count rate is obtained as a function of

5

the count rate in the region of interest of the interfering
element. The calculation is performed in FRAME C by means
of a parameter called the <u>overlap coefficient</u>, which depends
on the line widths and positions and on the choice of regions,
but is independent of specimen composition. Hence, it is
calculated once only for each analytical situation, and
stored for later use. We will define these <u>overlap coeffi-</u>
<u>cients</u> more rigorously on page 11.

To establish regions of interest we must know either a
priori or from inspection of the spectrum which elements are
present in the specimen. It is possible to check after the
analysis has been performed if all lines were accounted for
correctly. This is done in FRAME C by synthesizing the line
spectrum from the analytical result and comparing it with
the spectrum collected from the unknown specimen. If the
synthesized spectrum is subtracted from the original,
ideally only the continuum should remain. If a line has
been overlooked, it will be visible in the residual spectrum.

## II. General Description

Figure 1 shows the configuration of the system used for
analysis and data evaluation.[3] The broken line indicates
connection of the computation sector to a high-speed external
mass storage device (e.g., floppy disc) which will be provided
in future systems but is not presently available in our system.
Therefore, available external memory is slow, and connected to
the MCA rather than the computation sector. This feature
limits the extent to which parameters such as line energy can
be stored for use in the computation sector. In the first
system used by us, the computations are programmed in BASIC.
If FORTRAN is used, instead, the speed of computation will
increase substantially.

[3]The computer is used in two discrete sectors. One of these
serves exclusively the MCA functions, and the other is
available for ocmputation in a users language.
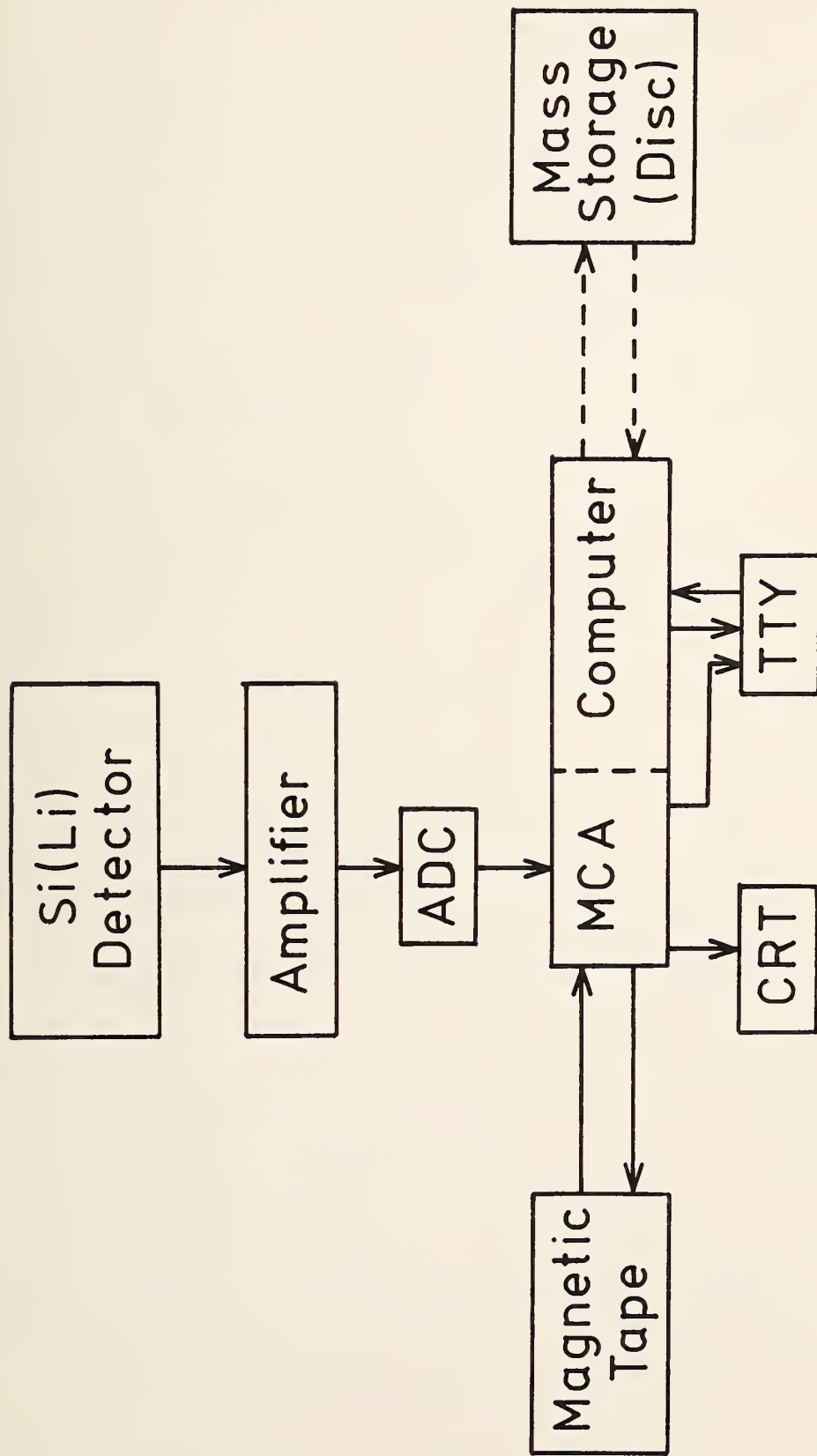
Figure 1. Block diagram of the data evaluation system in FRAME C.

A block diagram of the principal steps in a quantitative analysis by FRAME C is shown in figure 2. The first block in this figure contains all preliminary calibrations that the analyst must perform if accurate results are to be obtained. The first of these concerns the efficiency of the Si(Li) detector as a function of energy. Photons can escape detection by passing through the detector without being absorbed or by being absorbed by the beryllium detector window, the gold coating or the silicon dead layer, before entering the active region of the detector. By means of an auxiliary routine included with FRAME C, we can compute the necessary parameters from a spectrum of carbon in a calibration procedure separate from the remainder of FRAME C. Neglecting the effects of x-ray scattering and incomplete charge collection, we get for the detector efficiency the following expression:

$$P_e = \exp-[\mu(Be,E)t_{Be} + \mu(Si,E)t_{Si}^D] \, [1-\exp(-\mu(Si,E)t_{Si})] \quad [1]$$

Here, $t_{Si}^D$ and $t_{Si}$ are the thicknesses $(g/cm^2)$ of the silicon dead layer, and of the active detector region, respectively, and $\mu(Be,E)$ and $\mu(Si,E)$ are the mass absorption coefficients of beryllium and silicon at the energy E. Another parameter that must be determined for a particular detector is the full width at half-maximum (FWHM) of a peak such as the manganese $K\alpha$ x-ray peak. This width is necessary to compute the widths of all other peaks for the computation of peak interferences. The contribution due to incomplete charge collection [12] is only significant when an x-ray peak is measured near the low-energy side of another large x-ray peak. The approximation to the incomplete charge collection included in FRAME C will be sufficient to account for this effect in most detectors. Finally, the energy scale of the multichannel analyzer (e.g., 10 eV per channel) must be

8
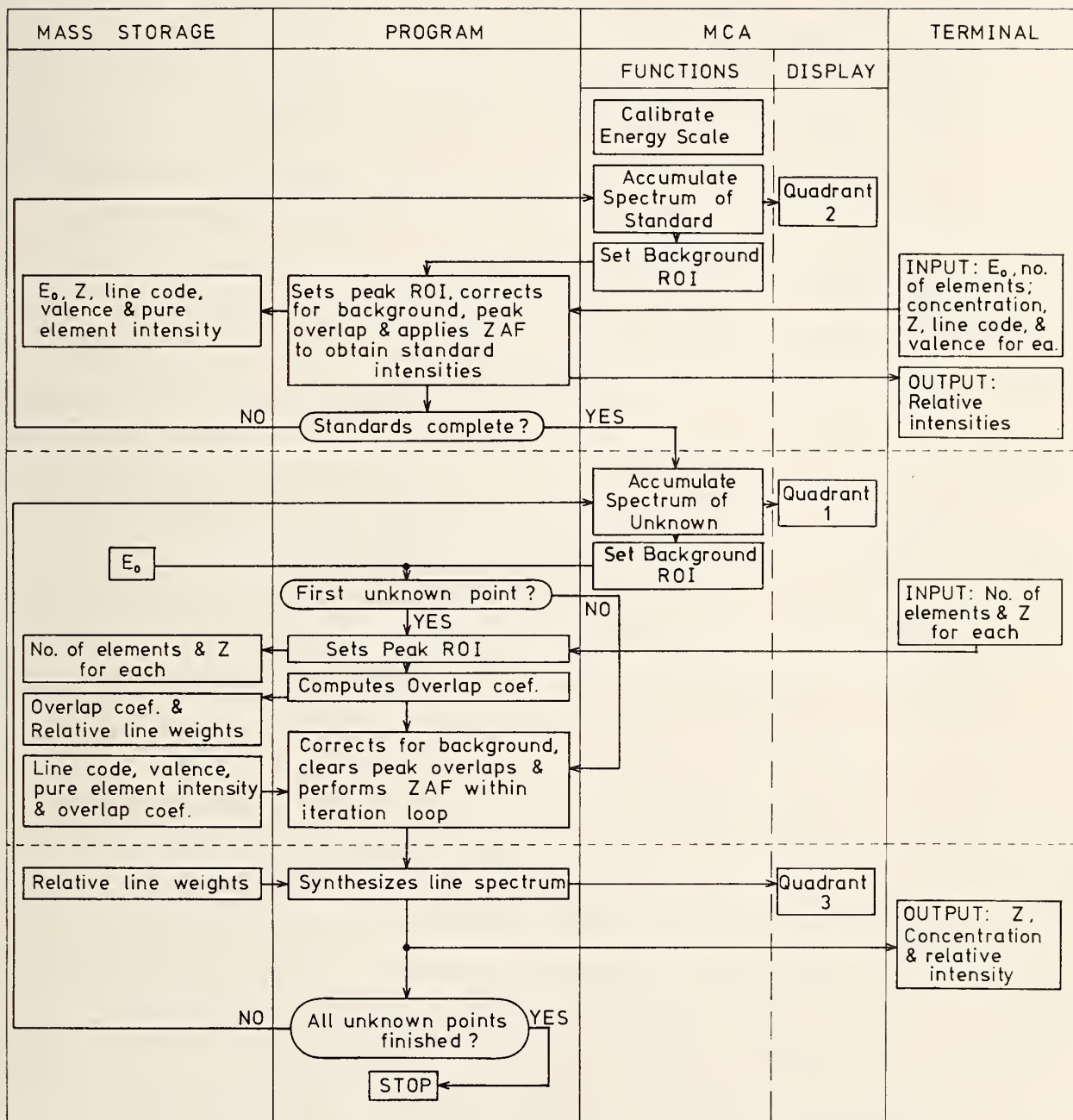
Figure 2. Block diagram of FRAME C showing all steps in an analysis.

9

calibrated. All of the above parameters need to be determined
at infrequent intervals; i.e., according to our experience,
every six months to one year.

Two more parameters must be entered before the program
is executed: The electron beam incidence angle and the
x-ray emergence angle. The blocks in Figure 2 are an outline
of a typical analysis. First, x-ray spectra must be collected
from standards for each element to be analyzed in the unknown
specimen. These spectra are processed by the standardization
portion of FRAME C. A multielement standard can serve as
a reference for several elements. In the present version of
FRAME C, all necessary information concerning each element
in the standard is stored in one quadrant of the multichannel
analyzer memory or in a high speed mass storage device such
as a floppy disc. Either method is satisfactory; however,
since we did not have a high speed mass storage device in
our first system, we used the fourth quadrant of the multi-
channel analyzer as our data file. (See Figure 1).

When all the standard spectra have been processed, the
spectrum from an unknown specimen can be analyzed. Once
regions of interest have been assigned for each element in
the spectrum of the specimen, the overlap factors are computed
for all interferences in the spectrum. Since these depend
only on the widths of the Gaussian peaks, the boundaries of
each region of interest, and the relative x-ray transition
probabilities, they are computed only once. If more than one
unknown is to be analyzed for the same elements, it is not
necessary to recompute these factors for each unknown.

The background subtraction [11] and the clearing of
x-ray line interferences ]13] require the x-ray absorption
factor, f, for each analytical x-ray line and, in the case of
line interferences, for each interfering x-ray line. In
principle, one would assume that the absorption factor for
continuous radiation would be different from that for

10

characteristic radiation.  We find, however, that an expression
such as proposed for characteristic x-radiation in reference
[10] produces a correction for the absorption of the continuum
in the target withoug an identifiable residual error.  For
this application the particular energy of interest of the
continuous radiation, $E_{cm}$ is substituted for the critical
excitation potential, $E_q$:

$$f_{cm} = [1 + 1.2 \times 10^{-6} \cdot (E_o^{1.65} - E_{cm}^{1.65}) \cdot \chi]^{-2} \qquad [2]$$

where $\chi = \mu \csc \psi$, $\mu$ the appropriate mass absorption coeffi-
cient, and $\psi$ the x-ray emergence angle.  Since the absorption
factors depend on the specimen composition, they must be
recomputed for each iteration of the matrix correction
[figure 2].

The final step in each analysis is to synthesize an x-
ray line spectrum from the analytical results and display it
on the screen of the multichannel analyzer so that it can be
compared with the measured spectrum from the unknown.  If the
analysis has been correctly performed, no peaks should be
observed in the measured spectrum that are not in the synthe-
sized spectrum, and vice versa.

IIa.   Background and line interference corrections

In energy-dispersive electron probe microanalysis, the
background due to the x-ray continuum is a significant part
of the contents of the region of interest of a characteristic
x-ray peak.  We have used a simple but accurate technique
for background correction which is an extension and amplifi-
cation of schemes proposed by Ware and Reed [8] and by
Lifshin et al. [9].  The technique has been described by
Fiori et al. [11].

The original energy-dispersive version of the FRAME
program, FRAME B, [14] required that all analytical x-ray
peaks be clearly resolved from other x-ray peaks in the
spectrum.  This condition is frequently not met in energy-

dispersive analysis. We have developed a simple method [14] to overcome this limitation which is based on calculating the overlap of Gaussian peaks of one element into the region of interest of anothe element. One x-ray line (the analytical line) from each element will have a region of interest and be used in the ZAF computation to determine the specimen composition, but all other lines will be considered to determine if they overlap with the regions of interest of the analytical lines.

Given an x-ray peak near a region of interest, the fraction of this peak which falls within the region only depends on the relative positions of peak and region of interest and of the standard deviation of the Gaussian peak, but not on the composition of the specimen. If the interfering peak has its own region of interest, the fraction of the peak with its own region of interest is equally independent of composition. Therefore, the ratio between these two fractions, called the overlap factor, can be computed once early in the procedure and stored for all subsequent measurements. We will develop the argument for two unresolved peaks, A and B (see figure 3). We will only describe the computation of the overlap factor due to peak A on the intensity under peak B. Since peak B contributes counts to the region of interest for peak A and vice versa, the correction procedure in practice must be iterative.

Let $E_A$ be the center of peak A and $E_B$ the center of peak B. We can calculate the standard deviations $\sigma_A$ and $\sigma_B$ as a function of $E_A$ and $E_B$ [15] if the FWHM has been measured for a peak at any energy (e.g., Mn K$\alpha$). The number of counts due to peak A at any channel number $E_i$ is:

$$N_i = A_a \exp\left[ -\frac{1}{2} \left( \frac{E_A - E_i}{\sigma_A} \right)^2 \right]$$

[3]

12
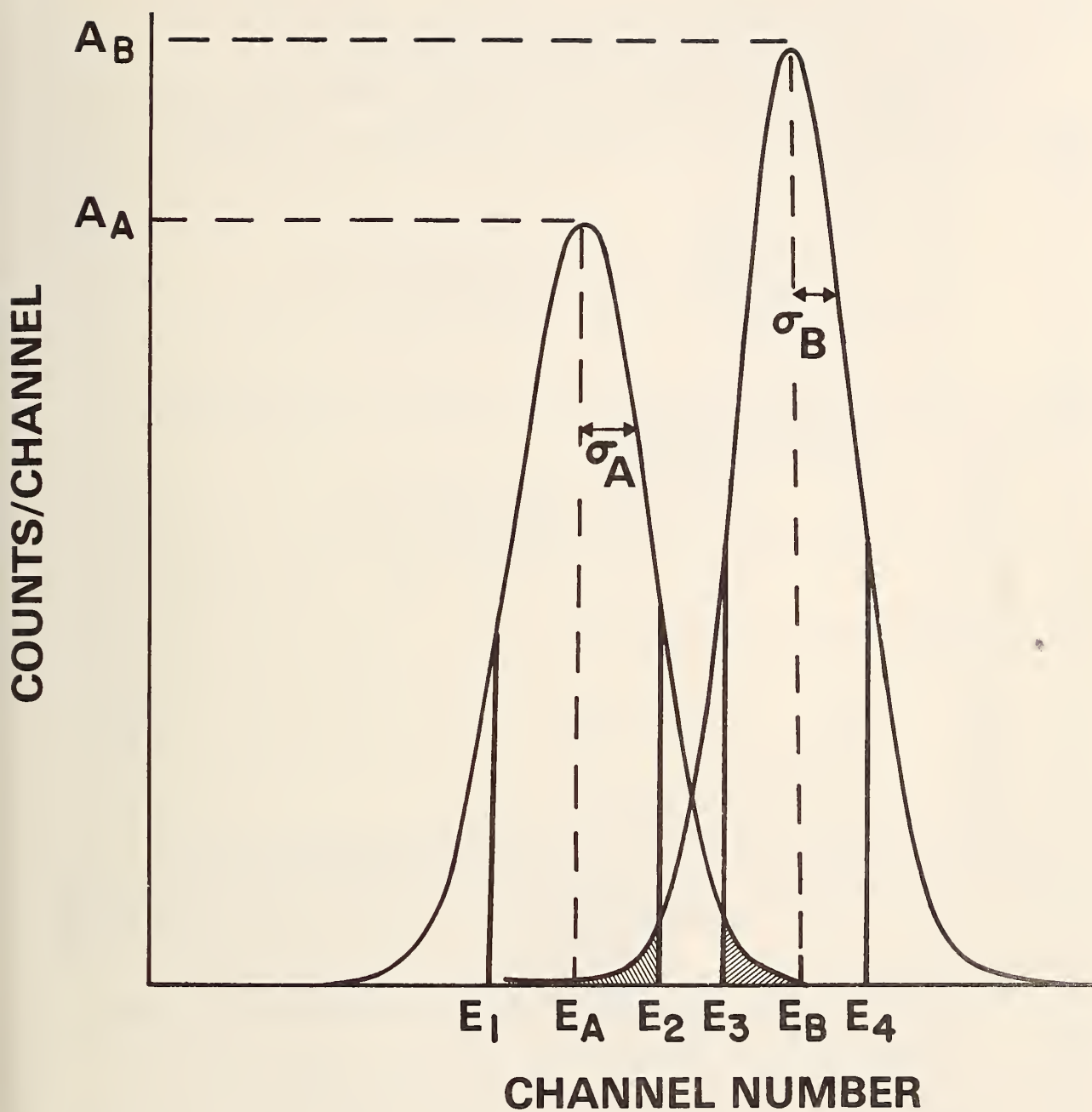
Figure 3. Schematic representation of two overlapping Gaussian peaks. Shaded areas are the overlaps of each peak into the region of interest of the other peak.

13

where $E_A$ is the centroid of the peak of A, and $A_A$ the counts
n a channel of narrow width centered around $E_A$.

Consequently, the counts $N_A$ obtained between the limits
$E_1$ and $E_2$ which define the region of interest of element A,
are:

$$N_A = A_A \int_{E_1}^{E_2} \exp\left[ -\frac{1}{2}\left(\frac{E_A - E_i}{\sigma_A}\right)^2 \right] dE_i \qquad [4]$$

while the counts between the limits $E_3$ and $E_4$ of the region
of interest of element B are:

$$N_{AB} = A_A \int_{E_3}^{E_4} \exp\left[ -\frac{1}{2}\left(\frac{E_A - E_i}{\sigma_A}\right)^2 \right] dE_i \qquad [5]$$

The overlap factor is defined as:

$$H_{AB} = \frac{N_{AB}}{N_A} \qquad [6]$$

The number of counts measured in peak A between the limits
$E_1$ and $E_2$ is multiplied by this factor to obtain the number
of counts contributed to the region of interest of peak B
by peak A.

A different type of interference occurs when a peak from
element A which is not used for data reduction (i.e., has no
region of interest) falls within the region of interest
selected for element B (figure 4). In this case, the intensity
of the interfering peak from element A must be obtained from
the count rate within the region of interest of the analytical
peak for element A. If the analytical line and the interfer-
ing line are both generated from ionization of the same
shell or subshell, their generated intensities are related
by their respective relative transition probabilities (or

14
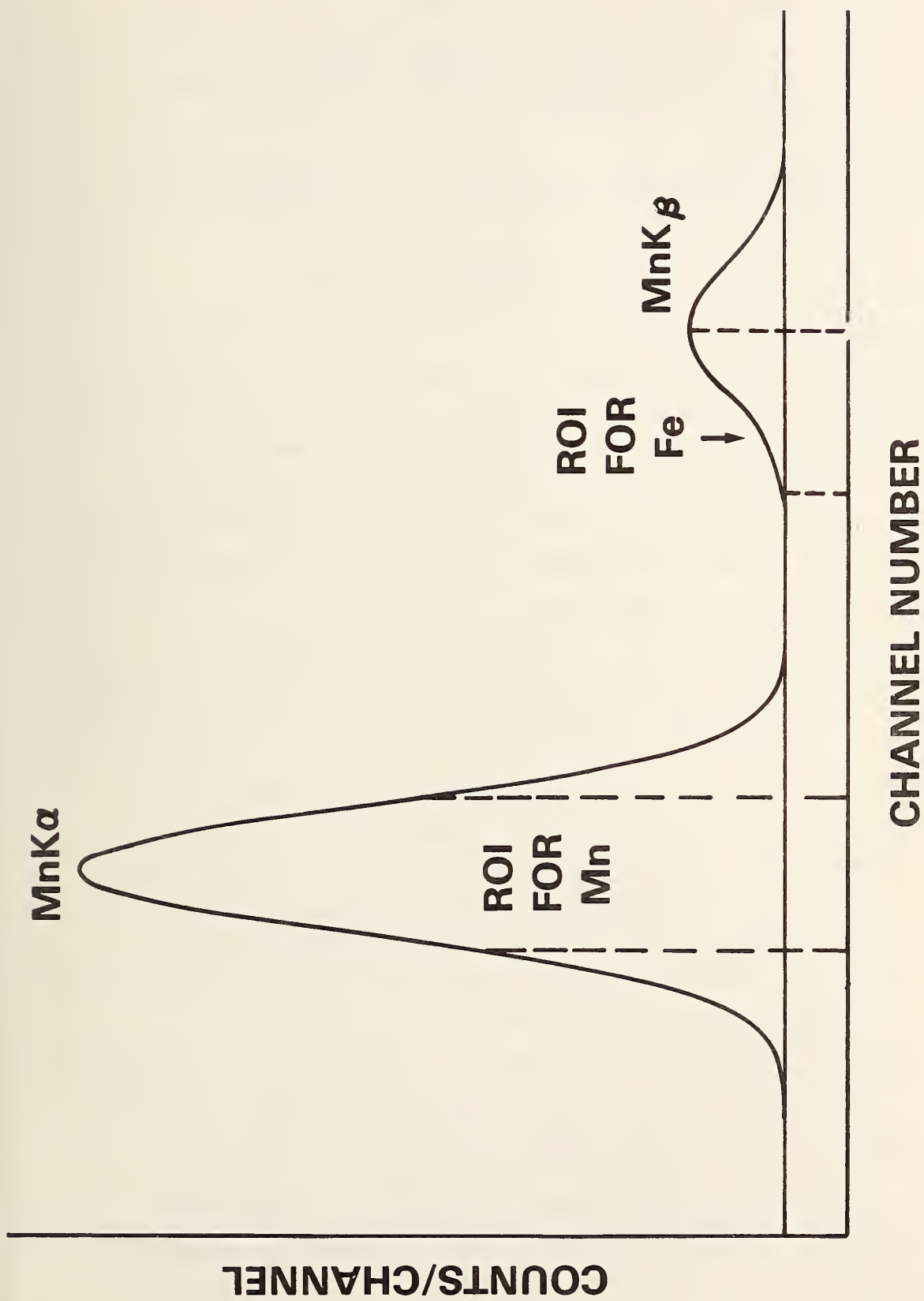
Figure 4. Spectrum of manganese showing region of interest (ROI) for FeKα overlapped by MnKβ .

15

weights of lines). A transition probability is the intensity of the line of interest divided by the sum of the intensities of all other lines arising from the same absorption edge. The emergent and detected intensities are also affected by the respective absorption factors, and the efficiency of the detector at the respective energies. For instance:

$$\frac{I'_{AK\beta}}{I'_{AK\alpha}} = \frac{\phi_{AK\beta}}{\phi_{AK\alpha}} \cdot \frac{f(AK\beta)}{f(AK\alpha)} \cdot \frac{P_E (AK\beta)}{P_E (AK\alpha)} \qquad [7]$$

where $\phi_{AK\beta} = I(AK\beta)/\Sigma I(AK)$ is the transition probability of the AKβ line, f(AKβ) is the corresponding absorption correction factor, and $P_E$ the detector efficiency at the energy E.

The procedure can be extended by a simple adjustment derived from the generation equation ("atomic number correction") to the relation of lines from different subshells of the same shell (e.g., $L\alpha_1$-$L\beta_1$).

When the two lines of interest belong to different shells (e.g., the analytical line is $AuL\alpha_1$, and the interfering line is Au Mα), the comparison of generated intensities, performed in FRAME C, is less accurate than in the previous case. This situation arises seldom in actual analysis; research is presently underway to improve the accuracy of such calculations. The correction for lines from different edges is made by calculating the relationship of line intensities for element A: From the emitted intensity of the line of A which has a region of interest, a calculation is made of the interfering line intensity of element A in the region of interest of element B. The relative transition probabilities (weights of lines) are used for this purpose. For example, if the interfering line is the Kβ peak of element A, then to relate the interference of AKβ with another peak BKα to the measured intensity of AKα, the overlap factor of AKβ into the region of interest of BKα is obtained by:

16

$$H_{AB} = \frac{I_{AK\beta}}{I_{AK\alpha}} \cdot \frac{f_p(AK\alpha)}{f_p(AK\beta)} \frac{P_{E(AK\alpha)}}{P_{E(AK\beta)}} \cdot \frac{N_{AB}}{N_A} \qquad [8]$$

where $I_{AK\beta}/I_{AK\alpha}$ is derived from the ratio of generated intensities (weight of line $\frac{I_{AK\beta}}{\Sigma I_{AK_i}}$), which is a known parameter of the K$\beta$ line and the K$\alpha$ line; $f_p$ is the absorption in the specimen and $P_E$ is the detector efficiency. The weights of the K$\beta$ x-ray lines of elements of atomic number 15 through 30 have been measured by us (see Table 1) as well as by others [16] and are better known than those of the L or M x-ray lines. For an extreme peak overlap consider the Cr K$\beta$ line overlapping the Mn K$\alpha$ line. A two percent error in the weight of the Cr K$\beta$ line will generate an error in the mass fraction of Mn of 0.0025 in a pure Cr specimen (see Table 2). The weights within each of the L and M series of lines, up to 10 keV, have been estimated by us and are probably within ±20 percent of their true value.

Table 1

Relative Transition Probabilities for Kβ X-ray Lines [20]

| Atomic Number | $K\beta/(K\alpha + K\beta)$ |
|:---:|:---:|
| 15 | .050 |
| 16 | .063 |
| 17 | .085 |
| 18 | .097[a] |
| 19 | .104 |
| 20 | .113 |
| 21 | .114[a] |
| 22 | .114 |
| 23 | .116 |
| 24 | .116 |
| 25 | .119 |
| 26 | .119 |
| 27 | .120 |
| 28 | .121 |
| 29 | .123 |
| 30 | .128 |

[a] Interpolated value

Table 2. Overlap Corrections

| Specimen | $E_o$ in keV | Analyzed for | Overlap with | Mass fraction found before correction | Mass fraction found after correction |
|----------|--------------|--------------|--------------|----------------------------------------|---------------------------------------|
| MgO | 15 | Al | MgK$\beta$ | .0026 | .0016 |
| Al$_2$O$_3$ | 15 | Mg | AlK$\alpha$ | .0132 | .0058 |
| Al$_2$O$_3$ | 15 | Si | AlK$\beta$ | .0039 | .0014 |
| SiO$_2$ | 15 | Al | SiK$\alpha$ | .0072 | -.0010 |
| Cr | 15 | Mn | CrK$\beta$ | .1311 | -.0024 |
| Mn | 15 | Fe | MnK$\beta$ | .1045 | .0019 |
| Fe | 15 | Co | FeK$\beta$ | .0653 | .0062 |
| Cu | 20 | Zn | CuK$\beta$ | .0206 | .0039 |
| Zr | 15 | Bi | ZrL$\beta_2$, L$\gamma_1$,L$\gamma_3$ | .0214 | -.0113 |
| Bi | 15 | Zr | BiM$\alpha$,M$\beta$, M$\zeta$ | .0213 | -.0009 |
| Zn | 20 | W | ZnK$\alpha$ | .1329 | .0010 |
| Ta | 20 | Cu | TaL$\alpha_1$[a] | .1968 | .0700 |

[a]The regions of interest for Cu K$\alpha$ and Ta L$\alpha$ overlap. These lines are too close to be separated well by this method.

The electron beam incidence angle is 90° and the x-ray emergence angle is 52.5°.

To compute overlap factors for all the L x-ray lines, we relate the intensity of each L line to the $L\alpha_1$ line (the measured line). We must, however, take into account that the ratios of line intensities of the L spectra vary with excitation potential. This is due to the fact that these lines arise from three subshells each of which has a different critical excitation potential. To relate the intensity of any line to the measured $L\alpha_1$ line, we compute an intensity factor which is the intensity of the line "i" divided by the intensity of the $L\alpha_1$ line $(I_{L_i}/I_{L\alpha 1})$.

To introduce an energy-dependent term into this factor, we have integrated the expression:

$$Y_{n1} = \frac{N}{A} \int_{E_o}^{E_c} \frac{Q(E)}{[dE/ds]} \, dE \qquad [9]$$

where s is the mass thickness along the electron path $(g/cm^2)$, in the same manner as Philibert and Tixier [17] to obtain the number of ionizations, $Y_{n1}$, in the level n1.

$$Y_{n1} = \frac{N}{A} \frac{Z_{n1}}{M} \left\{ U_o - 1 - \frac{1}{W} \ln W [ \text{li}(U_o W) - \text{li}(W)] \right\} \qquad [10]$$

M and N/A are constant and can be eliminated since we are calculating the ratios of the x-ray lines for the same element. $U_o$ is the overvoltage $E_o/E_{n1}$ where $E_{n1}$ is the ionization energy of the edge n1, W is 1166 $E_{n1}/J$ where J is the mean ionization potential, $U_o W$ is 1166 $E_o/J$ and li is the logarithmic integral. We have fitted an expression which approximates the logarithmic integral $(\text{li}(x) \overset{\sim}{=} 2.905 \sqrt{x} - 3.063)$ over the range of interest. The number of electrons in each subshell, $Z_{n1}$, is determined from basic quantum theory, and the pertinent values for the subshells of interest are as follows:

| Subshell | Number of Electrons |
|----------|---------------------|
| K        | 2                   |
| $L_1$    | 2                   |
| $L_2$    | 2                   |
| $L_3$    | 4                   |
| $M_1$    | 2                   |
| $M_2$    | 2                   |
| $M_3$    | 4                   |
| $M_4$    | 4                   |
| $M_5$    | 6                   |

The ratios of lines arising from different absorption edges are then corrected for differences in overvoltage by multiplying each line by $Y_{n1}$ (Eqn. 10). The total L line intensity factor, for any L line, thus becomes:

$$S_L = \frac{I_L \, Y_L}{I_{L\alpha_1} \, Y_{L\alpha_1}} \qquad [11]$$

The first step in computing the L overlaps is to determine the area of the $L\alpha_1$ line within its region of interest by subtracting the areas of all other L lines of the same element from the region of interest. This is done by calculating all the overlap factors for these lines and stripping them out in the same manner as is used for overlaps from other elements. Since the computed overlap factor for each L line is relative to the $L\alpha_1$ line alone, this step is necessary. Overlap factors for the measured lines of other elements are then computed in the same manner as for K lines except that the overlapping area of an interfering peak is multiplied by that peak's intensity factor, $S_L$. In the case of the ratio $L\alpha_1/K\alpha$, the ratio must be multiplied by the ratio of fluorescence yields, $\omega_L/\omega_K$, and an atomic number dependent factor which is at least partly due to the Coster-Kronig transitions.

$$y_L = 0.095Z - 1.69 \qquad\qquad [12]$$

M lines are treated in a similar manner. There are also provisions for determining the intensity of an M line from an L line or vice versa. Since we were unable to find an appropriate cross section for the M-series of x-ray lines, we fitted an empirical expression to the generated $M\alpha/L\alpha_1$ ratio for three elements at five different operating voltages.

$$Y_{n1}y_M = \exp\left[\frac{34.17}{\ln(U_p)} - \frac{30.03}{\sqrt{\ln(U_p)}} + 8.527\right] \qquad [13]$$

$U_p$ is the product of the L overvoltage, $E_o/E_{L3}$, and the M overvoltage, $E_o/E_{M5}$. Approximate results can be obtained by this technique; however, the factors used are not well known at this time.

In the previous discussion, we have assumed that the peaks have simple Gaussian shapes. In reality, however, the peaks are distorted on the low-energy side by the effect of incomplete charge collection (see Appendix 1). Consequently, the x-ray peaks observed by a Si(Li) detector are the convolutions of several contributions. Some peaks consist of several x-ray lines of the same series (such as $K\alpha_1$ and $K\alpha_2$). In most cases of multiple peaks (except $K\alpha_{1,2}$ and $K\beta_{1,3,5}$), we compute the peaks separately for each x-ray line in the same manner as the overlapping peaks from other elements. For the incomplete charge collection at the low-energy shoulder of each peak, we have developed an empirical expression:

$$I_{c_i} = A_A a(E_A - E_i) \exp[-b(E_A - E_i)] \qquad [14]$$

in which a and b are energy-dependent coefficients fitted for a particular detector and the other terms are as previously defined. $A_A$ was previously obtained as a measure of line intensity from Eqn. 3.

22

The remaining case of overlap that is computed is the interference of the escape peak of a characteristic x-ray line with an analytical line. The expression used to predict the number of counts in an escape peak based on the number of counts in the parent peak is that due to Reed and Ware [18]:

$$k_{esc} = 0.038\varepsilon/(1-0.038\varepsilon) \qquad [15]$$

where $k_{esc}$ is the integrated intensity ratio of the escape peak to the parent peak and

$$\varepsilon = \frac{1}{2} \left\{ 1 - \frac{\mu(Si,Si)}{\mu(Si,E_A)} \ln \left[ 1 + \frac{\mu(Si,E_A)}{\mu(Si,Si)} \right] \right\} \qquad [16]$$

$\mu(Si,Si)$ is the mass absorption coefficient for $SiK\alpha$ in silicon and $\mu(Si,E_A)$ is the mass absorption coefficient for the parent peak in silicon. An overlap coefficient is then computed in the same manner as previously described for a peak that has no region of interest. The standard deviation of the escape peak is that corresponding to its energy rather than of the parent energy; $k_{esc}$ is the intensity ratio of escape peak to parent peak.

## IIb. Description of Subroutines

### A. Main Program for Standards (100-390)

This program is executed for each spectrum of a standard whether the standard is a pure element or a multi-element material of known composition. On the spectrum, the operator must choose two regions of interest for the background determination. These regions must be the first two in the list of regions contained in the multichannel analyzer (regions 0 and 1). The following information must be entered via the terminal by the operator: 1. the number of elements in the standard and, for the first standard, the operating potential (kV). 2. the mass fraction, atomic number, x-ray line code

23

and valence of each element in the standard. Any elements that are present in the standard but are not needed for a particular analysis may be excluded by entering a zero for the x-ray line code. Otherwise, enter 1 for the $K\alpha$ line, 2 for the $L\alpha_1$ line and 3 for the $M\alpha$ line. The valence for each element in the unknown must be entered if you wish to compute the oxygen content of an unknown by stoichiometry. If this is not required, enter a zero for the valence.

The program automatically defines the region of interest for each peak the signal contents of which are then corrected for background and any overlap from other peaks. If the standard contains more than one element, a matrix correction is performed. The known composition is used to obtain the calculated intensity ratio ($k_c = I_{std}/I_{pure}$). The intensity of the measured peak is then divided by the calculated intensity ratio to obtain the intensity that would be emitted under identical conditions from the pure element ($I_{pure} = I_{meas.}/k_c$). If the standard is a pure element, the matrix correction is omitted.

The results (see figure 2) are then stored in a random access data file. In our version of FRAME C, one quadrant (1024 channels) of the multichannel analyzer was selected to be used as a data file in the TN 1700. The information stored in this area is the operating voltage, the number of elements that have been measured as standards, and, for each element standard, the atomic number, x-ray line, valence (if used), and the intensity for the pure element. The only results printed in the execution of this program are the calculated intensity ratios for each element in the standard.

B.   Main Program for Computing Concentrations in Unknowns 500-900

This program is similar to that for standards. The same subroutines are called but in slightly different order. The operator must again select the two background regions of interest as before and the number of elements and the atomic

24

number for each of them must then be entered via the terminal. All of the information stored in the standards file for each element is retrieved from the file. The region of interest for each element is assigned and the overlap correction factors are computed and stored in the file with the standards.

The matrix correction is then performed. The background subtraction and overlap corrections are included within the main iteration loop of the ZAF corrections and hence performed in each iteration. At the completion of the computation, the obtained mass fractions of all elements are printed, and the x-ray peaks are constructed in one quadrant of the multichannel analyzer. These peaks may then be compared with the original spectrum to see if all elements have been correctly identified and the compositions determined. Additional unknown spectra may then be analyzed for the same elements without entering any additional information. The overlap factors previously calculated and stored are also used in subsequent analyses, thereby saving the time required for this lengthy computation.

C.   Subroutine for retrieval of coefficients and constants
     (1000-1495)

The constants and functions needed by the program are stored in this subroutine as defined in the list of variables. The detector parameters (P6, P7, Q3) are also retrieved by this subroutine. These should be redetermined by each user to match his detector.

| Line | Variable | Definition |
|------|----------|------------|
| 1440 | Q1 | X-ray emergence angle in degrees. |
| 1450 | Q2 | Electron beam incidence angle in degrees. |
| 1454 | P6 | Thickness of Be window on detector (cm). |
| 1455 | P7 | Thickness of Si dead layer in detector (cm). |
| 1480 | Q3 | Full width at half maximum of MnKα peak (eV). |

D.  Subroutine for computing all necessary edge and line energies (1500-1610)

Nine x-ray absorption edge energies and 17 x-ray line energies are computed for each element. The general expression used for both edges and lines is:

$$E = \exp\left[a(\ln Z)^2 + b(\ln Z) - c\right] \qquad [17]$$

where Z is the atomic number and a, b, and c are coefficients stored in subroutine C. The x-ray lines are coded by numbers from 1 to 17 which refer to the Kα, Lα$_1$, Mα, Kβ, Lα$_2$, Lℓ, Lβ$_2$, Lβ$_1$, Lγ$_1$, Lη, Lβ$_3$, Lγ$_3$, Lβ$_4$, Mζ$_1$, Mβ, Mγ, and to the line from the M$_{II}$-N$_{IV}$ transition. The edges are in the order: K, L$_1$, L$_2$, L$_3$, M$_1$, M$_2$, M$_3$, M$_4$, and M$_5$. If the line energies are below 1 keV, the calculation is aborted by the program since the computed energies are of insufficient accuracy in this region to allow them to be used as the measured x-ray line for an element. Readers are warned to refrain from using these equations outside the limits of the regions for which they have been developed.

E.  Subroutine for computing mass absorption coefficients (1700-1980)

This subroutine will compute a mass absorption coefficient for x-rays of any energy above 0.5 keV in any pure element.

The absorption coefficients are calculated as proposed by
Heinrich [19]. Least squares fits were made to the logarithm
of the coefficient C and exponent n in the general relation:

$$\mu = C\lambda^n \qquad\qquad [18]$$

in which $\lambda$ is the wavelength of the x-ray in angstroms. A
comparison of the calculated values with those given by
Heinrich showed agreement within a few percent. To indicate
uncertainties which arise where lines close to absorption
edges are used, a warning is printed if the analytical line
falls within 100 eV of an absorption edge of another element
present in the specimen.

F.    Subroutine for computing detector efficiency (2000-2095)

The efficiency $P_E$ of the Si(Li) detector, at any photon
energy is determined by the loss of x-ray detection in the
detector due to absorption in the beryllium window, gold
surface layer and the silicon dead layer or by transmission
of the x-rays through the detector without absorption of
the photon:

$$P_E = \exp\,[-t_{Be}\mu_{Be}^E - t_{Au}\mu_{Au}^E - t_{Si}\mu_{Si}^E]\,[1-\exp(-t_{det}\mu_{Si}^E)] \qquad [19]$$

t is the thickness in cm of each layer of material, $t_{det}$ is
the total thickness of the detector, and $\mu_i^E$ is the <u>linear</u>
absorption coefficient for an x-ray of energy E in the
element i which is obtained in the program by dividing the
mass absorption coefficient by the density.

G.    Subroutine for computing the primary absorption factor
      in a specimen (2100-2140)

The x-ray absorption factor, $f_p$, used is that proposed
by Heinrich [10] and modified for oblique beam incidence.

$$f_p = [1 + 1.2 \times 10^{-6}\,\gamma\mu\sin(\varepsilon)\,\csc(\psi)] \qquad [20]$$

where $\mu$ is the mass absorption coefficient, $\psi$ (deg.) is the
x—ray emergence angle, and $\gamma = (E_o^{1.65} - E_q^{1.65})$. $E_o$ is

27

the operating potential (kV), $E_q$ is the critical excitation
potential (kV) and $\varepsilon$ (deg.) is the electron beam incidence
angle.

H.    Subroutine for computing the X-ray Continuum Background
      (2200-2620)

The method for computing the x-ray continuum is that
proposed by Fiori et al. [11]:

$$I_E = \frac{1}{E} [K_1(E_o-E) + K_2(E_o-E)^2] P_E f_p \qquad [21]$$

where $I_E$ is the intensity of the continuum at the photon
energy E, $E_o$ is the operating potential, and $P_E$ and $f_p$ are
defined in sections F and G respectively. $K_1$ and $K_2$ are
parameters fitted to the background curve, on the basis of
the measurements at the two background regions of interest
selected by the user for measurement. The fit must be
repeated in each iteration because the value of $f_p$ depends
on the specimen composition.

I.    Subroutine to store the information on standards into
      quadrant 4 of the TN 1700 multichannel analyzer
      (2700-2920)

This subroutine stores in quadrant 4 of the TN 1700, the
atomic number, line code, the background—and overlap—corrected
peak counts for the pure element, and the valence for each
element in the standard that is measured. If a data file
other than a quadrant in the multichannel analyzer is used,
this subroutine must be modified.

J.    Subroutine to compute the overlap factors (3000—3450)

This is the main program for computing the overlap
coefficients. In lines 3034-3200, the integrals of the measured
x-ray lines are computed from the assigned energy limits of
each peak together with the energy and width of the peak. The
incomplete charge collection is added to the Gaussian peak
after integration. From line 3205 to 3395, all possible over-
laps are computed one by one, beginning with overlap from

28

other lines of the same element (K1 = 0) and then each overlap
from other elements in the specimen (K1 = 1).  When K1 = 0,
an intensity factor for all observable x-ray lines of an
element relative to the measured x-ray line for the element
is stored in the random access data file for use in recon-
structing the x-ray spectrum of the unknown.

K.   Subroutine to compute relative peak intensities and
     to test for overlaps (3490-3850)

The x-ray generation cross-sections $Y_{nl}$ for electron
excitation that are required are computed by equations 10,
12 and 13 in lines 3490-3513 and multiplied by the fluores-
cence yield $\omega$.  In lines 3514-3645 the weight of each
x-ray line from an element relative to the measured line
for the element is determined.  The overlap coefficients are
calculated for each overlapping line in lines 3730-3850.

It must be emphasized that the values for the weights
of generated lines which appear in lines 3571-3605 are
estimates which will be changed as more information becomes
available.

L.   Subroutine to store the overlap coefficients in the
     random access data file (3855-3886)

The overlap coefficients are individually stored for
each element together with the atomic number and line of
the interfering x-ray peak.  A maximum number of 13 overlaps
per measured line can be stored.

M.   Subroutine to compute the relative weights of escape
     peaks (3890-3990)

The relative weight of an escape peak ($S_8$ in the program)
to its parent peak is determined by equations 15 and 16.

N.   Subroutine to compute the overlapping area of one peak
     on another (4000-4130)

The portion of an interfering peak that overlaps the
analytical peak for an element is computed by integrating
the area with the overlapping peak between the energy limits

of the analysis peak. Since the area is asymmetrically placed on the overlapping peak, the integrals from the peak energy to each energy limit are computed separately and algebraically summed to obtain the overlapping area. A correction for incomplete charge collection in the detector is also added on the low energy side of the peak.

O.    Subroutine to compute the incomplete charge collection of the detector (4200-4400)

The expression for incomplete charge collection (Equation 14) has been integrated to give:

$$N_{c_i} = \frac{a}{b^2} A_A \left\{ 1 - \exp\left[-b(E_A - E_i)\right] \cdot \left[1 + b(E_A - E_i)\right] \right\} \quad [22]$$

In the program, X1 = a and X3 = 1/b. X1 and X3 are varied as a function of the peak energy in lines 4220-4260.

P.    Subroutine to integrate the area under a Gaussian (4500-5090)

This subroutine produces the integral of the error function:

$$\mathrm{erf}(x) = \frac{2}{\sqrt{\pi}} \int_0^x e^{-t^2} \, dt \quad [23]$$

Since the integral under a Gaussian is of the form:

$$A(y) = \frac{2}{\sqrt{2\pi}\,\sigma} \int_0^y e^{-\left(\frac{E-E_A}{\sigma\sqrt{2}}\right)^2} \, dE \quad [24]$$

the integration may be performed with the error function if $x = t = \dfrac{E-E_A}{\sigma\sqrt{2}}$ and $dt = \dfrac{1}{\sigma\sqrt{2}}\, dE$. The integration limits are not necessarily symmetrical with respect to the peak; therefore, the integration must be don  twice, once for each limit, and half of each integral is summed to obtain the total for the area of the peak.

30

Q.  Subroutine to correct peaks for overlap, using the
    overlap coefficients (5100-5390)

This subroutine must be considered in relation to the
matrix correction.  Figure 5 is a flow chart emphasizing the
overlap correction while showing its relation to the rest of
the program.  The overlap coefficients for each peak are
recalled from the random access data file.  As long as
similar unknowns are being analyzed, these coefficients need
not be recalculated by subroutines J-P.

R.  Subroutine to compute the matrix corrections (5500-7150)

The expressions in the matrix correction will not be
defined here since they have been described previously [2].
Instead we will list the particular factor being computed
in each region of the subroutine.  All factors that are
independent of concentration are computed in the loop from
line 5510 to line 6400.  The overvoltage ($E_o/E_q$) should be
between 1.5 and 10 for each element.  The overvoltages are
computed and tested in lines 5530-5580.  If the overvoltage
is too low, a message is printed.  Absorption coefficients
of pure elements are calculated in lines 5590-5630.  The
absorption factors ($f_p$) are determined in lines 5750-5770.
Tests are made for characteristic fluorescence corrections
in lines 5780-6160 and the parameters for the characteristic
fluorescence corrections are defined in lines 6170-6381.
The backscatter losses and stopping powers are computed in
lines 6382-6400.  Initial intensity ratios and the first
estimates for concentrations are calculated in lines 6405-
6540.

The main iteration loop begins in line 6550 and the
loop ends in 7050.  The atomic-number and absorption correc-
tions are computed in lines 6580 to 6690.  The characteristic
fluorescence correction is calculated in lines 6700 to 6810.
The intensity ratios for the assumed concentrations are
determined in line 6820.  If the computation is being done

31
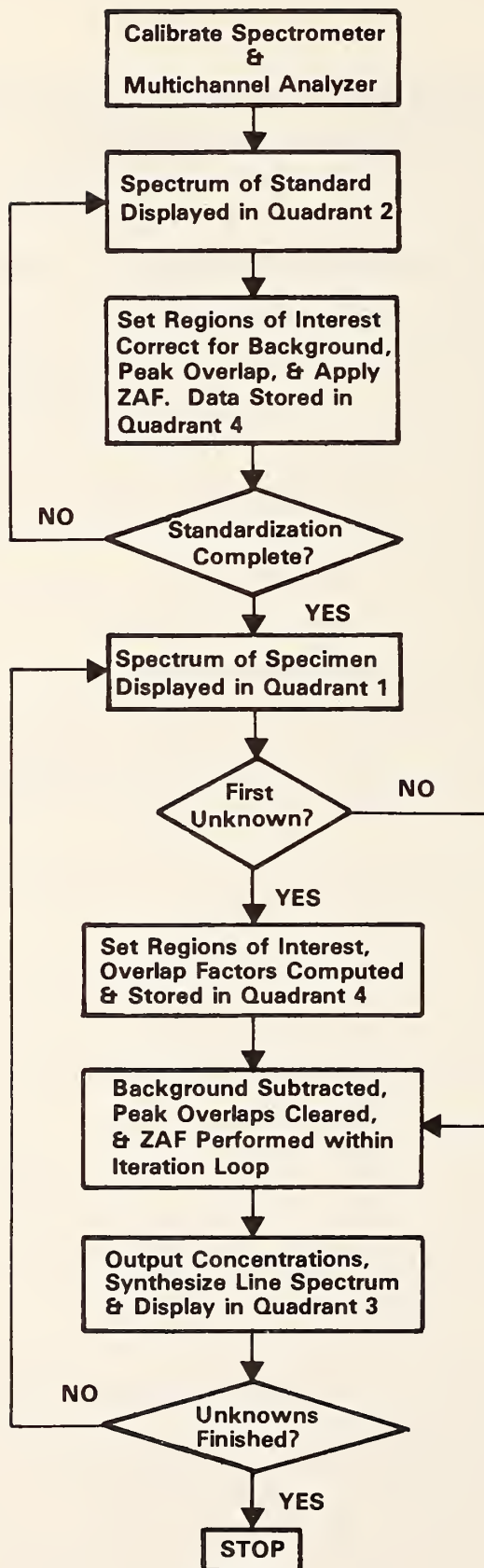
Figure 5. Short block diagram of procedures in FRAME C.

for a multielement standard, these intensity ratios are printed out (lines 6835-6850) and the values are returned to main program A. If an unknown specimen is being analyzed, new concentration estimates are obtained from the hyperbolic equation in lines 6870 and 6872. If the calculations are complete (line 6874), the spectrum may be redrawn on the multichannel analyzer (line 6876). In lines 6900-7040, the new concentration estimates are used to obtain a new background correction (line 6980), a new overlap correction (line 6990), and a new intensity ratio (lines 7000-7040). If the computation is completed, the results are printed in lines 7060-7140.

S.   Subroutine to set the regions of interest (ROI) for each measured line (8000-8140).

The instructions in this subroutine are specifically written for a Tracor-Northern TN 1700[4] multichannel analyzer. Line 8020 defines the value of K1 which is used to define the width of any ROI as a function of energy.

$$\text{Lower limit} = E_A - K1 \; \sigma \qquad\qquad [25]$$

$$\text{Upper limit} = E_A + K1 \; \sigma \qquad\qquad [26]$$

T.   Subroutine to redraw the spectrum in one quadrant of the multichannel analyzer (8200-8595)

The concentrations obtained by the program together with the relative peak weights generated in subroutine J are used to redraw the characteristic line spectrum (without the continuum) in quadrant 3 of our multichannel analyzer. The energy limits and intensity of the measured peak are determined in lines 8210-8315. The parameters for all other

---

[4]In order to adequately describe materials and experimental procedures, it was occasionally necessary to identify commercial products by manufacturer's name or label. In no instance does such identification imply that the particular products or equipment is necessarily the best available for the purpose.

peaks are determined in lines 8320-8460. The redrawing of
each peak is done in lines 8500-8595 (this is really a
separate subroutine; however, it is called from line 8310
and 8430 only).

U.    Subroutine to compute the concentration of an element
      either by stoichiometry or by difference (8600—8740)

One element in an unknown may be determined by difference:

$$C_n = (1 - \sum_{i=1}^{n-1} C_i) \qquad [27]$$

or if the unanalyzed element is oxygen, it may be determined
by the stoichiometric relationships to the analyzed elements.
If zeros were entered for the valences of the elements, the
element will be determined by difference (8720-8740). If
non-zero valences were entered for each element (main program
A), the oxygen content will be determined using the stoichi-
ometric relation of oxygen to each analyzed element (8680-
8690 and 8702).

V.    Main program for computing window thickness on a Si(Li)
      detector (100-312)

This procedure should be carried out three or four times
a year on each Si(Li) detector to determine the thickness of
the beryllium window and of the silicon dead layer. A
carbon continuum spectrum should be generated at a convenient
operating potential (15 kV). The operator must select back-
ground regions of interest coded 0 and 1 as they are normally
positioned (e.g., 3.5 kV and 7 kV). Then the operator must
select two more regions of interest: number 2 about half way
up the slope on the low energy side of the silicon K-absorption
edge and number 3 just on the high energy side of the silicon
K-absorption edge. The operator must then enter the atomic
number of the sample (6 for carbon) and the operating potential.
The program does 15 iterations and prints out the two thick-
nesses which can then be entered in lines 1454 for Be and

34

1455 for Si.  This program will overlay the main program A. It, therefore, requires no additional computer memory.

## IIc.  Results

As reported elsewhere [2], the ZAF portion of FRAME C has been extensively tested and compared with results obtained with the program COR 2 which includes all available refinements of the quantitation theory.  The prediction of the continuum has also been previously examined and shown to be adequate for the background corrections [11].  The effectiveness of the interference correction was tested by analyzing several specimens (pure elements and minerals) for elements that are not present in the specimens but the lines of which fall near x-ray lines from elements that are present.  For example, if pure manganese is analyzed for iron, the Mn K$\beta$ peak which overlaps with the Fe K$\alpha$ region of interest contributes a large number of counts to this region.  The overlap correction subtracts the counts due to Mn K$\beta$ from the region of interest of Fe K$\alpha$ (see figure 4).  Some examples of overlaps that are removed are shown in Table 2.  In most cases, the interference is removed efficiently; however, it must be noted that the incomplete charge collection is not at present adequately removed for some elements.  Figure 6 shows a mutual overlap of Zn K$\alpha$ and W L$\alpha$ in a spectrum from zinc tungstate ($ZnWO_4$), with the results obtained by FRAME C in Table 3.  It must also be noted that the statistical uncertainty of an overlap corrected peak is greater than the uncertainty of the same peak if it had no overlap.
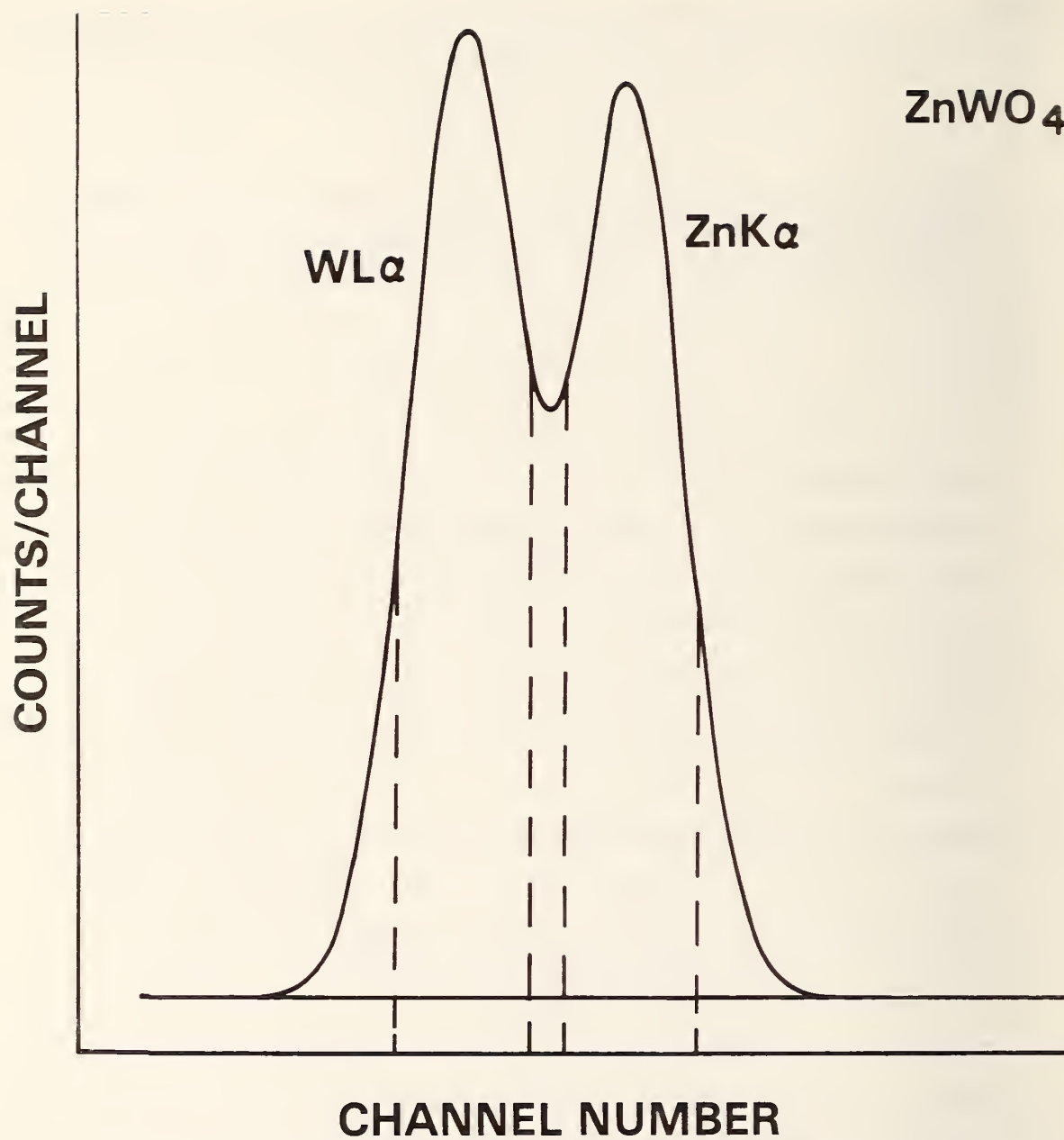
Figure 6.  Spectrum of $ZnWO_4$ showing the WLα and ZnKα overlapping peaks.

Table 3. Comparative Analyses of Zinc Tungstate, $ZnWO_4$

| | Relative Intensities (k ratios) | | | Calculated Mass Fractions | |
| | Crystal Spectrometer | Si(Li) Detector | | Crystal Spectrometer | Si(Li) |
| | | No Overlap Correction | With Overlap Correction | | With Overlap Correction |
| --- | --- | --- | --- | --- | --- |
| W(Lα) | .503 | .532 | .498 | .587 | .580 |
| Zn | .203 | .255 | .236 | .221 | .227 |

The operating voltage is 20 kV. The electron beam incidence angle is 90° and the x-ray emergence angle is 52.5°.

In this and subsequent tables, all analytical lines are Kα lines unless otherwise noted.

37

Since the magnitude of the interference from lines that
do not have a region of interest depends on the relative
weights of the lines, these must be known. FRAME C contains
estimates of the weights of lines which will be updated as im-
proved values become available from measurements in our labora-
tory or elsewhere. In the course of an analysis, a line spec-
trum of the unknown synthesized by the program is stored for
display in quadrant 3 of the multi-channel analyzer memory.
Gaussian peaks are constructed for each x-ray line from the
weights of lines, the analytical results, the line energies,
and the peak widths. The continuum is not synthesized for the
display since this procedure requires too much time.

The results of an analysis may be evaluated by comparing
the synthesized spectrum with the spectrum obtained experi-
mentally from the specimens. Part of an experimental spectrum
of Nunivak anorthoclase is shown in figure 7 together with
the spectrum synthesized by the program of the same specimen.
The comparison of spectra is particularly useful for detecting
elements which were inadvertently omitted in the analysis.
Results of energy-dispersive analyses of several minerals and
alloys are shown in Tables 4 and 5 together with the results
obtained by chemical analyses and the standards used for
each element. The standards K371, K409, and K412 are glasses
prepared at NBS as microanalytical standards. The steels
listed in Table 5 were analyzed by scanning the beam over an
area of 160 x 200 μm; however, this was not always sufficient
to prevent specimen inhomogeneity effects. Also, the large
incomplete charge collection present in the Fe Kβ signal is
not adequately removed from the Co Kα region of interest.
We are currently evaluating data collected from several
different Si(Li) detectors to obtain a better estimate of
the contribution of incomplete charge collection. The tests
conducted show that the proposed method for overlap corrections
in energy-dispersive x-ray analysis combined with the FRAME B
program is suitable for general use.
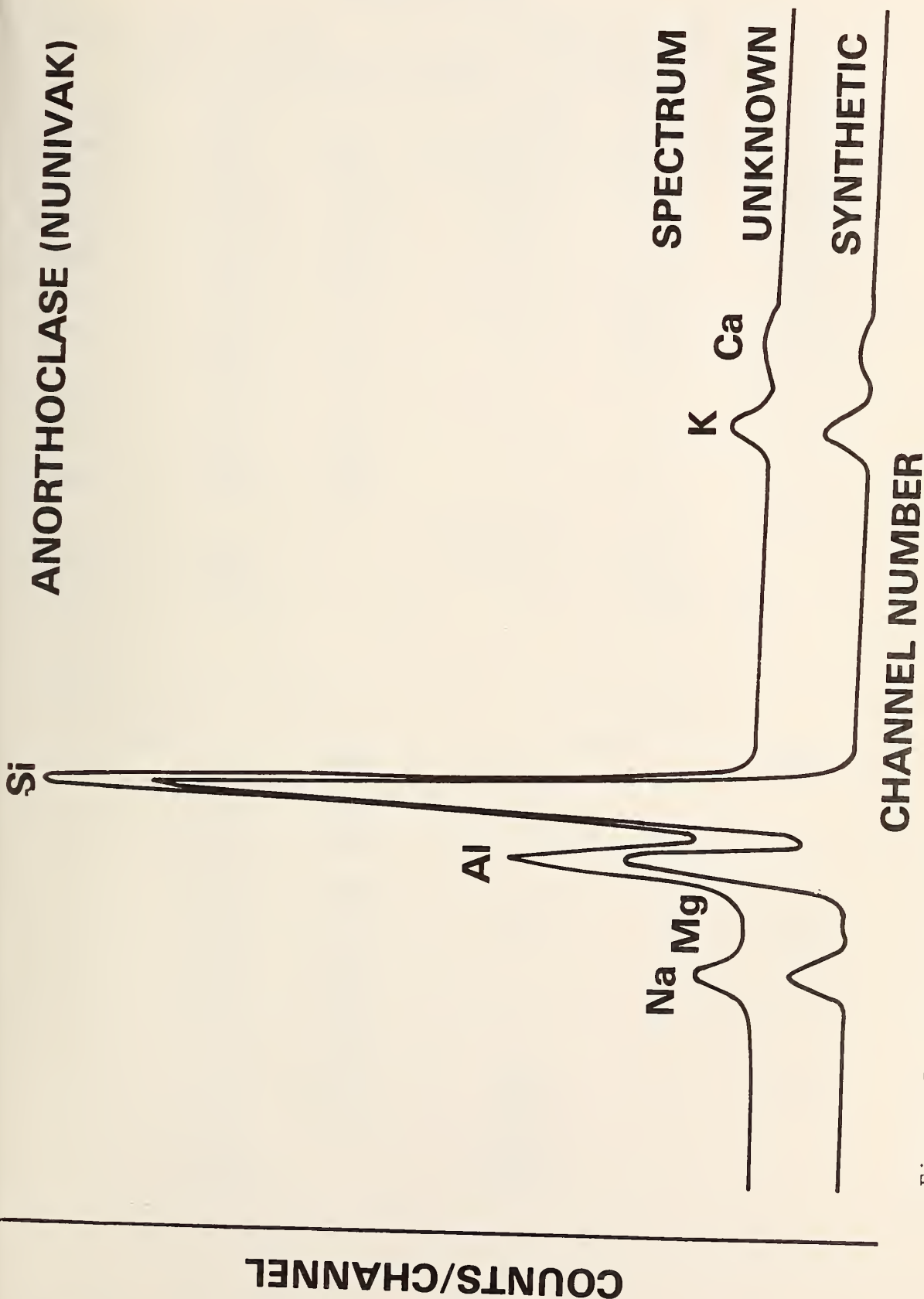
Figure 7. Spectrum of anorthoclase (Nunivak) compared to the synthetic spectrum of the same material generated by FRAME C.

39

## Table 4. Mineral Analyses

### Mass Fractions

#### Anorthoclase (Nunivak)[f]

| | Chem | FRAME C Set 1[a] | Set 2 |
|---|---|---|---|
| Na | .0611 | .0638[b] | .0639[b] |
| Mg | .00012 | .0038[b] | .0020[b] |
| Al | .1081 | .1048[b] | .1060[b] |
| Si | .3088 | .3087[b] | .3114[b] |
| K | .0291 | .0291 | .0289 |
| Ca | .0056 | .0073[b] | .0073[b] |
| Ti | .0001 | ND[e] | ND |
| Mn | - | - | - |
| Fe | .0016 | .0013 | .0013 |
| Zn | - | - | - |
| Ba(Lα) | .0013 | .0021 | .0020 |
| O | | .4789[c] | .4772[d] |
| Total | | .9998 | 1[d] |

#### Rhodonite (Bald Knob)[f]

| | Chem | FRAME C Set 1 | Set 2 |
|---|---|---|---|
| Na | - | - | (.0008)[b] |
| Mg | .0076 | .0096 | .0093 |
| Al | - | (.0044)[b] | (.0005)[b] |
| Si | .2194 | .2251 | .2265 |
| K | - | - | (-.0006) |
| Ca | .0567 | .0586 | .0580 |
| Ti | - | - | - |
| Mn | .2645 | .2735 | .2730 |
| Fe | .0131 | .0157[b] | .0136[b] |
| Zn | .0562 | .0609 | .0606 |
| Ba(Lα) | - | - | - |
| O | | .3893[c] | .3577[d] |
| Total | | 1.0371 | 1[d] |

#### Tephroite[f]

| | Chem | FRAME C Set 2 |
|---|---|---|
| Na | - | - |
| Mg | - | - |
| Al | - | - |
| Si | .1391 | .1443 |
| K | - | - |
| Ca | - | - |
| Ti | - | - |
| Mn | .5441 | .5410 |
| Fe | - | (.0008) |
| O | | .3139[d] |
| Total | | 1[d] |

#### Basalt (Juan de Fuca)[g]

| | Chem | FRAME C Set 1 |
|---|---|---|
| Na | .0194 | .0256[b] |
| Mg | .0405 | .0446[b] |
| Al | .0744 | .0723[b] |
| Si | .2375 | .2376[b] |
| K | .0016 | .0019 |
| Ca | .0795 | .0790[b] |
| Ti | .0111 | .0110 |
| Mn | .0017 | .0020 |
| Fe | .0919 | .0921[b] |
| O | | .4397[c] |
| Total | | 1.0058 |

## Table 4 (Continued)

### Composition of Standards (Chem. Analysis)

| Element | K409 | K412 | K371 | OR-1[h] | Apatite | Tephroite[f] |
|---------|------|------|------|---------|---------|--------------|
| Na | .0737 | – | – | .0085 | – | – |
| Mg | – | .1166 | – | – | – | – |
| Al | .0780 | .0491 | – | .0983 | – | – |
| Si | .2538 | .2120 | .2309 | .3010 | – | .1391 |
| K | – | – | – | .1239 | – | – |
| Ca | .0014 | .1090 | – | – | .391 | – |
| Ti | – | – | – | – | – | – |
| Mn | – | .0010 | – | – | – | .5441 |
| Fe | .1489 | .0774 | – | .0002 | – | – |
| Zn | – | – | .0307 | – | – | – |
| Ba | – | – | .4192 | .0073 | – | – |
| P | – | – | – | – | .1806 | – |

Table 4 (Continued)

## Standards Used

| Element | Set 1 | Set 2 |
|---------|-------|-------|
| Na | K409 | K409 |
| Mg | K412 | MgO |
| Al | K412 | $Al_2O_3$ |
| Si | K412 | $SiO_2$ |
| K | OR-1[h] | OR-1 |
| Ca | K412 | Apatite |
| Ti | $TiO_2$ | Pure |
| Mn | Tephroite[f] | Pure |
| Fe | K412 | Pure |
| Zn | Pure | Pure |
| Ba | K371 | K371 |

---

[a]Set 1 and Set 2 refer to the two sets of standards used for these analyses.

[b]Element corrected for overlap.

[c]Oxygen computed by stoichiometry.

[d]Oxygen computed by difference.

[e]ND is "not determined".

[f]Huebner, J. S., U.S.G.S., Reston, Va.

[g]Jarosewich, E., Smithsonian Institution, Washington, D.C.

[h]Synthetic glass, from Geophys. Lab, Washington, D.C.

The operating voltage is 15 kV. The electron beam incidence angle is 90° and the x-ray emergence angle is 52.5°.

Table 5.  Analyses of NBS Low Alloy Steel

Mass Fractions

| Element | Pure Fe | SRM 662 | | SRM 663 | |
|---|---|---|---|---|---|
| | | Chem. | FRAME C | Chem. | FRAME C |
| V | .00075 | .00041 | .00081 | .0031 | .0034 |
| Cr | .0009 | .0030 | .0039 | .0131 | .0144 |
| Mn | -.00175 | .0104 | .0093 | .0150 | .0134 |
| Fe | 1.000 | (.953) | .953 | (.944) | .942 |
| Co | .0010 | .0030 | .0100 | .00048 | .0069 |
| Ni | -.00089 | .0059 | .0054 | .0032 | .0024 |
| Cu | ND | .0050 | .0058 | .00098 | .0013 |

Brass Analysis

| | Chem. | FRAME C | FRAME[a] |
|---|---|---|---|
| Cu | .7675 | .777 | .769 |
| Zn | .2326 | .236 | .235 |

---

[a]Crystal Spectrometer data.

The operating voltage is 20 kV.  The electron beam incidence angle is 90°
and the x-ray emergence angle is 52.5°.

## IId.   Example

It is difficult to present an example of an analysis computed by FRAME C since the data are directly transferred from spectra stored in the multichannel analyzer into the program.  The contents of each region of interest needed for a particular spectrum are listed, together with each region's energy limits, instead of listing the contents of every channel in the spectrum.  ROI(0) and ROI(1) in each spectrum are the background regions set up by the operator.[5]  All other regions of interest are defined by the program for each element to be analyzed.

The example used in what follows is an analysis of an anorthoclase (Nunivak) mineral obtained from J.S. Huebner of the U.S.G.S.  Five different standards were used for the eight analyzed elements.  The oxygen content of the specimen was determined stoichiometrically from those of the eight other elements.

Standard 1:     glass K371                          Ba standard

| ROI | $E_{low}$ | $E_{high}$ | Counts |
|-----|-----------|------------|--------|
| 0   | 3.070     | 3.290      | 16462  |
| 1   | 7.139     | 7.679      | 13618  |
| 2   | 4.390     | 4.550      | 88572  |

---

[5]Each input typed by the operator is preceded by a question mark (?) typed by the computer.  The region of interest data that is read from each spectrum is listed before each computation.

```
     100 RUN
    ENTER NO. OF ELEMENTS
    ? 4
    ENTER EO
    ? 5
    ENTER CON, ATNO, LINE CODE AND VALUE FOR EACH
    ? ·4192? 56? 2? 2
    ? ·2309? 14? 0? 0
    ? ·0307? 30? 0? 0
    ? ·3192?  8? 0? 0
    MELS = ·335377
    ROI 0            3·07   3·29
    ROI 1            7·139  7·679
```

Standard 2:    Pure Fe                    Fe standard

| ROI | $E_{low}$ | $E_{high}$ | Counts |
|---|---|---|---|
| 0 | 3.070 | 3.290 | 19890 |
| 1 | 8.319 | 8.859 | 11529 |
| 2 | 6.320 | 6.489 | 305924 |

```
    *100 RUN
    ENTER NO. OF ELEMENTS
    ? 1

    ENTER CON, ATNO, LINE CODE AND VALUE FOR EACH
    ? 1? 26? 1? 2
    MELS = 1
    ROI 0            3·07   3·29
    ROI 1            8·319  8·859
```

Standard 3:    glass OR-1                 K standard

| ROI | $E_{low}$ | $E_{high}$ | Counts |
|---|---|---|---|
| 0 | 2.360 | 2.580 | 11212 |
| 1 | 5.710 | 6.250 | 9832 |
| 2 | 3.240 | 3.390 | 89255 |

```
*100RUN
ENTER NO. OF ELEMENTS
? 6

ENTER CON, ATNO, LINE CODE AND VALENCE FOR EACH
? ·1239? 19? 1? 1
? ·0085? 11? 0? 0
? ·0983? 13? 0? 0
? ·301?  14? 0? 0
? ·0073? 56? 0? 0
? ·4601?  8? 0? 0
MELS = ·110224
ROI 0           2·36    2·58
ROI 1           5·71    6·25
```

Standard 4:    glass K412              Mg, Si, Ca standard

| ROI | $E_{low}$ | $E_{high}$ | Counts |
|-----|-----------|------------|--------|
| 0 | 2.700 | 2.920 | 10912 |
| 1 | 7.649 | 8.189 | 5926 |
| 2 | 1.190 | 1.320 | 79419 |
| 3 | 1.670 | 1.800 | 194831 |
| 4 | 3.610 | 3.770 | .76100 |

```
*100RUN
ENTER NO. OF ELEMENTS
? 6

ENTER CON, ATNO, LINE CODE AND VALENCE FOR EACH
? ·1166? 12? 1? 2
? · 212? 14? 1? 4
? · 109? 20? 1? 2
? ·0491? 13? 0? 0
? ·0774? 26? 0? 0
? ·4349?  8? 0? 0
MELS = 8.32303E-2
MELS =  ·168803
MELS =  ·10142
ROI 0           2·7     2·92
ROI 1           7·649   8·189
```

Standard 5:    glass K409                  Na and Al standard

| ROI | $E_{low}$ | $E_{high}$ | Counts |
|-----|-----------|------------|--------|
| 0 | 2.820 | 3.040 | 10012 |
| 1 | 7.649 | 8.189 | 5926 |
| 2 | 0.981 | 1.100 | 23988 |
| 3 | 1.420 | 1.550 | 73492 |

46

```
*100RUN
ENTER NO. OF ELEMENTS
? 6

ENTER CON, ATNO, LINE CODE AND VALENCE FOR EACH
? •0737? 11? 1? 1
? • 078? 13? 1? 3
? •2538? 14? 0? 0
? •00136?20? 0? 0
? •1489? 26? 0? 0
? •4442?  8? 0? 0
MELS = 3•84375E-2
MELS = 5•74489E-2
ROI 0            2•82   3•04
ROI 1            7•649  8•189
```

Unknown:          Anorthoclase (Nunivak)

| ROI | $E_{low}$ | $E_{high}$ | Counts |
|---|---|---|---|
| 0 | 2.320 | 2.540 | 10275 |
| 1 | 8.269 | 8.809 | 4124 |
| 2 | 0.981 | 1.100 | 25843 |
| 3 | 1.190 | 1.320 | 9372 |
| 4 | 1.420 | 1.550 | 101766 |
| 5 | 1.670 | 1.800 | 286980 |
| 6 | 3.240 | 3.390 | 25055 |
| 7 | 3.610 | 3.770 | 11031 |
| 8 | 6.320 | 6.489 | 2910 |
| 9 | 4.390 | 4.550 | 4648 |

```
*500RUN
ENTER NO. OF ELEMENTS
? 9
ENTER AT• NO •FOR EACH ELEMENT
? 11? 12? 13? 14? 19? 20? 26? 56? 8
NO PLOT ENTER 0
? 1Z            C            F(X)        K
 11        6•20325E-2   •571227    3•97415E-2
 12        0•           •657226   -3•33924E-4
 13         •1          •76323     8•23842E-2
 14         •307338     •777802     •253665
 19        2•89234E-2   •915523    2•55711E-2
 20        7•01639E-3   •93084     6•40029E-3
 26        1•2845E-3    •986375    1•09671E-3
 56        1•64386E-3   •959155    1•18512E-3
  8         •469937
TOTAL =  •978176
ROI 0            2•82   3•04
ROI 1            7•649  8•189
```

47

The synthetic spectrum, drawn by the program, together with the original spectrum is shown in Figure 7. This comparison is an important part of the analysis and should not be neglected when analyzing an unknown material since minor elements could be missed entirely.

Versions of FRAME C are available in both BASIC and FORTRAN that do not contain the subroutine to synthesize the spectrum since they are not written for a computer-oriented multichannel analyzer. Users are warned that without this feature, elements could be overlooked. This does not mean that the program will always work either. For example, attempting to measure S $K\alpha$ and PbM$\alpha$ in the same specimen will not work since these peaks would occupy the same region of interest.

## III. References

[1]  Henoc, J., Heinrich, K.F.J., and Myklebust, R.L.,
     A Rigorous Correction Procedure for Quantitative
     Electron Probe Microanalysis (COR 2), NBS Tech.
     Note 769, August 1973.

[2]  Yakowitz, H., Myklebust, R.L., and Heinrich, K.F.J.,
     FRAME: An On-Line Correction Procedure for Quantita-
     tive Electron Probe Microanalysis, NBS Tech. Note 796,
     October 1973.

[3]  Heinrich, K.F.J., Myklebust, R.L., and Yakowitz, H.,
     A Simple Correction Procedure for Quantitative Electron
     Probe Microanalysis, NBS Tech Note 719, May 1972.

[4]  Russ, J.C., Scanning Electron Microscopy 1977, Vol. 1,
     IITRI, Chicago, Ill. 289-296 (1977).

[5]  Myklebust, R.L. and Heinrich, K.F.J., in Energy Dispersion
     X-ray Analysis: X-ray and Electron Probe Analysis, ASTM
     STP 485, 1971, pp. 232-242.

[6]  Reed, S.J.B. and Ware, N.G., X-ray Spectrometry, 2, 2,
     1973, pp. 69-74.

[7]  Smith, D.G.W., Gold, C.M., and Tomlinson, D.A., X-ray
     Spectrometry, 4, 3, 1975, pp. 149-156.

[8]  Ware, N.G. and Reed, S.J.B., J. Phys. E: Sci. Inst.,
     6, 1973, pp. 286-288.

[9]  Lifshin, E., Ciccarelli, M.F., and Bolon, R.B., X-ray
     Spectral Measurement and Interpretation, General Electric
     Tech. Information Series, Report No. 74CRD159, Sept. 1974.

[10] Heinrich, K.F.J., Yakowitz, H., Anal. Chem., 47, 14,
     1975, pp. 2408-2411.

[11] Fiori, C.E., Myklebust, R.L., Heinrich, K.F.J., and
     Yakowitz, H., Anal Chem. 48, 1, 1976, pp. 172-176.

[12] Gedcke, D.A., X-ray Spectrometry, 1, 1972, pp. 129-141.

[13] Fiori, C.E., Myklebust, R.L., and Heinrich, K.F.J.,
     Proc. 11th Annual Conf. of Microbeam Analysis Society,
     Miami Beach, Florida, Aug. 9-13, 1976, paper 12.

[14]  Fiori, C.E., Myklebust, R.L., Heinrich, K.F.J., and
      Yakowitz, H., Proc. 10th Annual Conf. of Microbeam Anal-
      ysis Society, Las Vegas, Nev., Aug. 11-15, 1975, paper 20.

[15]  Walter, V.J., in Energy Dispersion X-ray Analysis: X-ray
      and Electron Probe Analysis, ASTM STP 485, 1971, pp. 82-
      111.

[16]  Smith, D.G.W., Reed, S.J.B., and Ware, N.G., X-ray Spec-
      trometry 3, 149, 1974.

[17]  Philibert, J. and Tixier, R., in Quantitative Electron
      Probe Microanalysis, NBS Special Publ. 298, K.F.J.
      Heinrich, ed. 13-33 (1968).

[18]  Reed, S.J.B., and Ware, N.G., J. Phys. E: Sci. Inst. 5,
      1972, pp. 582-584.

[19]  Heinrich, K.F.J., The Electron Microprobe, McKinley,
      Heinrich and Wittry, editors, John Wiley, New York,
      296-377 (1966).

[20]  Heinrich, K.F.J., Fiori, C.E., and Myklebust, R.L., J.
      Appl. Phys. (to be published) (1979).

# Appendix 1

## ARTIFACTS OBSERVED IN ENERGY-DISPERSIVE X-RAY SPECTROMETRY IN THE SCANNING ELECTRON MICROSCOPY

C. E. Fiori and D. E. Newbury

Microanalysis Section, Bldg. 222
National Bureau of Standards
Washington D. C., 20234

## Abstract

X-ray spectra obtained with a lithium-drifted silicon detector attached to a scanning electron microscope often contain artifacts which limit the accuracy of qualitative and quantitative analysis. Three categories of artifacts are recognized: (1) artifacts which originate during the physical process of x-ray detection; (2) artifacts associated with the signal processing chain; and (3) artifacts which arise from the environment of the sample and detector. Artifacts in these categories include: (1) silicon x-ray escape peaks, peak broadening, and peak distortions; (2) dead-time effects, the formation of sum peaks, and anomalous background signals; and (3) detector microphony, excitation by stray radiation of regions which are remote from the beam impact point, and effects on x-ray intensities caused by contamination. Recognition of these artifacts is required for accurate qualitative analysis of unknowns, particularly of low intensity signals. A procedure is described for qualitative analysis based on the known properties of the family of x-ray lines for each element as well as the artifacts which can be observed. The implications of the presence of spectral artifacts on the accuracy of quantitative analysis is also discussed.

## Introduction

The addition of a silicon (lithium) energy dispersive x-ray spectrometer to a scanning electron microscope (SEM) provides a versatile and powerful instrument for the study of structure on the micrometer scale. Both the morphology and the chemical elements ($Z > 11$) present in micrometer-sized features of a specimen can be studied. For cursory work, a qualitative x-ray analysis for the principal constituents of a specimen can be obtained in a very short time, typically minutes. To extract the maximum amount of information available, specifically the composition of the region of interest, considerable effort must be expended and a careful, logical approach is required.

An accurate quantitative x-ray microanalysis is developed in four distinct but interrelated stages: (1) The proper choice must be made for instrument operating parameters, including beam energy and current; and spectrometer parameters, such as amplifier calibration and pulse processing time. (2) A systematic qualitative analysis is performed by identifying all peaks and recognizing spectral artifacts. (3) The x-ray intensities for the peaks of interest are extracted from the spectra of the unknown and standards after the continuum radiation is subtracted. (4) The x-ray intensities are converted into compositional values through the application of mathematical algorithms which correct for various matrix effects, such as electron deceleration, electron backscatter, x-ray absorption in the target, and production of x-rays by secondary excitation[1,2,3]. The mathematical algorithms are dependent on the particular specimen shape and have only been comprehensively developed and rigorously tested for one type of specimen: a flat, bulk target which is set normal to the electron beam. A number of

successful computer programs are available which have been developed from these algorithms[4,5,6]. In addition, a purely empirical approach based on correction factors determined from standards similar in composition to the unknown is available[7].

When energy dispersive x-ray spectrometry (EDS) is employed for x-ray microanalysis, special considerations relative to points (1), (2), and (3) come into play. Certain operating conditions must be fulfilled if a satisfactory EDS spectrum is to be obtained. However, even a spectrum obtained under optimum conditions may contain numerous artifacts which can affect the accuracy of both the qualitative and quantitative analysis. We shall describe the most significant artifacts which appear in the EDS spectrum under typical analytical conditions for x-ray microanalysis with a scanning electron microscope or electron probe microanalyzer (EPMA). A strategy for qualitative analysis which is based upon the physics of x-ray generation and the detection process will be presented. The steps required to extract x-ray intensities for quantitative analysis will be described.

The natural x-ray spectrum generated by the incident electron beam in the sample consists of (1) characteristic x-rays produced during electron transitions following ionization of an inner electron shell of an atom by the beam electron and (2) bremsstrahlung ("braking radiation") or continuum x-rays formed during deceleration of the beam electron in the coulombic field of the atoms[1,2,3]. The continuum forms a background extending from zero to the incident beam energy. The x-ray continuum, while limiting the sensitivity of the measurement of the characteristic intensity, is not an artifact, since it is a product of the electron beam-specimen interaction and does, in fact, convey information on the average atomic number of the specimen. Artifacts are the discrepancies introduced into the spectrum by the measurement process. The artifacts observed in EDS spectra can be broadly classified into three categories: (1) those which arise through the nature of the x-ray detection process; (2) those associated with signal manipulation following the detector; and (3) those arising from certain aspects of the detector — specimen chamber environment. Artifacts in category (1) include silicon x-ray escape peaks, peak broadening, and peak distortions due to incomplete charge collection. Such artifacts cannot, in general, be eliminated from the spectrum through any action on the part of the analyst. Artifacts in category (2)

include coincidence losses, sum peaks in the spectrum due to pulse pile-up, and the distortion of the background due to pulse pile-up and the background shelf. Artifacts in category (3) include detector microphony, excitation of the specimen or parts of the instrument by stray radiation (x-rays or electrons), entrance of energetic electrons into the detector, and effects on measured x-ray intensities caused by the build-up of contamination on the specimen.

Artifacts of the Detection Process

The Si(Li) x-ray detector[8,9,10,11] operates on the following principle (Figure 1). The lithium-doped silicon has the interesting electrical property that both negative charges (free electrons in the conduction band) and positive charges (holes in the valence band) can move easily through the solid when a bias is applied. An energetic photon or particle which enters the detector causes the formation of such charge carriers. The incident x-ray photon is first absorbed by a silicon atom and an energetic electron is emitted (the photoelectric process). This photoelectron then creates charge carriers as it travels in the detector silicon and scatters inelastically. The silicon atom is left in an energetic condition, retaining the energy required to eject the photoelectron. This energy is subsequently released in the form of either an Auger electron or a silicon x-ray. The Auger electron scatters inelastically and creates charge carriers. The silicon x-ray can be re-absorbed which initiates the process again, or it can be scattered inelastically. Thus, a sequence of events takes place leading to the deposition of all of the energy of the original photon in the detector, unless radiation generated during the sequence, such as a silicon Kα photon, escapes the detector. The detector is also sensitive to energetic electrons which enter; such electrons can directly form charge carriers.

A bias applied to the detector serves to collect the charges on the two surface electrodes. The ideal number of charges created per incident particle with energy E (ev) is given by

$$n = E/K \qquad (1)$$

where $K = 3.8$ eV for silicon. For example, if the detector captures one photon having an energy of 5 keV, then from equation (1) the total number of electrons swept from the detector is approximately 1300 which represents a charge of $2 \times 10^{-16}$ coulombs. This is an extraordinarily small charge. The
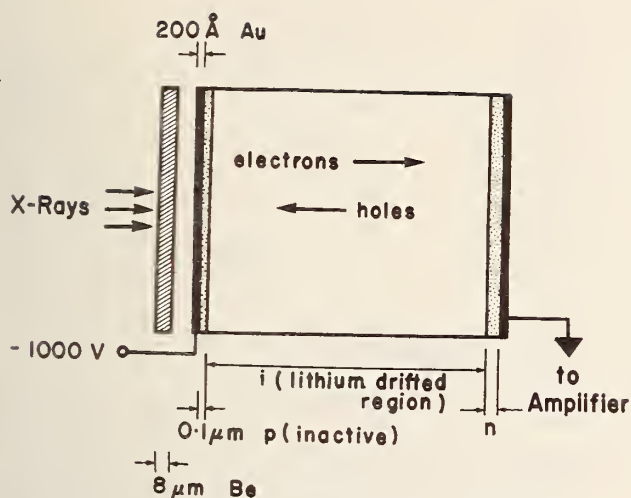
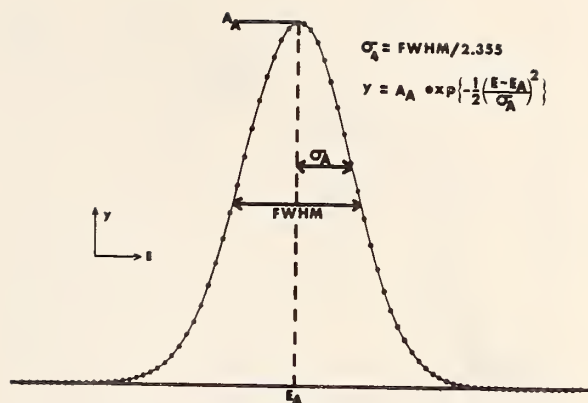Fig (1)  Schematic diagram of a typical lithium-drifted silicon detector.



Fig (2)  Theoretical Gaussian distribution which describes an EDS peak. σ is the standard deviation of the distribution, $A_A$ is the peak amplitude, and y is the amplitude at any energy

subsequent circuitry must be capable of amplifying this signal by about $10^{10}$.

Deviations from the ideal detector process result in the appearance of artifacts, principally peak broadening, peak distortion, silicon x-ray escape peaks, and silicon and gold absorption edges.

## Peak broadening

The natural width of an x-ray peak is of the order of one electron volt, measured at half the maximum of the peak intensity (the measured quantity is designated "full width, half maximum" (FWHM)).  For example for manganese Kα radiation (5.898 keV), the FWHM is approximately 2.3 eV, which makes the natural width about 0.039 percent of the peak energy.  The measured peak width from the Si(Li) spectrometer is degraded to a typical value of 150 eV for MnKα, or 2.5% of the peak energy.  This degradation in width of the peak occurs because:  (1) there is a distribution in the final number of charge carriers created by capturing photons of a single energy due to the discrete nature of the counting process and (2) an uncertainty is introduced by the thermal noise of the amplification process.  The distribution of numbers of charge carriers for a single photon energy is reasonably well described by a Gaussian distribution, shown schematically in Figure 2. The FWHM of this distribution can be calculated from the two sources of noise by quadrature addition, according to the equation

$$FWHM \propto \sqrt{C^2E+N^2} \qquad (2)$$

where C is the measure of the uncertainty in the formation of charge carriers

from a photon of energy E and N is the electronic noise of the amplification process. The immediate consequence of the peak broadening is a reduction in the height of the peak (counts per energy interval) as compared to the natural peak and an accompanying decrease in the peak-to-background ratio.

For practical work, the value of the FWHM as a function of the peak energy is conveniently described by the expression:

$$FWHM_1^2 = 2.5(E_1-E_2)+FWHM_2^2 \qquad (3)$$

where $FWHM_2$ is the known full width half maximum (eV) of a peak of energy $E_2$ (eV), and $FWHM_1$ and $E_1$ refer to those parameters for any other peak.  Thus, if the FWHM is known for MnKα, the FWHM appropriate to any other peak can be calculated.

The value of the FWHM is useful in estimating the extent of the overlap of peaks which have similar energies.  An estimate of the extent of overlap is vital when considering peak interferences in qualitative analysis, where the identification of a low intensity peak near a high intensity peak may be difficult, and in quantitative analysis, where the removal of the interference is necessary for accurate determination of the composition.  An example of the overlap of peaks is illustrated in the spectrum of KCl in Figure 3.  With a detector of 170 eV resolution (MnKα), the potassium Kα and Kβ peaks are nearly resolved, while the chlorine Kα and Kβ peaks are not.
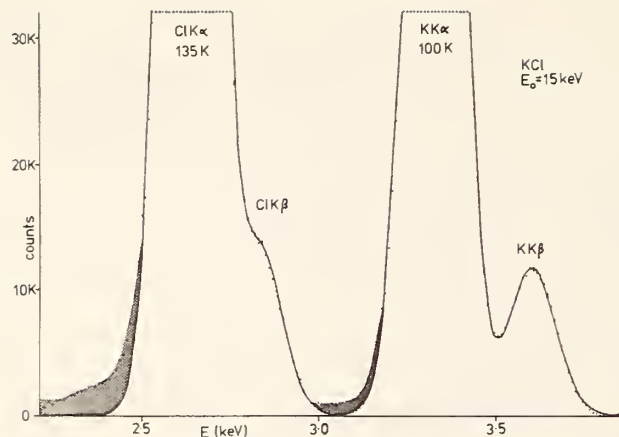
Fig (3) EDS spectrum of KCl illustrating peak overlap: Cl Kα,Kβ are not resolved while K Kα,Kβ are nearly resolved. The solid line is a Gaussian fit to the data points. The shaded area represents the deviation caused by incomplete charge collection.

## Peak distortion

Two different artifacts cause distortion, i.e., deviation from a Gaussian shape on the low energy side of a peak: (1) The collection of charge carriers created in certain regions of the detector near the faces and sides is imperfect due to trapping and recombination of the electron-hole pairs, leading to a reduction in the value of n predicted by equation (1) for the incident photon. The resulting distortion of the low energy side of the peak is known as "incomplete charge collection"[12,13] and its effect is illustrated in Figure 3 for chlorine Kα and potassium Kα peaks. The deviation from a Gaussian distribution (shown as a solid line) is a function of energy. For example, the magnitude of the effect is significantly different for chlorine and potassium, which are separated by an atomic number difference of only two. (2) The background shelf, Figure 4, is a phenomenon in which the presence of a peak increases the background at all energies below the peak value. Additional counts above the expected background result both from the incomplete charge collection phenomenon extending to low energy and from the escape from the detector of some of the continuum x-rays generated by the photoelectron as it scatters inelastically in the silicon. Any radiation lost from the detector reduces the number of charge carriers created. Both the incomplete charge collection and the loss of continuum x-radiation lead to a transfer of counts from the peak to the entire
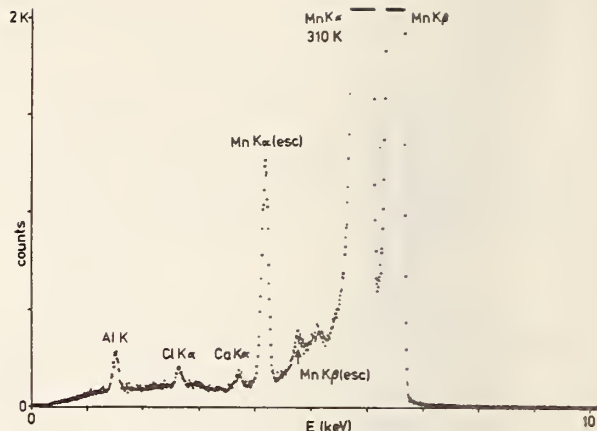


Fig (4) EDS spectrum derived from Fe radioactive source. The background shelf is easily observable at energies below Mn Kα down to the threshold at 300 eV. The Mn Kα and Kβ silicon escape peaks are noted. Extraneous characteristic peaks from the source holder are observed.

energy region down to zero. Typically, the background shelf at one-half the energy of a peak has a relative intensity of about 0.1 percent of the parent peak. The total number of counts lost to the full peak due to this effect is approximately 1 percent.

## Silicon x-ray escape peaks

The generation of a photoelectron leaves the silicon atom in an ionized state. If the photoelectron is emitted from the K-shell, the atom can subsequently undergo an electron transition to fill this K-shell vacancy, with subsequent emission of a silicon K x-ray or an Auger electron. The range of the Auger electron is only a fraction of a micrometer, and hence, it is highly probable that this electron will be re-absorbed in the detector and contribute its energy to the formation of charge carriers, yielding the correct value of energy deposited in the detector. The SiK x-ray, on the other hand, has a finite probability of escaping the detector (10 percent of the SiK initial intensity will remain after 30 μm of travel through silicon). When such an x-ray escape occurs from the detector, it robs the cascade being measured by the energy carried off in the x-ray, 1.740 keV for SiKα and 1.832 keV for SiKβ. Thus, an artifact peak, the "escape peak"[14] is formed at an energy equal to the energy of the parent line minus the energy of the silicon x-ray. In principle, both SiKα and SiKβ escape peaks are formed, but the probability for Kβ formation is about 2 percent of
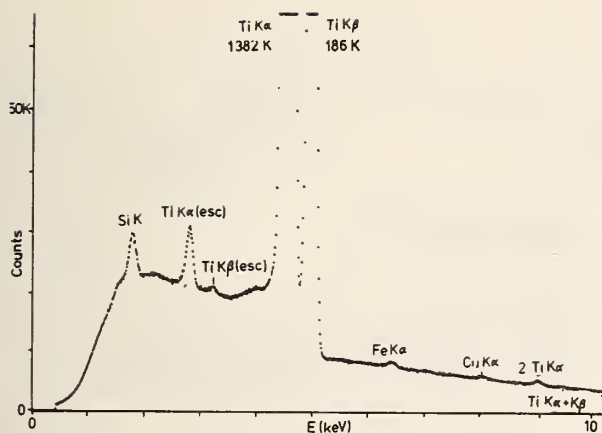
Fig (5)  Electron-excited EDS spectrum of titanium.  The Ti Kα and Kβ silicon x-ray escape peaks and the 2Kα and (Kα+Kβ) sum peaks are noted.  Extraneous peaks from the specimen chamber are also observed.



Fig (6)  Electron-excited EDS spectrum from carbon.  The silicon and gold absorption edges are illustrated.  Solid line represents a theoretical fit to the continuum.

the Kα, hence only one escape peak is observed per parent peak.  Escape peaks are illustrated in Figure 5, where the parent peaks are TiKα (4.51 keV) and TiKβ (4.93 keV) and escape peaks are found at 2.77 keV (TiKα-SiKα) and 3.19 keV (TiKβ-SiKα).  The magnitude of the escape peak relative to the parent peak varies from about 1 percent for phosphorus to 0.01 percent for zinc K x-rays.  Silicon x-ray escape peaks cannot occur for radiation below the absorption energy of the silicon K shell (1.838 keV).

## Absorption edges

The typical Si(Li) spectrometer has a protective window of beryllium (approximately 7.6 μm thick), a front surface electrode of gold (approximately 20 nm thick), and an inactive layer of silicon (20-200 nm thick).  X-rays must pass through each of these layers to reach the active silicon and be detected.  During passage of x-rays through the layers, absorption occurs.  Absorption in the beryllium window eliminates nearly all x-rays below about 600 eV.  Above 2 keV, virtually all x-rays are transmitted through the window.  Between these limits, the absorption increases with decreasing energy such that at 1.5 keV about 70 percent of the x-rays are transmitted while for an energy of 1 keV the transmission is 45 percent.  Absorption by the gold and silicon layers is much less significant due to the small mass thickness of these layers.  However, a noticeable change in the x-ray continuum is observed at the absorption edge of silicon and to a lesser degree

at gold, Figure 6.  Just above the energy of the absorption edge, the mass absorption coefficient increases abruptly, resulting in a decrease in the measured continuum x-radiation.  The height of the resulting step is an indication of the thickness of the layer.  Note that the action of the broadening effect of the detection process causes the absorption edge, which in reality is a sharp change of absorption over a range of about 1 eV, to be smeared over a much broader range, typically 100 eV for the silicon absorption edge.

The absorption of x-rays by the silicon dead layer causes fluorescence of Si K x-radiation. This results in the appearance in the spectrum of a small silicon peak, the so-called silicon internal fluorescence peak[14]. For most analysis situations, this fluorescence peak corresponds to an apparent concentration of 0.2 wt. percent or less silicon in the specimen.

## The Signal Processing Chain

The signal processing chain which follows the Si(Li) x-ray detector is illustrated in Figure 7.  Due to the wide variety of pulse processing systems available it is necessary here to describe a generalized system.  Figure 7, however, contains the essential features. In this circuitry, the small charge developed on the electrodes of the detector when a single photon is captured is converted into a voltage pulse of fixed shape and duration which is suitable for presentation to a multi-channel analyzer (MCA)[15]. The nature of the signals at various points in the

Fig (7) Schematic diagram of the signal processing chain of a generalized EDS system.

processing chain is shown in Figure 8. The signal produced by the detector at (1) has the form of a pulse with a rise time of less than 100 ns and a longer exponential tail. The passage of a second puls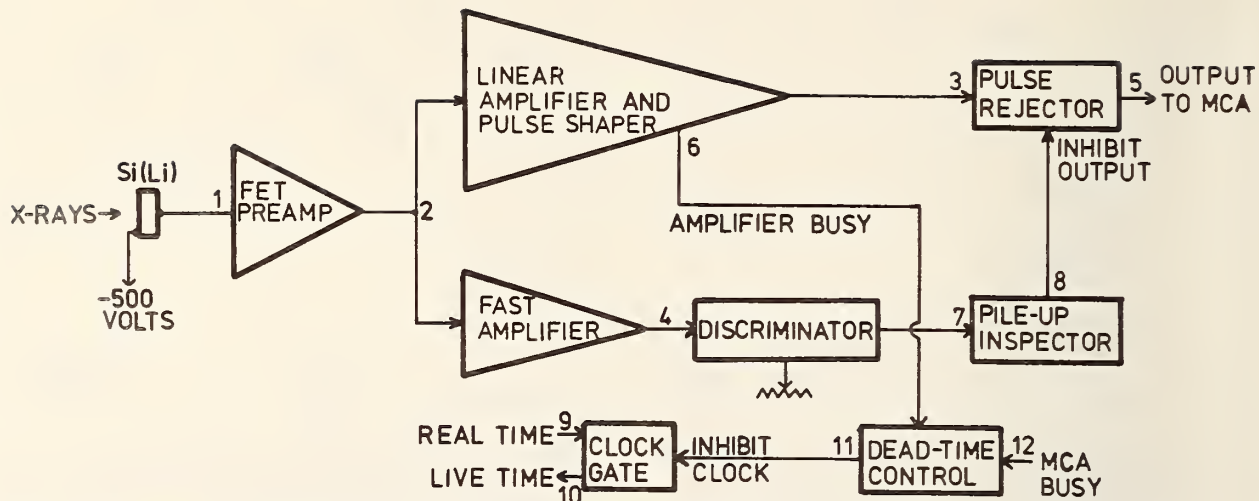e through the system is shown in dashed lines. The field effect transistor (FET) preamplifier has the function of amplifying the small detector signal with minimum degradation, to produce a step function (2), which, for clarity, is shown without noise. At this point, the signal is split into a slow and a fast channel[16]. The purpose of the slow channel is to amplify the pulse with the maximum possible signal-to-noise ratio which is necessary to yield a high resolution spectrum. Long time constants are required in these circuits, hence the designation "slow." The fast channel operates with a much poorer signal-to-noise ratio but serves as a monitor on the slow channel to eliminate pulses which would arrive too close to one another to be recognized as discrete by the slow channel.

In the slow channel, by a combination of differentiation and integration circuits in the linear amplifier, the pulse is shaped and the width is set in the range 5-80 μs (3). The choice of the width strongly affects the achievable resolution of the system. The time constants of the resistive-capacitive networks used in the integrators and differentiators of the pulse shaping circuit are commonly grouped into the parameter labelled "shaping time" on the amplifier. The magnitude of the shaping time is typically chosen in the range 2-20 μs. It must be noted, however, that the shaping time is not the deadtime. The deadtime of the amplifier is that period of time during which the voltage in the slow channel is raised above a

threshold value by the passage of a single pulse and during which time the slow channel is unavailable for subsequent pulses. The deadtime can be as much as ten times the value of the shaping time.

The discriminator on the fast amplifier channel sets a threshold level, adjustable by the analyst, which separates real pulses from the spectrum of noise which is passed and amplified by the fast amplifier. Note that a high energy pulse, such as that which results from a photon of CuKα, is well above this noise, while a low energy pulse, such as that from MgKα, is virtually at the same level as the noise and is therefore difficult to distinguish. The output of the discriminator is a normalized rectangular pulse of approximately the same duration as the fast amplifier pulse. The pile-up inspector examines the separation of the discriminator pulses to determine if one or both pulses in the slow channel must be rejected at the pulse rejector. If the first pulse in the slow channel has passed its peak before the second pulse arrives, it is necessary to reject only the second slow channel pulse. If the second pulse arrives before the first has reached its peak, then both pulses are rejected. The output pulses from the pile-up rejector are passed to the multichannel analyzer for sorting.

Deadtime correction functions will be treated subsequently.

## Artifacts of Signal Processing

Pulse pile-up. Artifacts associated with the processing of the signal originate primarily from pulse coincidence effects, that is, the nearly simultaneous arrival of x-ray photons in the
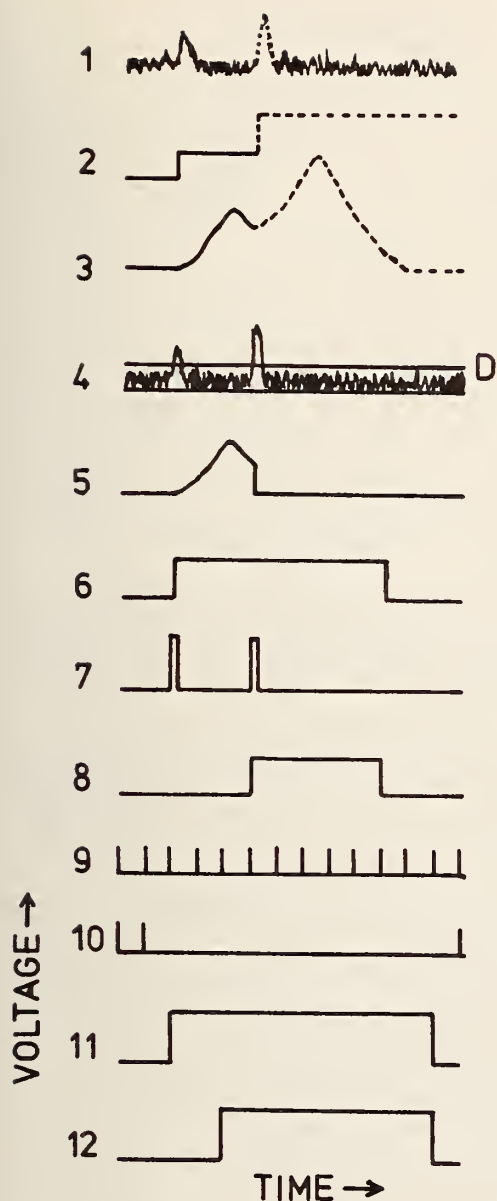
56

Fig (8) Schematic illustration of signals found at various points in Figure 7.

detector. If a second photon of energy $E_2$ enters the detector during that period of time in which the system is engaged in processing the pulse developed from the first photon of energy $E_1$, then a combined pulse is developed which has a value equal to $E_1+fE_2$, where f has a range $0 \le f \le 1$. The factor f can take on a continuous range of values since the arriving cascades generated by the photons can overlap in any proportion. The coincidence effect is illustrated schematically in Figure 8. Pulse coincidence or "pulse pile-up"[17] has the effect of reducing the total count in

the peaks $E_1$ and $E_2$ (consider $E_1 < E_2$), while creating artifact summation peaks at $2E_1$, $2E_2$ and $E_1 + E_2$ as well as a continuum of intermediate values between $E_1$ and $2E_2$. The summation peaks are readily apparent in the example of Figure 9(a) and the distortion of the background by the full range of intermediate summation values is also illustrated. The magnitude of the pulse pile-up effect is dependent on the rate of arrival of x-ray pulses at the detector and the value of the system time constant. The higher the counting rate and the longer the time constant, the more likely the coincidence of pulses becomes. Thus, the relative magnitude of the summation peaks is not a constant as in the case of escape peaks, but depends on amplifier parameters. At an input count rate of 10,000 c/s under a peak and a system time constant of 8 μs, the double energy peak is typically 0.25 percent of the parent peak.

The action of a pulse pile-up rejector circuit, which is an integral part of a modern system, is illustrated in Figure 9(b), where a significant reduction in summation peak height as well as the intermediate background with respect to Fig. 9(a) is obtained. The summation peaks are not totally suppressed by the pile-up rejector because the time resolution of the rejector has a limiting value. Pulses which arrive closer in time than the pulse pair resolution of the fast channel will be passed and treated as one pulse. Moreover, the pulse pile-up rejectors can have operational defects and are often ineffectual for low energy peaks for which the pulse in the fast channel is close to the noise. This failure is also illustrated in Figures 9(a) and (b) where adequate pulse pile-up rejection is achieved for silicon, but the rejector circuit fails for magnesium.

A second technique of coincidence control is that of Goulding[18]. In this approach, when the pulse monitoring circuitry detects a photon in the processing system, the SEM electron beam is blanked off and prevented from reaching the specimen for the duration of the pulse processing period, thus preventing the formation of additional photons which might cause coincidence. The Goulding technique has the considerable advantage that far fewer pulses are discarded, thus increasing the amount of information which can be obtained in a given time.

Deadtime Correction. The Si(Li) system detects photons sequentially; it is not possible to process more than one photon at a time. The period of time which the system requires to process a
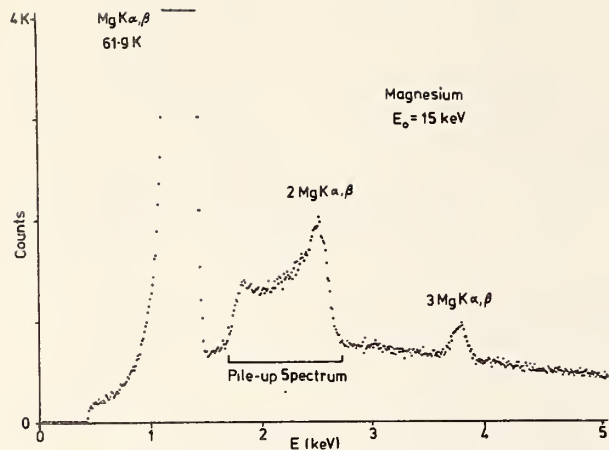
57

Fig (9) (a) Electron-excited EDS spectrum of magnesium.



Fig (9) (b) Electron-excited EDS spectrum of silicon.

pulse and during which it is unavailable for detecting subsequent photons is known as the deadtime[19]. In order to compensate for the loss of photons which arrive during the periods in which the system is occupied, the internal clock of the multichannel analyzer (9 in Figure 8) is gated "off" during the processing of a pulse by a signal derived from the slow channel. The deadtime varies with the energy of the pulse, and the counting time is auto-matically compensated for this effect by control of the clock pulses. If the system counting period is pre-set to give a value of T (seconds), the compen-sation for deadtime is carried out by the internal circuitry by effectively extending the counting period to $T + n\tau^*$, where $\tau^*$ (seconds) is the variable deadtime appropriate to each pulse of any energy and n is the number of counts in the whole spectrum. The system deadtime $\tau$ is, in general, a function of both the amplifier deadtime and the time which the multichannel analyzer requires to sort the pulse. In Figure 8, the clock pulses (9) are gated off when the detec-tor pulse first crosses a threshold value A. Although the pulse to the MCA is terminated after a time $t_B$, the clock remains off while the MCA sorts the pulse, which results in an extended interruption (10) in the clock. A modern MCA, operating with an amplifier set to optimize resolution, will com-plete its sorting function before the amplifier is ready to accept another pulse, and thus the system deadtime is only that of the amplifier. The system deadtime varies with the choice of ampli-fier parameters in the range 5 - 80 µs. The best resolution is obtained for the longest shaping time constant, and conse-quently, the longest deadtime. Values ob-tained from measurements on a typical sys-tem are as follows, where the resolution is measured as the FWHM at Mn Kα at a count rate of 1000 cps:

| Shaping time | Pulse width | Resolution |
|---|---|---|
| 8 µs | 75 µs | 144 eV |
| 6 µs | 47 µs | 147 eV |
| 4 µs | 30 µs | 152 eV |
| 2 µs | 17 µs | 169 eV |

The deadtime correction method which is discussed here is only one of the meth-ods currently in use, but it seems to be very popular. Other methods are available but are beyond the scope of the present discussion. The circuitry of the dead-time correction section of the signal pro-cessing system is capable of making a sufficiently accurate correction to satis-fy most practical analysis situations. The analyst must not, however, presume that he can use any arbitrary high count rate with the assumption that the deadtime correction will automatically accommodate that rate. Indeed, at high count rates, peak pile-up loss becomes significant. Every pulse in a double energy peak repre-sents the loss of two pulses from the par-ent peak. In the generalized schematic diagram of Figure 7, pulses lost from a peak due to pile-up are not correctly ac-counted by the deadtime circuit. However, by using a count rate where the sum peaks are not in evidence in the spectrum, this effect is reduced to an acceptable level.

For those applications where the out-put count rate of the amplifier is used directly, such as intensity modulation of a cathode ray tube for x-ray area mapping and x-ray line profiling which are appli-cations where a high count rate is espe-cially useful, the analyst should be aware of the following insidious artifact.
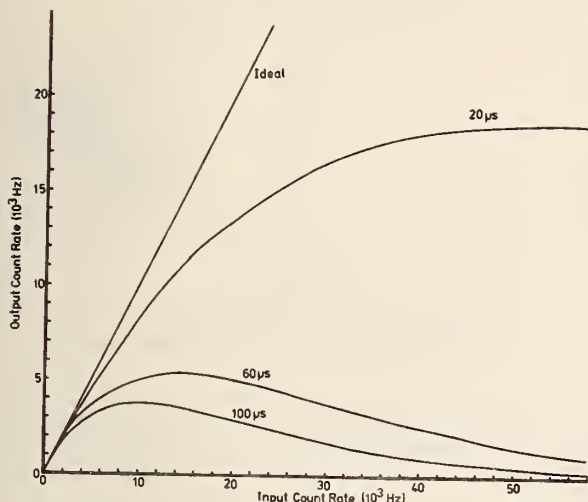
Fig (10) Relationship of output and input count rates for the generalized system of Figure 7 for three different values of the pulse width.

In Figure 10, the output count rate measured at point (5) in the system schematic, Figure 7, is plotted as a function of input count rate at point (7). The output count rate increases with increasing input count rate only up to a certain point. The arrival of pulses eventually becomes so frequent that the rejection process begins to dominate, and a point of diminishing returns is reached. Further increases in the input count rate actually lead to a decrease in output count rate. Operation in this high count rate region can lead to errors in analysis. Due to the shape of the roll-off, the same output count rate is observed for two widely different input count rates, which could correspond to two different specimen compositions.. Note that the input count rate refers to the entire spectrum from the beam energy down to the pre-set threshold (typically several hundred eV) and not to the count rate of a particular peak or range of energy being viewed in the MCA. Thus, if a 30 keV beam is used while the MCA monitors the x-ray range 0-10 keV, x-rays generated in the range 10-30 keV must still be considered as part of the total spectrum count rate. For a typical system where resolution is emphasized, the input count rate should not exceed about 5000 cps. Through the shaping time parameter, it is possible to achieve a higher limiting count rate at the price of system resolution. Curves in Figure 10 show the count rate response as a function of pulse width. This figure shows general trends; the exact curve varies with each system.

## Artifacts of the Detector/Microscope System

### Microphony

The Si(Li) spectrometer contains a detector and electronic circuitry of extraordinary sensitivity which can respond to radiation of energies other than x-rays. In particular, stray electromagnetic and acoustic radiation can affect the recorded x-ray spectrum. The coaxial cable through which the detector/pre-amplifier communicates with the main amplifier must be carefully routed to prevent it from becoming an antenna. The detector must be shielded against mechanical and acoustic vibration to which the detector acts as a sensitive microphone. The analyst can move a poorly routed cable to eliminate electro-magnetic interference but is generally powerless to do anything about the mechanical isolation of the detector. Thus, it is important when evaluating a new detector prior to acceptance to check for microphonic and antenna effects. In Figure 11(a), a spectrum obtained under non-microphonic conditions contains characteristic peaks and a continuum spectrum with a typical shape showing cutoff at low energies due to absorption in the beryllium window. In Figure 11(b), the same spectrum was recorded with several sources of mechanical and acoustic vibrations in the vicinity of the detector — the operation of a wavelength dispersive spectrometer motor, conversation, etc. The detector responded to these sources, producing an extremely high background in the region from 2 keV down to 0 keV. The characteristic peaks are broadened due to the noise in 11(b) as compared to Figure 11 (a). While virtually every detector has some microphonic response to high intensity noise, the detector should be isolated well enough to be insensitive to normal laboratory environment noise and vibration. The response in Figure 11(b) is quite unacceptable.

The main amplifier should also be carefully positioned. In general, it should be kept isolated from transformers and devices containing extensive logic circuits such as computers or scalers.

### Sensitivity to Stray Radiation

Origin. One of the features of the Si(Li) detector which is normally considered a great advantage is the rela-
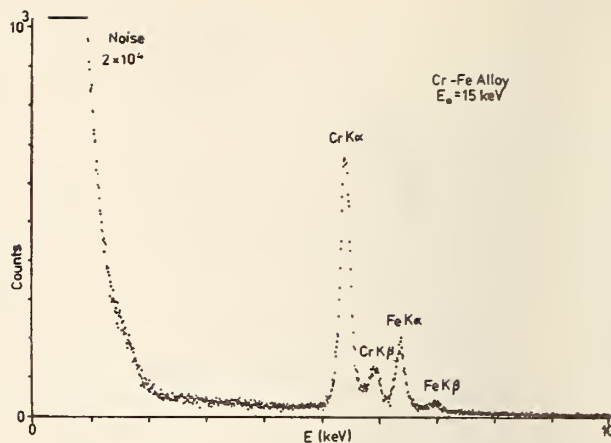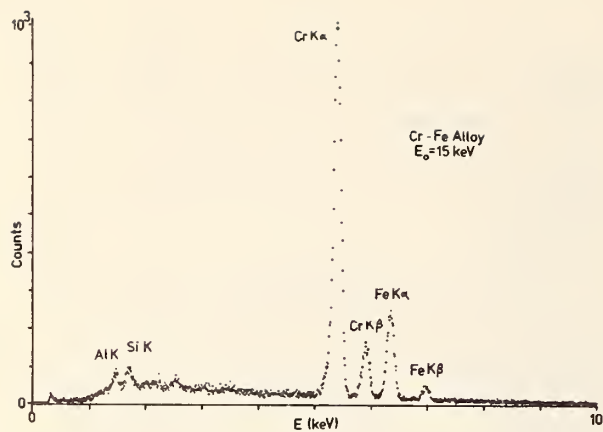
59

Fig (11) (a) Electron-excited spectrum of chromium-iron alloy. (b) Spectrum obtained under same beam conditions as (a) but with acoustic interference.

tively large solid angle of collection as compared to the focusing wavelength-dispersive spectrometer. The solid angle of collection is usually considered from the point of view of the electron-excited source in the specimen, with the apex of the cone placed at the beam impact point, Figure 12. To appreciate the complete collection situation, however, we must also consider the solid angle of collection from the point of view of the detector, Figure 12. It is obvious from Figure 12 that the true solid angle of collection is very large indeed, including not only the entire specimen but often a large portion of the sample stage and chamber walls. The difference in the collection angle between the points of view represented in Figure 12 would be immaterial if the excitation were really confined to the volume directly excited by the focused electron beam. Unfortunately, excitation can occur at a considerable distance from the region of impact of the focused beam. A schematic diagram of some typical sources of this remote excitation is shown in Figure 13. Electron-induced remote sources include scattering from apertures, backscattering from the specimen, and re-scattering from the polepiece. In this regard it should be noted that a significant fraction of the backscattered electrons from heavy elements retain 50% or more of the incident energy and are thus capable of exciting x-rays from the specimen environment (walls, stage, polepiece). Interaction with several surfaces is possible before an electron comes to rest. X-ray induced remote sources

originate principally from characteristic and continuum x-rays generated by those electrons which strike the upper surface of the final beam-defining aperture. These x-rays can propagate through the aperture and illuminate a large portion of the sample chamber as an x-ray fluorescence source. The significance of this source of remote excitation depends on (a) the material of the aperture, (b) its thickness, and (c) the beam energy. Thin film "self-cleaning" apertures of molybdenum produce a strong source of remote excitation, since self-absorption of the $MoK\alpha$ (critical excitation energy, 20 keV) radiation is low and the thin film (12.5 μm) transmits about 78 percent of the radiation. Considering that this final aperture may intercept 80 percent of the total beam, it is obvious that the x-ray fluorescence effect can be extremely deleterious to accurate analysis[20].

Recognition. It is not always obvious that a remote source exists, but its effects can usually be recognized by employing the following procedure. A Faraday cup is fabricated from a block of metal (iron, brass, titanium, etc.) e.g., by drilling a blind hole of 3 mm diameter and a few mm in depth and press fitting a microscope aperture (20 μm to 100 μm diameter) into this hole, Figure 14. The aperture material should be different from that of the block. Spectra are then recorded with the focussed beam alternately in the hole, on the aperture material, and on the block. If no remote sources exist, then with the beam falling into the aperture no spectrum should be obtained. If this so-called "in-hole" spectrum contains x-ray signals of the Faraday cup materials, then the ratios of the intensities
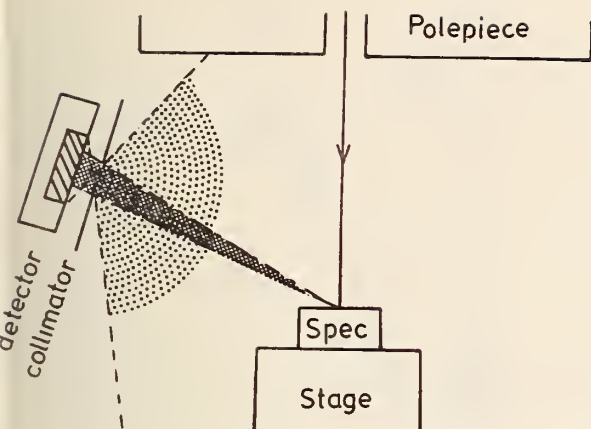
Fig (12) Solid angle of collection from the point of view of the specimen (dense hatching) and from point of view of EDS detector (light hatching).



Fig (13) Possible sources of remote x-ray excitation in an electron beam/EDS system. Solid lines - electron paths; dashed lines - x-ray paths.

of the characteristic lines to the values obtained from the spectra of the aperture and block are an indication of the magnitude of the problem. For example, a strong signal for the aperture material in the in-hole spectrum indicate a source of radiation in the vicinity of about 1 mm of the beam, while a high signal for the block material indicates a more distant source. The extraneous radiation has been observed to be as high as 20 percent and is typically between 0.01 and 1 percent[20] of that obtained with the beam directly on the aperture. Examination of the peak-to-background ratio of characteristic peaks observed in the in-hole spectrum can also indicate the type of remote excitation — electron or x-ray. Excitation by x-rays produces a much lower continuum. If the peak-to-background ratio is higher in the in-hole spectrum than in the directly excited spectrum of the aperture or block containing the element, the remote excitation is most likely by x-rays.

Observation of characteristic lines of the chamber wall or stage materials indicates excitation at great distances from the beam impact on the specimen. In this respect, it should be noted that a flat non-tilted specimen and a specimen of rough surface may behave differently. A rough specimen is more likely to scatter electrons in all directions to the surroundings, whereas the backscattered electrons from a flat, specimen normal to the beam follow a cosine distribution peaked about the normal, with little scattering in the horizontal plane.

## Correction of Stray-Radiation Problems

Eliminating stray radiation following its recognition is very much dependent on the particular instrumental configuration. General guidelines only can be given here.

X-ray fluorescence problems originating in the final aperture can be minimized by: (1) use of thick apertures and (2) choosing aperture materials of higher atomic number, such as platinum or tantalum. Typical beam energies (30 keV or lower) are insufficient to generate K x-rays, and the L lines of both materials have energies of less than 10 keV. For apertures of 12.5 μm thickness, the transmission of Lα x-rays of the aperture material is less than 3 percent for Pt and 4 percent for Ta. Transmission of 20 keV continuum is 6 percent for Pt and 15 percent for Ta.

Electron scattering problems are more difficult to deal with. Apertures should be kept clean, as debris particles on the circumference can produce unwanted scattering. Electrons often scatter in the column and pass around apertures if passages exist. Aperture alignment should be optimized. Double apertures can be employed with some success, although their alignment is difficult.

Scattering from the specimen is difficult to control, especially if the sample is rough, such as a fracture surface. Adjacent stage, polepiece, and chamber wall surfaces can be coated with carbon-dag or beryllium sheets to prevent generation of characteristic x-rays
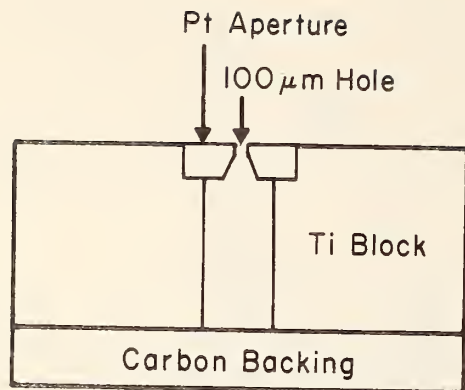
Fig (14)  Schematic illustration of cross-section through a Faraday cup suitable for detecting remote sources of radiation.



Fig (15)  Range of electrons in beryllium predicted by the equation of Heinrich (21)

$$z = \frac{7 \times 10^{-3}}{\rho} (E_O^{1 \cdot 65} - E_C^{1 \cdot 65})$$

$\rho (g/cm^3), E(keV), z(\mu m)$

in the energy region of interest by the scattered electrons.  After all obvious sources of remote excitation have been minimized, a remnant "in-hole" spectrum may still exist.  This "in-hole" spectrum can be subtracted from that of an unknown, but the procedure is risky, since the background spectrum may depend on scattering from the specimen, and the surroundings of the specimen and the standard.

<u>Direct entrance of electrons into the detector</u>.  The Si(Li) detector is capable of responding to an energetic electron which enters the active region of the detector.  A pulse is developed the height of which is a measure of the energy of the electron.  When the beam electrons strike the sample, a significant fraction, about 30 percent for copper with a beam normally incident, are backscattered with a wide energy range.  Many of these backscattered electrons retain a substantial fraction of the incident energy.  It is inevitable that some of those electrons will be scattered in the direction of the detector.  The beryllium window with a typical thickness of 7.6 μm (0.3 mil) is capable of stopping electrons with an energy below about 25 keV.  The range of electrons incident upon a 7.6 μm beryllium film as a function of energy according to the range equation of Heinrich[21] is shown in Figure 15.  Above energies of 25 keV, electrons will begin to penetrate the window and activate the detector, although with a loss of energy due to inelastic scattering in t  beryllium. When higher energy (>25 k  beams are employed, the electrons which enter the detector can have a substantial effect on the background.  An example is shown in Figure 16 for a 40 keV beam incident

on arsenic.  The background below 20 keV is greatly distorted by the electron contribution added to the expected x-ray continuum as shown by the solid curve.  Above 25 keV, the background is mostly due to the normal x-ray continuum; virtually no electrons are able to penetrate the beryllium window and retain energies in this range.  Note that the analyst usually examines the region between 0-10 keV or 0-20 keV.  In the example of Figure 16, it may not be obvious that the background is anomalous unless the entire spectrum is examined.

Artifacts arising from scattered electrons entering the detector can be eliminated with magnetic shielding in front of the detector snout. In the windowless variety of Si(Li) spectrometer, such shielding is an absolute necessity. The artifact may become more pronounced for samples with a high atomic number or with surfaces highly tilted relative to the beam.  These two conditions will produce the greatest number of high energy backscattered electrons.  Light element targets which are flat produce a relatively minor effect.  Operation with an acceleration voltage below 20 keV will also minimize the effect.

<u>Contamination Effects</u>

Contamination deposited during the electron beam-specimen interaction may considerably affect the measured x-ray intensities.  The effects of contamination are observed regardless of the
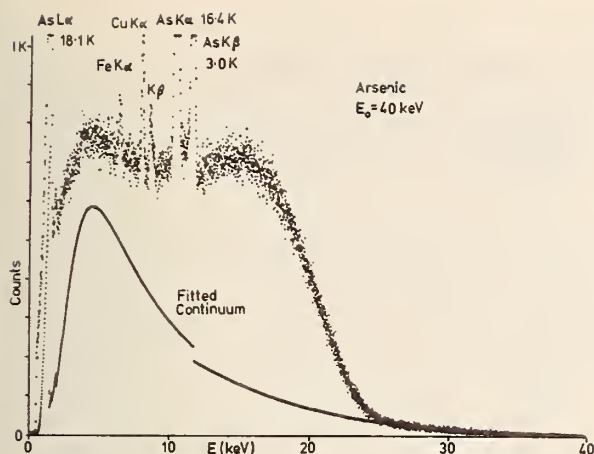
Fig (16) Electron-excited spectrum of arsenic showing background below 25 keV due to electrons entering the detector.



Fig (17) Electron-excited spectrum of carbon from an unsatisfactory detector showing an extremely thick silicon dead layer.

type of x-ray spectrometer which is employed, but the capability of the energy dispersive spectrometer to measure the entire spectrum makes the recognition of such artifacts easier.

The rate of contamination of a specimen is a complicated function of many parameters — current density, beam energy, specimen character, residual gases in the vacuum system, and extraneous substances which exist on the surface of the specimen[22]. Generally, the rate of contamination increases with increasing beam current density. Thus contamination effects are more noticeable when the electron beam is fixed on a point of the specimen as compared with a scanning raster. Contamination from previous bombardment can often be recognized in images due to differences in the secondary electron emission in the contaminated area compared to the rest of the specimen. In such cases, x-ray emission will often be affected as well.

The build-up of a contamination layer on a sample would be intuitively expected to affect the measured x-ray intensities through differential absorption effects, i.e., low energy lines would be more strongly absorbed than high energy lines. The following experiment, performed on an SEM in which contamination was very much in evidence in images, reveals the reverse behavior. X-ray spectra were recorded on polished bulk samples with normal beam incidence, a beam energy of 17.4 keV, and an x-ray take-off angle at 30° above the surface. Two cases were measured: (1) beam in a focused, fixed, position and (2) beam scanned over an area of 100 μm x 100 μm.

The ratios of intensities of the elements measured in the point mode spectrum to the scanning mode spectrum are given in Table 1. A consistent decrease in intensity with increasing x-ray energy is observed in the point mode as compared to the scanning mode. The deviation reaches 10 percent at the highest energy measured. Clearly, this is not an absorption effect, since the most energetic lines are the most strongly affected. A plausible explanation of the effect is that the increased build-up of contamination in the point mode causes the incoming electrons to lose a portion of their energy due to inelastic scattering before reaching the specimen proper. This energy loss reduces $E_o$, the initial interaction energy in the sample. Characteristic x-ray emission, $I_p$ is strongly dependent on the difference between $E_o$ and $E_c$, the critical excitation energy:

$$I_p \propto (E_o - E_c)^{1.7}$$

The difference $(E_o - E_c)$ decreases as the critical excitation energy increases for a fixed value of $E_o$. A decrease in $E_o$ due to contamination will thus have a larger effect on the intensity of the more energetic radiation, since $(E_o - E_c)$ is smaller. This effect is calculated in Table II. The real behavior observed in the experiment of Table I is a combination of the absorption effect and overvoltage effect. Absorption affects the low energy x-ray lines most strongly

63

Table I  Effect of Contamination on X-ray Signals Observed from NBS Glass K-309

| Element | Line | Energy (keV) | Point to Area Ratio |
|---------|------|--------------|---------------------|
| Al | $K\alpha$ | 1.49 | .98 |
| Si | $K\alpha$ | 1.74 | .97 |
| Ca | $K\alpha$ | 3.69 | .93 |
| Ba | $L\alpha$ | 4.47 | .93 |
| Fe | $K\alpha$ | 6.4 | .90 |

Table II  Calculation of Predicted X-ray Intensities from NBS Glass K-309

| | $K_{ab}$ | $E_o = 15$ $(E_o - E_c)^{1.7}$ | $E_o = 14.5$ $(E_o - E_c)^{1.7}$ | $I_{p(14.5)}/I_{p(15)}$ |
|----|---------|--------|--------|--------|
| Si | 1.838 | 79.955 | 74.86 | 0.936 |
| K | 3.607 | 62.558 | 57.962 | 0.926 |
| Fe | 7.111 | 33.492 | 29.963 | 0.895 |
| Cu | 8.980 | 21.150 | 18.251 | 0.863 |

while the decrease in $(E_o - E_c)$ affects the high energy lines. The experiment indicates that the overvoltage effect dominates.

Contamination problems can be significantly reduced with proper attention to the vacuum system and to specimen preparation. For conventional systems with oil diffusion pumps, the use of liquid nitrogen cold traps and chilled surfaces in the specimen chamber is invaluable. Diffusion pump fluids which decompose to gases rather than a solid deposit are available[23]. It is important to recognize that much of the contamination routinely observed results from residual substances on the specimen (oils, etc.). Careful solvent cleaning and vacuum baking can frequently remove such substances and greatly reduce contamination.

Initial Detector Set Up and Testing

The wide variety of Si(Li) spectrometer — MCA systems precludes a specific description for proper set up and testing which is applicable to all instruments. The manufacturer provides specific instructions on the proper installation and adjustment of his instrument. It is usually left to the analyst in the field to make the actual installation. In this section, we shall provide some general guidelines and suggestions to supplement the manufacturers' procedures in order to highlight the critical areas in the operation of these systems:

(1)  Before the Si(Li) detector is installed on the instrument, it is very useful to test the system separately by activating the detector with a radioactive source, preferably Fe[55]. The Fe[55] source emits MnK$\alpha$ and MnK$\beta$ x-radiation with negligible continuum. The x-ray spectrum of this source should be recorded with the detector placed on a vibration-free surface such as plastic foam at least 5 cm from the source. The amplifier should be electrically isolated from other electronics. The manufacturer's instructions for setup for optimum resolution should be followed. The total spectrum count rate should be 1000 HZ or less. A total of 100,000, or more, counts should be collected. It is best if this spectrum can be retained in digital form by storage on magnetic or paper tape. If digital recording is unavailable, the spectrum should be written on graph paper in several scale expansions centered about MnK$\alpha$. The merits of this source spectrum are the following:

64

(a)  The source spectrum serves as a permanent reference to the as-received condition of the system.  In the event of a question arising in the future about the quality of the system, a benchmark is available.

(b)  The resolution in the as-delivered condition can be measured at the usual value, the FWHM for Mn Kα.

(c)  To measure the degree of incomplete charge collection, the peak-to-tail ratio and the asymmetry of the MnKα peak should be determined.  The peak-to-tail ratio is typically measured by taking the ratio of the counts in the peak channel of MnKα to the counts in a background channel at half the energy of MnKα.  Because of the low background counts, an average over at least 10 channels should be used.  For a typical detector, this ratio should be about 1000:1.  The asymmetry of the MnKα peak is typically determined by measuring the full width of the peak at one-tenth the maximum amplitude (FWTM).  The FWTM should be no worse than 1.9 FWHM.

(2)  After installing the spectrometer on the SEM or EPMA, a spectrum should be obtained from a manganese target excited with a 15-20 keV electron beam at the same count rate and total MnKα counts as the reference spectrum. The resolution measured on this spectrum should not be degraded by more than a few eV over the reference spectrum.  If the resolution has deteriorated significantly and/or large numbers of counts are observed in the low energy region, e.g., Figure 11(b), there are several possible sources of trouble:  microphony, lack of electrical ground isolation between circuit components (ground loops), and stray radiation from transformers, computers, etc.  Remedies for these problems depend on the local situation. Ground loops can usually be eliminated by connecting all components of the system to a single high quality ground and not interconnecting them.

(3)  An eloctron-excited spectrum should be obtained from spectrographically pure carbon with a scanning beam to minimize possible contamination. This specimen should provide a continuum spectrum which is devoid of characteristic peaks.  Such a spectrum from a typical detector, Figure 6, has the following characteristics:

(a)  The intensity of the lowest energy channels should nearly reach the baseline, within about 3 percent of the intensity maximum in the continuum hump. If not, this failure may be indicative of a poorly set slow channel discriminator, microphony, stray radiation, or ground loops.

(b)  A silicon K absorption edge and a silicon internal fluorescence peak are always observed, as shown in the spectrum obtained with a normal detector, Figure 6 In an abnormal detector, Figure 17, the silicon absorption edge and the silicon fluorescence peak are much more pronounced, and the magnitude of the absorption edge will be a function of the bias voltage on the silicon detector.

(4)  At this point, the analyst should examine the entire carbon continuum spectrum up to the beam energy for other artifacts.  Specifically, the presence of any characteristic peaks, e.g., Figure 17, is an indication of stray radiation and a clue to its source.

(5)  Spectra should be obtained from elements which give characteristic lines throughout the energy range of interest to check the energy linearity of the system.

(6)  The performance of the pulse pile-up rejector should be examined as a function of x-ray energy and count rate. It can be expected that the pile-up rejector should work well for radiation as energetic as silicon Kα and greater. Below silicon Kα, the pile-up rejector frequently becomes progressively less satisfactory.  Spectra illustrating the pile-up performance from an optimally adjusted system (maximum resolution and maximum allowed count rate), Figure 9(a) and (b), show adequate pulse pile-up rejection for silicon but an almost total failure for magnesium.  A pile-up continuum below the double energy peak and even a triple energy peak are observed in the magnesium spectrum.  In the silicon spectrum, only the double energy peak, which corresponds to coincidence within the time resolution of the pulse rejector, is observed.  As a figure of merit, the area of the silicon Kα double energy peak should be less than 1/200 of the parent peak at allowed system count rates.

(7)  For accurate quantitative analysis, the performance of the deadtime correction circuit should be tested. The x-ray production in the specimen at any beam energy is proportional to the beam current striking the sample.  This fact provides a way to vary the input count rate to the spectrometer system in a controlled fashion.  A flat, pure element target such as iron should be scanned with a beam energy of 15-20 keV. The current should be set initially to give a total spectrum count rate of about 500 HZ.  The beam current is measured in a Faraday cup.  The integrated counts across the peak (Peak plus background) are then plotted as a func-

tion of beam current for a fixed live time (e.g., 100 s). The plot of counts versus current will be linear over that count rate range where the deadtime correction mechanism is functioning properly.

## Qualitative Analysis

Qualitative analysis of energy dispersive x-ray spectra requires a consideration of basic x-ray physics, a knowledge of the EDS spectrometer system, intuition, and common sense. From basic x-ray physics, we require such information as the energies of the family of lines for each element and the approximate weight of the lines. Knowledge of the artifacts of the EDS spectrometer system is needed to identify spurious peaks in the spectra. Intuition can be developed as a result of practice. Finally, the analyst must always be ready to apply common sense to a problem. For example, scandium is an exceedingly rare element, and therefore before identifying it in the spectrum of an unknown, one should check all possibilities for other spectral lines.

Typical sources of information on x-ray energies used for qualitative analysis include "energy slide rules" available from several manufacturers, charts, tables[24], and "KLM" markers available on sophisticated MCA's. All of these sources of information are valuable, but each has limitations at present which can lead to misidentification of peaks. The energy slide rules are extremely convenient, but frequently omit lines which are observed in spectra, such as Ll and $M_{II}N_{IV}$. Since the analyst has a tendency to identify all lines from the source of information at hand, these lines may be misidentified. Tables, such as Bearden's definitive compilation[24], are the ultimate reference, but the extraordinary detail of such tables is overwhelming for practical use. For example, twenty-five L series lines are listed for the heavy elements, of which nine L lines at most might be seen in analysis under practical conditions. Existing KLM markers have the deficiency that certain lines are not included and usually only one series (K,L, or M) can be seen at a time. To supplement these sources, a plot of the energies of lines in the range 1-10 keV observable under practical operating conditions is given in Figure 19. The lines are those which have been observed in the spectra of pure elements where the full spectrum integrated count is $5 \times 10^6$, a condition considered to be a practical upper limit (1000 s. live time at 5000 cps). The

spectra were measured with a 155 eV resolution detector fitted with a 7 μm beryllium window. The energies are derived from Bearden's table[24]. This plot has the advantage that it allows the analyst to see simultaneously all lines which might appear at a particular energy. The plot is useful for assessing situations in which overlap might exist. At the top of the plot, the resolution of a typical 155 eV resolution detector is shown as a function of energy in 1 keV increments.

## Guidelines for Qualitative Analysis

The following guidelines have been developed to give a logical approach to the problem of qualitative analysis with the energy dispersive spectrometer. The problem is sufficiently complicated, however, that it is difficult to provide a rote method which cannot fail. The suggestions are simply guidelines and not iron-clad rules. The analyst must use all his resources and be prepared to deal with unexpected situations. (Note: We will assume that a 1024 channel MCA is used with 10 eV/channel, 0-10 keV, beam energy 20 keV.)

### General Guidelines

(1) Always accumulate an adequate number of counts in the spectrum to give statistically significant peaks. If it is difficult to decide whether a peak exists against the continuum because of statistical fluctuations in the count in each channel, then either more counts should be accumulated to "develop" the peak or else the analyst should not identify it.

(2) EDS systems become increasingly prone to the introduction of spectral artifacts as the count rate increases. For a system set up to operate at the optimum resolution, the total spectrum input count rate should be kept below 5000 cps.

(3) Try to identify an element by more than one peak. This increases the confidence with which an identification is made. In order to excite as many lines as possible for each element, it is best to use a high accelerating potential, 20 kV or more.

### Specific Guidelines: Major Peaks

(1) Begin with the most intense peaks and, preferably work downwards in energy. Reason: The peaks of a given family, K, L, or M, are generally more separated in energy at the high energy end of the spectrum and are probably resolved by the energy dispersive spectrometer.

66

(2)  Determine the energy of a large peak.  If you suspect it is a Kα peak, look immediately for a Kβ peak at about 10 percent of the Kα height.  For K lines of sulfur (2.31 keV) and above, the Kα-Kβ peaks will be resolved with an ordinary 155 eV detector.  If peak ratios are found to be significantly different than expected, the analyst should be suspicious of the assigned identification and consider the possibility of an interference.

(3)  If a Kα-Kβ pair doesn't fit, try L lines.  If an Lα peak is suspected, look for the family $L\alpha_{1,2}(1)$, $L\beta_1(.7)$, $L\beta_2(0.2)$, $L\gamma_1(.08)$, $L\gamma_3(.03)$, Ll (.04) and Lη(.01).  The weights listed are only approximate and vary with atomic number and beam energy.  Below 3 keV, the L family is not well resolved, and the resultant peak appears asymmetric.

(4)  M family lines can be observed for elements such as cerium and above. The observed lines are Mα(1), Mβ(.6), Mζ(.06), Mγ(.05), and the $M_{II}N_{IV}$(.01) transition.  Mα and Mβ are often not resolved, but since Mβ is typically 0.6· Mα a pronounced asymmetry results.

(5)  When an element is identified, all of its peaks should be marked before going to the next element.  When K lines are observed at high energies (iron Kα and greater), look to see if the L lines for that element can be identified. Similarly, for L lines of cerium and above, look to see if the M lines can also be identified.

When all of the high intensity peaks have been identified, and the accompanying families of lines have been marked, then the remaining low intensity peaks can be attempted.

## Minor Peaks

(1)  Sort out the spectral artifacts. Identify the SiKα escape peaks ($E_{line}$-1.74 keV) which accompany all high intensity peaks with an energy greater than the absorption energy for silicon K-radiation (1.84 keV).

(2)  Identify the sum peaks which result from the coincidence of pulses at high counting rates.  For example, if there are large peaks with energies $E_A$, $E_B$, and $E_C$, look for sum peaks at $2E_A$, $2E_B$, $2E_C$, $(E_A+E_B)$, $(E_A+E_C)$, and $(E_B+E_C)$.

(3)  Note that a low level silicon signal will often be found, caused by fluorescence of the silicon dead layer at the surface of the detector at an apparent level of roughly 0.2 percent by weight in a specimen.

(4)  Any peaks remaining after the above procedure has been carried out have a reasonable chance of arising from an element rather than an artifact, and elemental identifications can now be made.  Again, the analyst should start at high energy and work toward the low energy end of the scale.

(5)  The analyst should always remember what stray radiation peaks due to the sample chamber are present in the spectrum and their approximate magnitude when assigning elements in the specimen.

If a computer-based MCA is available, as the final step in a combined qualitative/quantitative analysis, it is invaluable to reconstruct the spectrum and compare this reconstruction with the original.  In this way, any oversights can be recognized.

## Quantitative Analysis

The subject of quantitative analysis is covered extensively in other references and in the present proceedings[25]. For completeness, we shall cover several major points which are involved in the first stage of quantitative analysis with the Si(Li) detector, that is, the extraction of characteristic intensities from the spectrum.

When we are interested in extracting accurate values of the x-ray intensities from the spectrum, close attention must be paid to the artifacts of the detection and signal amplification processes. Particular care must be given to the count rate limitations of the amplifier. High counting rates, in excess of 5000 cps, are to be avoided because of potential problems with pulse pile-up, dead-time correction, peak broadening, and peak shift.

At the same time, it is important in quantitative analysis to accumulate an adequate number of counts under the peaks of interest to reduce statistical fluctuations in the count to an acceptable level.  For example, to reduce the uncertainty due to counting statistics alone to ±3 percent (99.7 percent confidence), at least 10,000 counts integrated under the desired peak are required.

The requirements of a relatively low counting rate and high values of the integrated count forces the analyst to use long counting periods, typically in excess of 100 s per spectrum.  This places stringent requirements on the stability of the electron beam instrument, and a procedure in which the beam current is repeatedly monitored to correct for drift is needed.  A principal advantage of the Si(Li) spectrometer system is its inherent long-term stability.  An analy-
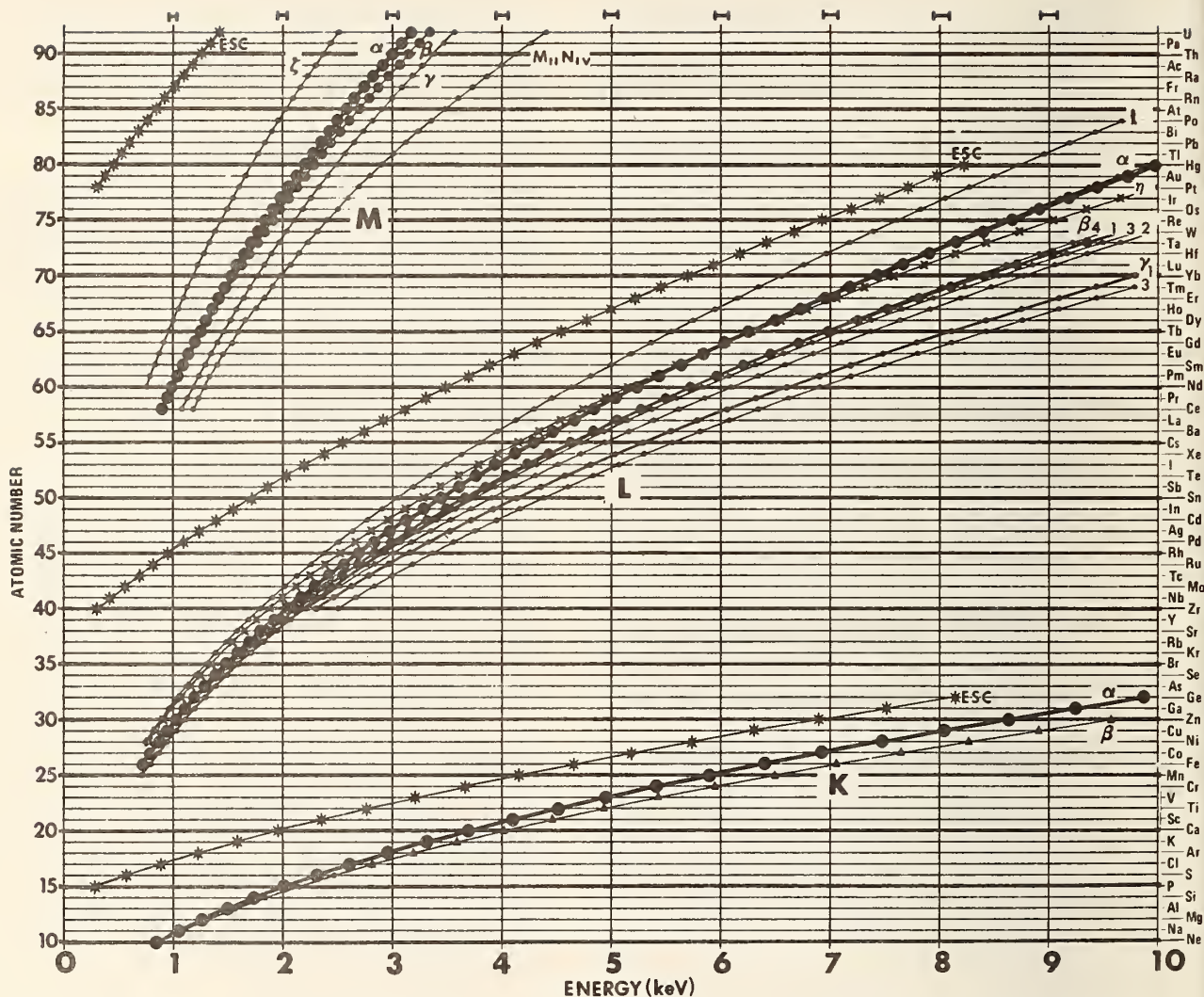
Fig (18)  Plot of the energies of x-ray lines likely to be observed in EDS spectra containing about 5,000,000 counts in the full spectrum.  The silicon escape peak for the major line of each series (K,L,M) is also indicated.  Solid bars at the top are the FWHM values produced by a 155 eV(Mn Kα) detector in each 1 keV interval.

tical procedure can be developed in which stored reference spectra obtained under standardized conditions are utilized over long periods of time, e.g., weeks to months.

In the absence of other artifacts, the two principal modifications which must be applied to a spectrum to extract the characteristic intensity are the subtraction of the background[26,27,28] under the peak and the subtraction of peak overlaps[27,28,29].  Both of these corrections are dependent upon the composition of the sample which is sought, and therefore the correction procedures are usually incorporated into the iteration loop of a matrix correction procedure[30].

The analyst who is seeking to carry out fully quantitative analysis of unknowns with the Si(Li) spectrometer is advised to first test his instrument, spectrometer system, and data reduction scheme on samples known to be satisfactory for quantitative microanalysis. Suitable samples which are known to be microspatially homogeneous and for which the composition is certified are available from the National Bureau of Standards, Washington DC, 20234.

### Acknowledgements

68

## References

1. K.F.J. Heinrich, Quantitative Electron Probe Microanalysis, NBS Special Publication 298, U.S. Government Printing Office, Washington, D.C. 20402, 1968.
2. S.J.B. Reed, Electron Microprobe Analysis, (Cambridge University Press, Cambridge) 1975.
3. J.I. Goldstein, H. Yakowitz, D.E. Newbury, E. Lifshin, J. Colby, and J. Coleman, Practical Scanning Electron Microscopy (Plenum Press, New York) 1975.
4. J. Henoc, K.F.J. Heinrich, and R.L. Myklebust, "A Rigorous Correction Procedure for Quantitative Electron Probe Microanalysis (COR2)", NBS Technical Note 769, U.S. Government Printing Office, Washington, D.C., 1973.
5. H. Yakowitz, R.L. Myklebust, and K.F.J. Heinrich, "FRAME: An On-Line Correction Procedure for Quantitative Electron Probe Microanalysis", NBS Technical Note 796, U.S. Government Printing Office, Washington, D.C., 1973.
6. J.W. Colby, "Quantitative Microprobe Analysis of Thin Insulating Films", in Advances in X-ray Analysis, J.B. Newkirk, G.R. Mallett, and H.G. Peiffer, eds., (Plenum Press, New York)11, 1968, 287-305.
7. A.E. Bence and A. Albee, "Empirical Correction Factors for the Electron Microanalysis of Silicates and Oxides", J. Geol. 76, 1968, 382-403.
8. R. Woldseth, X-ray Energy Spectrometry Kevex Corporation, 1101 Chess Dr., Foster City, CA 94404.
9. D. Gedke, "The Si(Li) X-ray Energy Analysis System: Operating Principles and Performance", X-ray Spec., 1, 1972, 129 - 141.
10. R. Fitzgerald and P. Ganzel, "X-ray Energy Spectrometry in the 0.1 to 10 A Range", Energy Dispersion X-ray Analysis: X-ray and Electron Probe Analysis, ASTM STP-485, American Society for Testing and Materials, 1971, 3-35.
11. R.L. Heath, "The Application of High-Resolution Solid State Detectors to X-ray Spectrometry - A Review", Advan. X-ray Anal., 15, 1972, 1-35.
12. H.U. Freund, J.S. Hansen, E. Karttunen, and R.W. Fink, "Photon Spectrometry in the Low Energy Region of 500 eV to 100 keV", Proc. Intern. Conf. on Radioactivity and Nucl. Spect., 1969, 623-649.
13. E. Elad, C.N. Inskeep, R.A. Sareen, and P. Nestor, "Dead Layers in Charged-Particle Detectors", IEEE Trans. Nucl. Sci., 20, 1973, 534-544.
14. S.J.B. Reed and N.G. Ware, "Escape Peaks and Internal Fluorescence in X-ray Spectra Recorded with Lithium Drifted Silicon Detectors", J. Phys. E: Sci. Instr 5, 1972, 582-584.

15. G. Williams, "Role of Multichannel Analyzer in Data Handling", Energy Dispersion X-ray Analysis: X-ray and Electron Probe Analysis, ASTM STP-485, American Society for Testing and Materials, 1971, 125-139.
16. C.W. Williams, "Reducing Pulse Height Spectral Distortion by Means of DC Restoration and Pile-up Rejection", IEEE Trans. Nucl. Sci. NS-15(1), 1968, 297-302.
17. S.J.B. Reed, "Pulse Pile-up Rejection in Si(Li) X-ray Systems", J. Phys. E: Sci. Instr., 5, 1972, 1-4.
18. J.M. Jaklevic, F.S. Goulding, and D.A. Landis, "High Rate X-ray Fluorescence Analysis by Pulsed Excitation", IEEE Trans. Nucl. Sci., 3, 1972, 392-400.
19. P.J. Statham, "Pile-up Rejection: Limitations and Corrections for Residual Errors in Energy-Dispersive Spectrometers 6, 1977, 94-102.
20. R.B. Bolon and M.D. McConnell, "Evaluation of Electron Beam Tails and X-ray Spatial Resolution in the SEM", in SEM/1976, O. Johari, ed, 1,1976, 163-170.
21. K.F.J. Heinrich, personal communication. (Details available from authors).
22. W. R. Bottoms, "Contamination in the SEM" in SEM/1973, IITRI, Chicago, 1973 181-188.
23. L. Laurenson, "Perfluoropolyethers as Vacuum Pump Fluids", Research/Development 28, 1977, 61-72.
24. J.A. Bearden, "X-ray Wavelengths and X-ray Atomic Energy Levels", Rev. Mod. Phys., 31,1967, 1-66.
25. R.B. Bolon, these proceedings.
26. C.E. Fiori, R.L. Myklebust, K.F.J. Heinrich, and H. Yakowitz, "Prediction of Continuum Intensity in X-ray Dispersive Microanalysis", Analyt. Chem., 48, 1976, 172-176.
27. D.G.W. Smith, C.M. Gold, and D.A. Tomlinson, "The Atomic Number Dependence of the X-ray Continuum Intensity and the Practical Calculation of Background in Energy Dispersive Electron Microprobe Analysis", X-ray Spec., 4, 1975, 149-156.
28. F.H. Schamber, "A Modification of the Linear Least-Squares Fitting Method which Provides Continuum Suppression", in X-ray Fluorescence Analysis of Environmental Samples, T.G. Dzubay, ed.(Ann Arbor Science Pub., Ann Arbor, Mich.) 1977, 241-257.
29. C.E. Fiori, R.L. Myklebust, and K.F.J. Heinrich, "A Method for Resolving Overlapping Energy Dispersive Peaks of an X-ray Spectrum; Application to the Correction Procedure FRAME B", Proc. 11th Ann. Conf. Microbeam Analysis Society, 1976, 12A-12C.

30. R.L. Myklebust, C.E. Fiori, and K.F. J Heinrich, "FRAME C: A Compact Procedure for Quantitative Energy Dispersive Electron Probe X-ray Analysis", Proc. 12th Ann. Conf. Microbeam Analysis Society, 1977, 96A-96D. (Available from author).

## DISCUSSION WITH REVIEWERS

Reviewer I: Could you provide an applicable reference for the numbers given concerning the natural width of an x-ray peak, in the first paragraph on "Peak Broadening"?

Authors: A suitable reference is L. G. Parratt, Phys. Rev. 44, 1933, pp. 63-68. It should be noted that there is some controversy over exact values and our intention in giving a value for $MnK\alpha$ was merely to demonstrate how badly a Si(Li) detector will degrade a natural x-ray spectrum. A $MnK\alpha$ peak of 1000 counts amplitude and natural width of 2.3 eV will be degraded to a peak of typically 150 eV width and amplitude of 15 counts (assuming 10 eV/channel).

Reviewer I: Please explain what the "dead layer" (inactive layer) on the front face of the Si(Li) crystal detector is, and why its presence is unavoidable (which I understand to be the case). Can its depth be minimized? How?

Authors: The dead layer is a region in which the desired electrical properties of the Si are altered by an excess presence of "dopant" and by the presence of the gold electrode. The dead layer can be considered to have two regions. The first region is a completely inactive layer of Si which will differentially absorb incoming radiation. The second region is a partially active layer in which an insufficient number of electron-hole pairs will be collected for radiation captured in it. This has the effect of shifting an output pulse to a lower energy. The depth of the dead layer can be controlled somewhat by changing the bias applied to the detector. However, other factors determine the recommended bias. For example, a higher bias will reduce the thickness of the dead layer and will improve the charge collection characteristics of the detector-but the leakage current will increase and introduce noise which will degrade resolution.

Reviewer I: It seems to me that in an actual spectrum, it would be difficult to distinguish among the normal low-energy tail of a major peak, the associated absorption edge, and the resulting background shelf. Can this be done other than by comparison with theoretical fits? How?

Authors: The effect of the background shelf can be isolated by the use of monochromatic x-ray lines. For $MnK\alpha$ an $Fe^{55}$ radioactive source can be used. For other x-ray lines it is possible to use x-ray fluorescence. The essense of the method is as follows. If one wished to determine the peak to tail ratio of

$CaK\alpha$, a thin foil of Ti metal can be placed above a specimen of, say, $CaF$ in the SEM. The foil will completely stop the SEM electron beam, but will transmit $TiK\alpha, K\beta$ and some Bremstrahlung radiation. Obviously, the thickness of the foil and the kilovoltage of the electron beam will have to be correctly chosen. The detector will then see an essentially monochromatic source of $CaK\alpha$ x-rays. We have found that the small deviation between our theoretical fits and an observed spectrum is mostly explained by incomplete charge collection.

Reviewers I, III: The authors state in their introduction that the continuum "conveys information on the average atomic number of the specimen". What are the features of the continuum which contain this information and are there any practical examples of its use?

Authors: For a fixed analysis time and constant electron beam current and energy the number of counts in any background channel of the MCA is very nearly proportional to the average atomic number of the specimen. Double the average atomic number of the specimen and the number of counts in the given background channel will double. This fact permits a simple and convenient estimate of the average atomic number to be made. If the analyst is examining a series of points in an alloy and, suddenly, all characteristic intensities seemed too low for one point, he could use the above property of the continuum to determine if, for example, an oxide or carbide phase had been encountered. On the other hand, the above property can work against the analyst when "line profiling" or "x-ray area mapping". If the background under a peak is a significant fraction of the peak it is possible to encounter situations where the line profile or x-ray area map is more indicative of the average atomic number than of the chemical element one is attemping to analyze for.

Reviewer IV: Many of the commercially available MCA systems offer "data enhancement" capabilities such as smoothing to reduce statistical noise and forms of automatic background subtraction to remove the continuum. Do the authors have an opinion on the utility of such features as an aid to qualitative and/or quantitative analysis of EDS spectra?

Authors: At the risk of being labeled unbelievers in sophisticated statistical methods we make the following observation: Nothing can beat an unmodified spectrum with a lot of counts. If a peak stands clearly above the background then it is indeed a peak. How-

ever, smoothing the data with, for example, a weighted polynomial function, can alter the statistical variations in the continuum in such a manner that a novice will very likely see "trace" peaks where none exist. To explain to a customer the physics of an EDS spectrum is usually enough. To explain a "smoothed" EDS spectrum is masochism. For applications where all concerned understand the underlying statistics such functions are indeed valuable. In general, we feel that if the analyst is displeased with the appearance of a spectrum due to statistical noise, he should gather more counts rather than push a "smooth" button. In regards to automatic background correction schemes a similar argument holds. If the user trusts and understands the physical or mathematical model he can push the appropriate buttons and make intelligent use of the results. But this places a non-trivial problem of documentation on the manufacturer. The basis of our concern is a fear that the above buttons are used more often for artistic purposes than physical purposes.

Reviewer IV: The authors have discussed the excitation of characteristic radiation from the silicon dead-layer of the detector. Is it possible to obtain significant secondary radiation from any of the other components of the detector, its associated mountings, or its x-ray collimator?
Authors: For applications of the Si(Li) detector mounted on a scanning electron microscope, where the energy of any x-ray will typically be below 30 keV, the possibility of secondary radiation from other components in the detector is very small. Furthermore, the presence of the continuum tends to mask such signals. However, if the counting statistics permit, it is possible to see the gold $M_V$ absorption edge from the gold layer on the face of the detector. See figure 6 in the text.

Reviewer I: The experiment described in the section "Contamination Effects" indicates that contamination layers effectively reduce the measured x-ray intensity for higher-Z elements (Fe) more than for lower-Z elements (Al, Si), due to predominance of the overvoltage effect. It has been reported occasionally that an intense stationary beam has produced a "cratered" contamination spot with the contamination effectively removed (or not deposited) in the central, highest-intensity area. Could not the experimental results reported in Table I have been caused by this sort of phenomenon? If not, please indicate why.

Authors: We examined the contamination spots at high magnification and did not observe a cratered effect. A cratered contamination spot would not decelerate the electrons sufficiently to explain the effect. It could be that the brightness of our instrument is insufficient to cause "cratering".

Reviewer I: In paragraph 2 of "Initial Set Up and Testing", you recommend that the $Fe^{55}$ test source should be at least 5 cm. from the detector. What is the reason for recommending so great a minimum distance here (Manufacturers' service people often tape the source to the collimator.)?
Authors: The degree of distortion to a peak on its low energy side and the magnitude and shape of the background "shelf" extending to zero energy can be very sensitive to the angle at which photons arrive at the detector. Collimation is important. When a test source is taped to the face of the detector, photons will enter the detector over a wide range of angles. If one is merely characterizing the resolution at FWHM of the detector this arrangement will more than likely not cause any difficulty. Furthermore, a considerably higher count rate is available. However, if one is characterizing the peak shape and, or, the background shelf, it is advisable to move the test source back. We feel that the shaded area in figure 6 is an example of the above effect. Internal fluorescence of the silicon dead layer provides a source of totally uncollimated x-rays since they are generated exactly at the surface of the active silicon. The resulting peak is highly distorted on the low energy side due to incomplete charge collection. There is no combination of silicon K absorption edge and Gaussian peak of the appropriate resolution which will explain the shape of the continuum below the energy of silicon in figure 6.

Reviewer III: The authors recommend an $Fe^{55}$ source for initial set up of the ED system. This is the only source which should be used for the peak-to-tail check described. However, a $Co^{57}$ source has the benefit of producing Fe K x-rays as well as a 14.4 keV gamma ray. The presence of two such separated peaks permits calibration of the EDS system before installation on the column. For a beginning analyst who is not quite sure of the nature of stray x-rays from his chamber, composition of sample holders or mounts, contaminant or coating elements in his "standards", etc., the calibration capability is more useful than the

71

peak-to-tail measurement. Resolution can be checked on the Fe Kα line using equation (3) in the text, although this is not as exact as direct measurement of the Mn Kα. What comments do the authors have about the use of Co$^{57}$ as a calibration source.

Authors: We agree the Co$^{57}$ is an acceptable calibration source. Our only objection is that it is a "dirty" source, emitting several extremely energetic gamma rays (122 and 136 keV) in addition to those stated and a significant Bremsstrahlung spectrum. The higher energy gamma rays could be confusing if the amplifier gain settings were initially set low. As observed, Co$^{57}$ should not be used to test the peak-to-tail ratio.

Fe$^{55}$, Co$^{57}$ and other useful radioactive standards are available from the National Bureau of Standards, Office of Standard Reference Materials. These are calibrated sources (photons/sec./steradian). SRM 4260-B, Fe$^{55}$, is particularly useful as it is a point source mounted on a 2.54 cm disk suitable for mounting in the specimen position of a SEM.

Reviewer I: While it is not directly part of your subject, could you address a few comments to the question of whether integrated peak height, or simple peak height (counts in peak channel) should be used in quantitative EDS analyses, and why. There still seems to be considerable confusion concerning this matter.

Authors: Presumably, the reason for using only the counts in the peak channel is to reduce interference from another, nearby, peak. A better way to reduce this interference is merely to integrate half of the peak on the side opposite from the interfering peak. In another question we note that a natural x-ray line of 1000 counts amplitude and width of 2.3 eV is degraded by the Si(Li) detector into a peak of typically 150 eV width and amplitude of 15 counts. One simply throws away a totally unacceptable amount of information by using the peak channel.

Reviewer I: When peak height or integrated peak height is used in this paper, does it refer to the usual integration over 1.2 x FWHM?

Authors: In all cases an "integrated" peak or a "full" peak means the total area of a fitted Gaussian to the data. "Amplitude" means the number of counts in a 10 eV wide area centered at the mean energy. This corresponds to one channel of a multichannel analyzer calibrated with 10 eV/channel.

Reviewer II: The Si(Li) detector has to be kept at liquid nitrogen temperature. Are there artifacts which would be caused by accidental failure to maintain that temperature? How would one know if the detector has been damaged during routine operation?

Authors: Most systems have a circuit built in, or sold as an option, to protect the detector in the event of a warm-up. We strongly recommend such a circuit. When warm-up occurs the analyst is alerted by either an alarm buzzer, or the detector simply stops working. In the event that a protection circuit is not available the analyst might initially see a deterioration in resolution and an increase in noise at the lower energy end of the spectrum, such as seen in figure 11b. Since the detector assembly is cryogenically pumped a temperature is eventually reached where increasing pressure will permit a detector bias induced gas discharge to occur. This discharge can destroy the FET of the preamplifier. With modern day Si(Li) detectors it is possible to survive a number of warm-ups without ill effects (if the bias supply has been turned off). However, this is not one of the manufactures specifications which we recommend testing.

Reviewer II: What artifacts would be observed due to a vacuum leak in the detector? What artifacts would be observed in a windowless detector due to ice build-up (from moisture in the environment) and or contaminants on the detector surface?

Authors: Again, a vacuum leak sufficient to cause a gas discharge to occur can cause destruction of the FET in the preamplifier.
The build up of ice and/or contaminants causes the following difficulty. One of the most important characteristics of the Si(Li) "chip" is its surface resistance. Anything which will degrade this parameter will degrade the performance. Differential absorption of low energy x-rays will also occur in the surface layers of contamination.

# Appendix 2

## 2a. General Variables

A. Subscripted Variables (Element Number J)

| | |
|---|---|
| A(I) | Atomic weight for atomic number I |
| B(I) | Kβ/ΣK ratios for atomic number I |
| C(J) | Mass fractions |
| D(3,3) | Coefficients for computing the constants in mass absorption coefficient equations. |
| E(I,J) | Energies of absorption edges (edge number I). |
| G(I,J) | Energies of x-ray lines (line number I). |
| H(I,J) | Mass absorption coefficients (absorber I). |
| K(I,J) | Coefficients for computing energies of absorption edges (edge number I). |
| L(J) | Code number for x-ray lines: Kα = 1, Lα₁ = 2, Mα = 3, etc. |
| O(J,J) | Characteristic fluorescence correction (all terms that are independent of C(J)). |
| P(J,J) | Code numbers for identifying the characteristic fluorescence correction. |
| 0 | none |
| 1 | Kα exciting Kα |
| 2 | Lα exciting Kα |
| 3 | Kα exciting Lα |
| 4 | Lα exciting Lα |
| 5 | Kα exciting Mα |
| 6 | Lα exciting Mα |
| R(I) | Edge jump ratios (edge number I). |
| T(I,J) | Coefficients for computing energies of x-ray lines (line number I). |
| V(J,J) | Overvoltage or, after line 6394, back-scatter factors (R). |
| Z(J) | Atomic numbers. |

73

2a.  General Variables (Continued)

B.  Unsubscripted Variables

D2            Detector Efficiency, $P_E$.

EO            Opérating voltage (in kV), $E_o$.

L1            Memory address for a particular channel
                     number.

L9            Switch for computing line energies
                     (L9 = 2) or edge energies (L9 = 1).

M3            X-ray emission angle $\psi$.

N             Number of elements in specimen.

N3            Switch:  If N3 = 0, compute standard inten-
                     sity ratio from known concentrations.  If
                     N3 > 0, compute concentrations in unknown.
                     N3 + 1 is the number of iterations.

N4            Switch for analyzing more than one similar
                     unknown point.  For first point, N4 = 0;
                     for additional points N4 is set to 1 by
                     the program.

N9            N9/10 is the number of element standards
                     currently in the standards data file.

P6            Thickness of Be window on detector (cm),
                     $t_{Be}$.

P7            Thickness of Si dead layer in detector
                     (cm), $t_{Si}$.

Q1            csc $\psi$.

Q2            Initially, the electron beam incidence
                     angle, $\theta$.  After line 1470, sin $\theta$.

Q3            Initially, the full-width at half-maximum,
                     FWHM, for Mn K$\alpha$ (eV).  After 1485, Q3 =
                     $[(Q3)^2 - 14737.5]$ which is used for computing
                     peak widths, $\sigma$, as a function of energy.

Variables used as index variables unless otherwise defined:
I, J, M1, M3, J1, I1, I2, K1, L2, B1, T1, D1, N1, K2.

2b.  Local Variables (for listed subroutines only)

A.  Main Program for Standards (100-390) (For subscripted variables, the element number is J).

M(J)                Background-and overlap-corrected intensities (counts).

Q(J)                Valence for each element.

W(J)                Same as M(J).

E1                  Operating voltage, $E_o$ (eV).

K1                  One half of the width integrated for each peak in units of the standard deviation, $\sigma$, for a Gaussian peak.

B.  Main Program for Unknown (500-900)

Q(J)                Background and overlap corrected intensities for pure elements (counts).

C.  Subroutine for coefficients and constants (1000-1495)
    All variables are global.
    List of functions:

FNA(I)              Returns the contents of MCA channel I to the calling routine.

FNE(I)              Returns the energy (kV) of MCA channel I.

FNC(I)              Returns computer memory address of MCA channel I.

FNN(I)              Returns the MCA channel number of energy I.

FNS(I)              Returns peak width (standard deviation, $\sigma$), of energy I.

FNG(I)              Returns x-ray line energy of the measured line of element I.

FNF(I)              Returns the atomic number (I) dependence of the $L\alpha_1/K\alpha$ ratio.

FNJ(I)              Returns the mean ionization potential for atomic number I.

FNL(I)              Returns the logarithmic integral for I.

2b. Local Variables (Continued)

FNM(I)              Returns the $M\alpha/L\alpha_1$ ratio.

D. Subroutine for computing x-ray line and edge energies (1500-1610)

Z1                  ln $(Z(J))$; natural logarithm of the atomic number.

E. Subroutine for computing mass absorption coefficients (1700-1980)

A1                  Mass absorption coefficient, $\mu = C_k\lambda^n$.

C2                  Constant in absorption coefficient equation ($C_k$, $C_{k1}$, $C_{1m}$).

E1                  Energy at which absorption coefficient is computed.

Z1                  ln $(Z(J))$.

F. Subroutine for computing detector efficiency (2000-2095)

A1                  Mass absorption coefficient $\mu(\lambda, I)$.

A3                  $t_{Be}$ $\mu(\lambda, Be)$

A4                  $t_{Au}$ $\mu(\lambda, Au)$

G. Subroutine for computing primary absorption in specimen, $f_p$ (2100-2140)

A2                  Absorption coefficient $\mu(\lambda, I)$

E1                  Energy of x-ray line ($E_1$).

F1                  $f_p$, the absorption factor.

G1                  $\gamma \sin\theta = (E_o^{1.65} - E_1^{1.65}) \sin\theta$.

X3                  $\chi = \mu(\lambda, I)$ csc $\psi$.

H. Subroutine for computing the continuum background (2200-2620)

F(1,J)              Primary absorption factor for specimen, $f_p$.

76

2b. Local Variables (Continued)

M(I)            Integrated counts in the region of interest I, (ROI(I)).

U(I)            $(E_0-E_1)^2$ for ROI(I).

W(I)            Mean energy (kV) of ROI(I)

X(I)            $(E_0-E_1)$ for ROI(I).

Y(I)            M(I)/T1.

A1              $\mu(\lambda,I)$ mass absorption coefficient.

A2              $\bar{\mu} = \sum\limits_{I=1}^{N} [C(I) * \mu(\lambda,I)]$ average mass absorption coefficient.

D1              X(0) U(1) - U(0) X(1).

E1              Same as W(I).

F1              $f_p$ absorption in specimen.

G1              $T1 * (K1 * X1^2 + K2 * X1)$.

G2              Number of MCA channels in a region of interest.

K1              Quadratic coefficient in background equation (Y(1) X(0) - Y(0) X(1))/D1.

K2              Linear coefficient in background equation (Y(0) U(1) - Y(1) U(0))/D1.

T1              $f_p * P_E/E_1$.

T5              Contents of a region of interest.

X1              $E_0-E_1$

I.  Subroutine for storing information on standards in a file (2700-2920)

M(J)            Integrated intensity in counts (background and overlap corrected) for a pure element.

Q(J)            Valence of element J if oxygen is to be computed by stoichiometry.

2b. Local Variables (Continued)

J. Subroutine for computing the overlap factors (3000-3450)

M(J)     Total calculated integral of Gaussian-shaped peak plus incomplete charge collection.

S(I,J)     Relative weights of x-ray lines (line number I).

W(J)     Same as M(J).

D3     4 standard deviations, $4\sigma$, for a peak.

E1     Calculated integral of lower energy half of peak.

E2     Calculated integral of upper energy half of peak.

E3     Lower energy limit of integral.

E4     Upper energy limit of integral.

E7     Energy of an x-ray line.

E8     Result of integration of Gaussian peak.

G4     Result of integration of incomplete charge collection function.

O2     Computed overlap factor.

S6     Standard deviation, $\sigma$, for a peak of energy E7.

T5     (a) Contents of a ROI, or
       (b) The energy of an interfering x-ray line.

X2     Value to be integrated by erf(X2)
       X2 = ((E3 or E4) - E7)/(S6*$\sqrt{2}$) or in line
       3340, X2 = 1/ln $(U_L U_M)$

K. Subroutine for computing each type of interference for subroutine J (3500-3850)

S(I,J)     Relative weights of x-ray lines (line number I).

78

## 2b. Local Variables (Continued)

| | |
|---|---|
| U(I) | Computed x-ray cross-section for edge I. |
| W(J) | Computed integral of measured peak. |
| X(I) | Fluorescence yields for K, L, or M lines. |
| A1,A2,A3, A4,A5 | Relative x-ray cross-sections. U(I)/U(K1) where K1 is measured line, I is any other line. |
| D3 | 4 $\sigma$ for a peak. |
| E1 | Overvoltage $E0/E(I,J)$. |
| E2 | Part of cross-section equation 1166 $E(I,J)/FNJ(Z)$. |
| E7 | Energy of x-ray line. |
| O1 | Integral of overlap fraction. |
| O2 | Overlap factor for one peak on another. |
| R1 | Weight of K$\beta$ line, K$\beta$/$\Sigma$K. |
| S6 | Standard deviation, $\sigma$, for energy E7. |
| S8 | Relative weight of escape peak to parent peak. |
| T5 | X-ray line energy for an analyzed line. |
| X1 | E1*E2 |

## L. Subroutine for storing overlap factors in a data file (3860-3886)

| | |
|---|---|
| E9 | Index for determining proper memory address. |
| I2 | Line code of the overlapping line. |
| O2 | Computed overlap factor. |
| X2 | Computed overlap factor * 100000. |

2b.  Local Variables (Continued)

M.  Subroutine for computing overlaps by escape peaks
    (3890-3990)

| | |
|---|---|
| A1 | Mass absorption coefficient. |
| D3 | 4 $\sigma$ for the overlapped peak. |
| E1 | Energy of the parent peak that produces the escape peak. |
| E7 | Initially the same as E1, then the energy of the escape peak (E1-1.74). |
| S6 | Sigma, $\sigma$, for the escape peak. |
| S7 | Factor in expression for relative weight of escape peak. |
| S8 | Relative weight of escape peak. |
| T5 | Energy of peak overlapped by escape peak of energy E7. |

N.  Subroutines for integrating the overlapping area of any
    peak (4000-4130)

| | |
|---|---|
| E2 | Integrated area from lower energy limit, E3, to center of Gaussian peak. |
| E3 | Lower limit of integration. |
| E4 | Upper limit of integration. |
| E7 | Energy of the Gaussian peak. |
| E8 | Integrated area from center of Gaussian peak to upper limit, E4. |
| G4 | Integrated area of incomplete charge collection. |
| O1 | Total integral of overlap area. |
| S6 | Standard deviation, $\sigma$, of Gaussian peak of energy E7. |
| X2 | Function to be integrated by erf(X2) $X2 = ((E3 \text{ or } E4) - E7)/(S6*\sqrt{2})$. |

80

2b.  Local Variables (Continued)

O.  Subroutine for computing the integrated area of the
    incomplete charge collection (4200-4400)

    E7              Energy of the x-ray peak.

    G4              Calculated integral of the incomplete
                    charge collection expression
                    $G4 = X1 * (S3)^2 [1 - \exp(X2)*(1 - S2)]$.

    X1,X3           Empirical fitting coefficients for the
                    incomplete charge expression.

    X2              [(E3 or E4) - E7]/X3 where E3 and E4 are
                    the integration limits.

P.  Subroutine for the integration of the areas under
    Gaussian peaks by integrating erf(X) (4500-5090)

    All variables in this subroutine are used only within
    the subroutine.

    E8              Area calculated by the integration.

    X2              The argument to be integrated.
                    $X2 = [(E3 \text{ or } E4) - E7]/(S6 * \sqrt{2})$.

    All other variables in this subroutine are not
    individually defined but are listed for information.
    They are all temporary variables and their values
    are not used in the rest of the program.

    | A5 | F3 | S1 |
    |----|----|----|
    | B1 | F4 | S2 |
    | C1 | G1 | T1 |
    | D1 | G2 | T2 |
    | E9 | G3 | U1 |
    | F1 | P2 | W1 |
    | F2 | P3 | Y1 |
    |    |    | Y2 |

81

2b. Local Variables (Continued)

Q. Subroutine for correcting overlaps using the overlap coefficients (5100-5390)

$F(3,J)$            Detector efficiency, $P_E$, times primary absorption factor, $f_p$, for element J.

$M(J)$            Integrated counts in peak of element J.

$W(J)$            Integrated counts in peak of element J corrected for overlaps.

A1            Mass absorption coefficient $\mu(\lambda, J)$

A2            Average mass absorption coefficients

$$\bar{\mu} = \sum_{J=1}^{N} C(J) * \mu(\lambda, J).$$

E1            Energy of an x-ray line.

F1            Primary absorption factor, $f_p$.

G1            Line code of an overlapping peak.

R1            Number of counts in overlapping region.

Y1            The computed overlap factor.

R. Subroutine for computing the matrix (ZAF) correction (5500-7150)

$F(I,J)$            Absorption factor $f_p$ (I = 0 for standard, I = 1 for unknown.

$M(J)$            Number of counts in the measured x-ray peak or the measured intensity ratio (k).

$Q(J)$            Number of counts in a peak from a pure element.

$S(I,J)$            Stopping power (S) (I = other element number).

$U(J)$            Overvoltage $(E_o/E_q)$.

$W(J)$            Number of counts in the measured x-ray peak corrected for background and overlap.

## 2b. Local Variables (Continued)

| | |
|---|---|
| A1 | Mass absorption coefficient, $\mu(\lambda, I)$. |
| A2 | Average mass absorption coefficient, $\bar{\mu}$. |
| A3 | $\bar{\mu}$ of exciting x-ray line in fluorescence correction. |
| B1 | Initially, the edge number of a measured x-ray line. Then one of the factors in the secondary fluorescence correction. |
| C1,F3, L2,P3 | Factors used for determining if the secondary fluorescence correction is needed. |
| D1 | In fluorescence correction, the weight of the x-ray line, $P_{ij}$, times the fluorescence yield, $\omega$. |
| E1 | Energy of x-ray line. |
| F1 | Absorption factor, $f_p$. |
| F2 | Characteristic fluorescence correction factor. |
| F4,X1 | Intermediate factors for computing the secondary fluorescence correction. |
| G1,G2,P2 | Intermediate variables for computing the backscatter correction R. |
| G3 | Computed intensity ratio, $k_c$. |
| G4 | Switch for including or omitting the drawing of the reconstructed spectrum. |
| S1 | Summation of mass fractions. |
| S2 | Average stopping power, $\bar{S} = \Sigma C_i S_i$. |
| T1 | Fluorescence yield of K-lines. |
| T2 | Fluorescence yield of L-lines. |
| T5 | Number of counts in a region of interest. |
| U1 | Overvoltage $E_o/E_q$. |

2b.  Local Variables (Continued)

W1                    $(R/\bar{R})$ $(S/\bar{S})$.

X2                    Average of backscatter factors, $\bar{R} = \Sigma C_i R_i$.

S.  Subroutine for assigning regions of interest in a TN 1700
    MCA.  (8000-8140)

E1                    Lower energy limit of a region of interest
                      $E_{peak} - K_1\sigma$.

E2                    Upper energy limit of a region of interest
                      $E_{peak} + K_1\sigma$.

K1                    Width factor $(K_1)$:  $2 K_1\sigma$ = width integrated
                      by the region of interest.

S1                    Standard deviation, $\sigma$, for an x-ray peak.

T.  Subroutine to draw the x-ray peaks predicted by the
    program (8200-8595)

F(3,J)                $f_p * P_E$

Q(J)                  Measured intensity for a pure element.

A1                    Mass absorption coefficient, $\mu(\lambda,J)$.

A2                    Average mass absorption coefficients, $\bar{\mu}$.

E1                    Energy of x-ray peak.

E2                    Amplitude of x-ray peak.

E3, E4                Lower and upper energy limits of region
                      of interest.

F1                    $f_p$

G1                    Computed integral within a region of
                      interest, $\Sigma T1$.

G3                    Computed intensity ratio, $k_c$.

J1                    Energy of channel J.

K2                    Energy width of integrated peak (in terms
                      of standard deviation).

84

2b. Local Variables (Continued)

S1,S2                   Standard deviation, $\sigma$, for energy, E1.

S6                      Peak overlap factor.

T1                      Intensity of spectrum at channel J.

T5                      Generated x-ray peak intensity for unknown.

U.   Subroutine for computing an element, for which a line is
     not measured, by stoichiometry (oxygen) or by difference.

F3                      Oxygen concentration in an oxide.

G3                      Valence of an element.

S1                      Summation of mass fractions.

V.   Main program for computing window thickness on a Si(Li)
     detector. (This program will overlay main program A)
     (100-312)

M(I)                    The average number of counts per channel
                        in ROI(I).

S(I)                    The mean energy (kV) of ROI(I).

U(I)                    $\ln (K1*X1^2 + K2*X1) - \ln(M(I)) +$
                        $\ln(F1/E1) - A3$

X(I)                    $\mu(\lambda,Be)\rho_{Be}$

Y(I)                    $\mu(\lambda,Si)\rho_{Si}$

A1                      Mass absorption coefficient for element I
                        $\mu(\lambda,I)$.

A2                      Same as A1.

A3                      $\mu(\lambda,Au)\rho_{Au}t_{Au}$

D1                      X(0) Y(1) - Y(0) X(1).

E1                      Same as W(I).

F1                      $f_p$ absorption in specimen.

G1                      $\ln (M(I))$.

85

2b.  Local Variables (Continued)

      P2               Iteration number.

      T1               $\ln (f_p/E_1)$

      X1               $E_0 - E_1$

```
100     REM      THIS PROGRAM READS STANDARD SPECTRA FROM QUADRANT 2
120     GOSUB   1000
130     PRINT "ENTER NO. OF ELEMENTS"
135     INPUT N
140     PRINT
141     CALL 4,(1)
142     CALL 4,(3)
143     IF   FNA(2)= 0 GOTO   146
144     LET E0= FNA(2)/1000
145     GOTO  151
146     PRINT "ENTER E0 (YOUR TOA IS";M3;"DEG)"
147     INPUT E0
148     LET E1=(E0+.00001)*1000
149     LET L1= FNC(2)
150     CALL 3,L1,E1
151     LET L1= FNC(3)
152     CALL 3,L1, 0
154     CALL 4,(3)
155     CALL 4,(1)
160     LET Z[N]=4
170     LET Z[N+1]=14
180     LET Z[N+2]=79
181     PRINT
185     PRINT "ENTER CON, ATNO, LINE CODE AND VALENCE FOR EACH"
190     FOR I= 0 TO N+2
200       IF I>N-1 GOTO   230
210       INPUT C[I],Z[I],L[I],Q[I]
220       PRINT
230       LET L9=1
240       GOSUB  1500
250       IF L[I]= 0 GOTO   280
260       LET L9=2
270       GOSUB   1500
274       IF   FNG(I)>=1 GOTO   280
275       PRINT "LINE OF ";Z[I];" BELOW 1 KV"
276       GOTO   380
280     NEXT I
285     GOSUB  8000
290     LET N3= 0
291     CALL 4,(1)
292     CALL 4,(3)
293     LET L1= FNC(5)
294     CALL 3,L1,K1*10000
295     CALL 4,(3)
296     CALL 4,(1)
300     GOSUB  3000
310     GOSUB  2200
312     CALL 4,(1)
```

```
316    CALL 4,(3)
320    GOSUB  5100
330    FOR I= 0 TO N-1
335      LET M[I]=W[I]
340    NEXT I
352    CALL 4,(3)
356    CALL 4,(1)
360    GOSUB  5500
370    GOSUB  2700
380    STOP
390    END
500    REM    THIS PROGRAM READS A SPECIMEN SPECTRUM FROM QUADRANT 1
501    REM             THE STANDARDS INFORMATION FROM QUADRANT 4 AND PRINTS
502    REM    QUANTITATIVE RESULTS. A1, B1 AND DISPLAY ON.
520    GOSUB  1000
530    CALL 4,( 0)
550    CALL 4,(3)
570    LET N9= FNA(1)
575    LET N4= FNA(3)
576    LET L1= FNC(3)
577    CALL 3,L1,1
579    IF N4=1 GOTO  595
580    PRINT "ENTER NO. OF ELEMENTS"
590    INPUT N
591    LET L1= FNC(4)
592    CALL 3,L1,N
595    LET E0= FNA(2)/1000
596    LET N= FNA(4)
600    PRINT
610    LET Z[N]=4
620    LET Z[N+1]=14
630    LET Z[N+2]=79
635    IF N4=1 GOTO  650
640    PRINT "ENTER AT. NO. FOR EACH ELEMENT"
650    FOR I= 0 TO N+2
660      IF I>=N GOTO  680
665      IF N4=1 GOTO  675
670      INPUT Z[I]
671      LET L1= FNC(900+I)
672      CALL 3,L1,Z[I]
673      GOTO  680
675      LET Z[I]= FNA(900+I)
680      LET L9=1
690      GOSUB  1500
700      IF I>=N GOTO  800
710      FOR J=10 TO N9 STEP 10
720        IF  FNA(J)=Z[I] GOTO  750
730      NEXT J
740      GOTO  800
750      LET L[I]= FNA(J+1)
```

```
760      LET Q[I]= FNA(J+2)
770      LET L9=2
780      GOSUB  1500
790      GOTO   810
800      LET L[I]= 0
810   NEXT I
815   PRINT
820   CALL 4,(3)
840   CALL 4,( 0)
855   GOSUB  8000
860   LET N3=3
865   IF N4=1 GOTO   880
870   GOSUB  3000
880   GOSUB  5500
890   STOP
900   END
1000  REM            THIS SUBROUTINE READS IN COEFFICIENTS FOR COMPUTING
1001  REM       ENERGIES, ABSORPTION EDGE RATIOS, ATOMIC WEIGHTS,
1002  REM       KB/K RATIOS, AND ELECTRON INCIDENCE AND X-RAY
1003  REM       EMISSION ANGLES
1005  DIM C[12],Z[12],L[12],Q[12],E[8,12],G[16,12]
1006  DIM M[12],W[12],X[3],Y[3],U[12],F[3,12],S[16,12]
1007  DIM O[12,12],H[24,12],V[12,12],P[12,12]
1010  DIM K[8,2],T[16,2],R[9],A[92],B[50]
1020  DEF   FNA(I)= DTA ((I- LCN (118))/ LCN (120))
1025  DEF   FNE(I)= ECL ((I- LCS (134))/ LCS (136))
1030  DEF   FNC(I)=(I- LCN (118))/ LCN (120)
1035  DEF   FNN(I)=1000*(I- FNE ( 0))/( FNE(1000)- FNE ( 0))
1036  DEF   FNL(I)=2.905* SQR (I)-3.063
1037  DEF   FNJ(I)=9.76*I+58.5*I^(-.19)
1038  DEF   FNF(I)=.2567*I-6.8176
1039  DEF   FNM(I)= EXP (34.165*I-30.027* SQR (I)+8.5268)/1.6
1040  FOR I= 0 TO 9
1050     READ R[I]
1060  NEXT I
1070  DATA  1, 1, 1.17, 1.63, 1, 1.16, 1.4, 1.621, 1.783, 1
1080  FOR J= 0 TO 2
1090     FOR I= 0 TO 8
1100        READ K[I,J]
1110     NEXT I
1120  NEXT J
1130  DATA -3.97931E-2,-.033916,-8.65397E-2,-.228343, 1.25179
1140  DATA  .834903, .442217, .25141, .272951
1150  DATA  2.423, 2.82526, 3.32315, 4.31172,-7.838
1160  DATA -4.14925,-.979241, .931913, .688906
1170  DATA  5.5091, 9.03526, 10.2505, 12.0025,-11.5803
1180  DATA -3.33802, 3.15348, 8.03561, 7.4243
1190  FOR J= 0 TO 2
1200     FOR I= 0 TO 16
1210        READ T[I,J]
```

```
1220     NEXT I
1230   NEXT J
1240   DATA -1.99726E-2,-.123941,-.47555,-.060101
1242   DATA -.117102,-.192466,-.197431,-3.22523E-3, .035676
1244   DATA  2.88553E-3, 9.57107E-2, .092961, 5.05888E-2
1246   DATA -.390705,-.386042,-.603132, .322877
1250   DATA  2.22412, 3.29533, 6.84662, 2.52781
1252   DATA  3.22414, 3.83158, 4.01718, 2.48613, 2.29113
1254   DATA  2.49221, 1.69157, 1.7559, 2.0035
1256   DATA  6.17432, 6.14822, 7.75598, .102358
1260   DATA  5.17774, 9.75836, 20.0833, 5.6437
1262   DATA  9.58711, 10.9293, 11.3323, 8.37742, 8.09392
1264   DATA  8.60965, 6.76302, 6.81839, 7.30182
1266   DATA  19.0119, 18.7034, 21.4878, 5.58269
1270   FOR I=11 TO 30
1280     READ B[I]
1290   NEXT I
1300   DATA  .011, .027, .04, .055, .066, .078, .085, .097
1310   DATA  .108, .114, .115, .117, .119, .119, .121
1311   DATA  .121, .121, .123, .1235, .125
1320   FOR I=1 TO 92
1330     READ A[I]
1340   NEXT I
1350   DATA  1.008, 4.003, 6.94, 9.013, 10.82, 12.011
1351   DATA  14.007, 16, 19, 20.18
1360   DATA  22.99, 24.31, 26.98, 28.09, 30.97, 32.06
1361   DATA  35.45, 39.95, 39.1, 40.08
1370   DATA  44.96, 47.9, 50.94, 52, 54.94, 55.85
1371   DATA  58.93, 58.71, 63.54, 65.37
1380   DATA  69.72, 72.59, 74.92, 78.96, 79.91
1381   DATA  83.8, 85.47, 87.62, 88.91, 91.22
1390   DATA  92.91, 95.94, 99, 101.1
1391   DATA  102.9, 106.4, 107.9, 112.4, 114.8, 118.7
1400   DATA  121.8, 127.6, 126.9, 131.3, 132.9, 137.3, 138.9
1401   DATA  140.1, 140.9, 144.2
1410   DATA  145, 150.4, 152, 157, 158.9, 162.5
1411   DATA  164.9, 167.3, 168.9, 173
1420   DATA  175, 178.5, 180.95, 183.85, 186.2
1421   DATA  190.2, 192.2, 195.1, 196.97
1430   DATA  200.6, 204.4, 207.2, 209, 210, 210
1431   DATA  222, 223, 226, 227, 232
1432   DATA  231, 238
1440   LET M3=40
1450   LET Q2=90
1454   LET P6=9.165E-4
1455   LET P7=8.579E-6
1460   LET Q1=1/ SIN (M3/57.2958)
1470   LET Q2= SIN (Q2/57.2958)
1480   LET Q3=149
1485   LET Q3=Q3^2-14737.5
```

```
1490    DEF   FNS(I)= SQR (2500*I+Q3)*4.2466E-4
1492    DEF   FNG(I)=G[L[I]-1,I]
1495    RETURN
1500    REM     THIS SUBROUTINE COMPUTES ALL OF THE NECESSARY
1501    REM     EDGE AND LINE ENERGIES
1520    LET Z1= LOG (Z[I])
1530    IF L9=2 GOTO  1580
1540    FOR M1= 0 TO 8
1550      LET E[M1,I]= EXP (K[M1, 0]*Z1*Z1+K[M1,1]*Z1-K[M1,2])
1560    NEXT M1
1570    IF L9=1 GOTO  1610
1580    FOR M1= 0 TO 16
1590      LET G[M1,I]= EXP (T[M1, 0]*Z1*Z1+T[M1,1]*Z1-T[M1,2])
1600    NEXT M1
1610    RETURN
1700    REM     THIS SUBROUTINE COMPUTES ALL MASS ABSORPTION
1701    REM     COEFFICIENTS REQUIRED
1710    DIM D[3,3]
1720    LET D[ 0, 0]=-.232229
1730    LET D[ 0,1]=-.254471
1740    LET D[ 0,2]=.256216
1750    LET D[ 0,3]=1.35917
1760    LET D[1, 0]=4.07005
1770    LET D[1,1]=4.76925
1780    LET D[1,2]=1.15119
1790    LET D[1,3]=-9.49212
1800    LET D[2, 0]=-6.22075
1810    LET D[2,1]=-10.3788
1820    LET D[2,2]=-5.68485
1830    LET D[2,3]=18.6408
1840    LET D[3,2]=2.6
1850    LET D[3,3]=2.22
1860    LET Z1= LOG (Z[I])
1870    LET D[3, 0]= EXP (-4.5522E-3*Z1*Z1-6.8535E-3*Z1+1.07018)
1880    LET D[3,1]=2.73
1890    IF Z[I]<42 GOTO  1910
1900    LET D[3,1]= EXP (-.11316*Z1*Z1+.836883*Z1-.545969)
1910    FOR M1= 0 TO 9
1920      LET M3=M1+1
1930      IF M1=9 GOTO  1945
1940      IF E1<E[M1,I] GOTO  1970
1945      LET L1=M1- INT (M3/3)- INT (M3/4)- INT (M3/7)
1950      LET C2= EXP (D[ 0,L1]*Z1*Z1+D[1,L1]*Z1+D[2,L1])/R[M1]
1955      LET A1=C2*(12.398/E1)^D[3,L1]
1960      GOTO  1980
1970    NEXT M1
1980    RETURN
2000    REM         THIS SUBROUTINE COMPUTES THE DETECTOR EFFICIENCY
2010    LET I=N
2020    GOSUB  1700
```

```
2030    LET A3=A1*1.82*P6
2040    LET I=N+2
2050    GOSUB  1700
2060    LET A4=A1*19.3*8E-7
2070    LET I=N+1
2080    GOSUB  1700
2090    LET D2= EXP (-A3-A4-A1*2.33*P7)*(1- EXP (-A1*2.33*.469))
2095    RETURN
2100    REM     THIS SUBROUTINE COMPUTES THE ABSORPTION FACTOR
2101    REM     FOR ANY LINE
2110    LET X3=A2*Q1
2120    LET G1=(E0^1.65-E1^1.65)*Q2
2130    LET F1=1/(1+1.2E-6*G1*X3)^2
2140    RETURN
2200    REM     THIS SUBROUTINE COMPUTES BACKGROUND UNDER EACH PEAK
2220    FOR I= 0 TO 1
2230      LET M[I]= ROI (I)/( LCN (158)- LCN (157))
2240      LET W[I]= FNE(( LCN (157)+ LCN (158))/2)
2250    NEXT I
2260    FOR J= 0 TO 1
2270      LET A2= 0
2280      LET E1=W[J]
2290      FOR I= 0 TO N-1
2300        GOSUB  1700
2310        LET A2=A2+C[I]*A1
2320      NEXT I
2330      GOSUB  2000
2340      GOSUB  2100
2350      LET T1=D2*F1/E1
2360      LET X[J]=E0-E1
2370      LET Y[J]=M[J]/T1
2380      LET U[J]=X[J]*X[J]
2390    NEXT J
2400    LET D1=X[ 0]*U[1]-U[ 0]*X[1]
2410    LET K1=(Y[1]*X[ 0]-Y[ 0]*X[1])/D1
2420    LET K2=(Y[ 0]*U[1]-Y[1]*U[ 0])/D1
2425    IF L[ 0]=10 GOTO  2620
2430    FOR J= 0 TO N-1
2440      IF L[J]= 0 GOTO  2610
2450      LET J1=L[J]-1
2460      LET E1=G[J1,J]
2470      LET T5= ROI (J+2)
2480      LET A2= 0
2490      FOR I= 0 TO N-1
2500        GOSUB  1700
2510        LET A2=A2+C[I]*A1
2520      NEXT I
2530      GOSUB  2000
2540      GOSUB  2100
2550      LET T1=D2*F1/E1
```

```
2560      LET X1=E0-E1
2570      LET G1=T1*(K1*X1*X1+K2*X1)
2580      LET G2= LCN (158)- LCN (157)
2590      LET M[J]=T5-G1*G2
2600      LET F[1,J]=F1
2610    NEXT J
2620    RETURN
2700    REM      THIS SUBROUTINE WRITES STANDARDS INFORMATION INTO
2701    REM          QUADRANT 4.
2710    CALL 4,(1)
2730    CALL 4,(3)
2750    LET N9= FNA(1)
2760    FOR I= 0 TO N-1
2770      IF L[I]= 0 GOTO  2850
2780      LET N9=N9+10
2790      LET L1= FNC(N9)
2800      CALL 3,L1,Z[I]
2810      LET L1= FNC(N9+1)
2820      CALL 3,L1,L[I]
2830      LET L1= FNC(N9+2)
2840      CALL 3,L1,M[I]
2842      LET L1= FNC(N9+3)
2843      CALL 3,L1,Q[I]
2850    NEXT I
2860    LET L1= FNC(1)
2870    CALL 3,L1,N9
2880    CALL 4,(3)
2900    CALL 4,(1)
2920    RETURN
3000    REM      THIS SUBROUTINE COMPUTES OVERLAP FUNCTION OF ONE
3001    REM          PEAK ON ANOTHER.
3010    LET G4= 0
3015    IF N3> 0 GOTO  3025
3017    CALL 4,(1)
3020    GOTO  3027
3025    CALL 4,( 0)
3027    CALL 4,(3)
3029    FOR I=300 TO 899
3030      LET L1= FNC(I)
3031      CALL 3,L1, 0
3032    NEXT I
3034    FOR I= 0 TO N-1
3035      IF L[I]= 0 GOTO  3200
3040      LET E7= FNG(I)
3050      LET S6= FNS(E7)
3052      LET T5= ROI (I+2)
3056      LET E3= FNE( LCN (157))
3060      LET E4= FNE( LCN (158))
3070      LET X2=(E3-E7)/S6/1.4142
3080      GOSUB  4500
```

```
3085      GOSUB  4200
3090      LET E1= ABS (E8)/2
3100      LET X2=(E4-E7)/S6/1.4142
3110      GOSUB  4500
3120      LET E2= ABS (E8)/2
3130      IF E3<=E7 GOTO  3160
3140      LET W[I]=E2-E1
3150      GOTO  3195
3160      IF E4>=E7 GOTO  3190
3170      LET W[I]=E1-E2+G4
3180      GOTO  3195
3190      LET W[I]=E1+E2÷G4
3195      LET M[I]=W[I]
3200    NEXT I
3205    FOR K1= 0 TO 1
3230      FOR I1= 0 TO N-1
3240        IF L[I1]= 0 GOTO  3390
3245        LET J1= 0
3250        LET T5= FNG(I1)
3260        LET D3=4* FNS(T5)
3270        LET I=N+1
3280        LET S6= ROI (I1+2)
3290        LET E3= FNE( LCN (157))
3300        LET E4= FNE( LCN (158))
3310        FOR J= 0 TO N-1
3320          IF L[J]= 0 GOTO  3350
3325          IF K1=1 GOTO  3340
3330          IF J=I1 GOTO  3340
3335          GOTO  3350
3340          LET X2=1/ LOG (E0*E0/E[3,J]/E[8,J])
3345          GOSUB  3500
3350        NEXT J
3360        IF K1=1 GOTO  3390
3381        FOR J= 0 TO 16
3382          LET L1= FNC(I1*20+700+J)
3384          LET O2=S[J,I1]*100000
3385          IF O2> 0 GOTO  3387
3386          LET O2= 0
3387          CALL 3,L1,O2
3389        NEXT J
3390      NEXT I1
3395    NEXT K1
3400    CALL 4,(3)
3410    IF N3= 0 GOTO  3440
3420    CALL 4,( 0)
3430    GOTO  3450
3440    CALL 4,(1)
3450    RETURN
3490    REM      COMPUTE OVERLAPS FOR EACH LINE
3500    LET O2= 0
```

```
3501    LET X[1]= EXP (2.373* LOG (Z[J])-8.902)
3502    LET X[2]= EXP (2.946* LOG (Z[J])-13.94)
3503    LET X[3]=2.27E-5*Z[J]^2-.001359*Z[J]-.00657
3504    FOR L2= 0 TO 8
3505      LET M1=L2+1
3506      LET I2=M1- INT (M1/3)- INT (M1/4)- INT (M1/7)
3507      LET M3=2*( INT (M1/I2)- INT (M1/6)+ INT (M1/7))
3508      IF E[L2,J]>=E0 GOTO  3513
3509      LET E1=E0/E[L2,J]
3510      LET E2=1166*E[L2,J]/ FNJ(Z[J])
3511      LET X1=E1*E2
3512      LET U[M1]=M3*(E1-1- LOG (E2)/E2*( FNL(X1)- FNL(E2)))*X[I2]
3513    NEXT L2
3514    LET A4=1
3515    LET A5=1
3516    LET A1=1
3517    LET A2=1
3518    LET A3=1
3519    IF L[J]=3 GOTO  3530
3520    IF L[J]=2 GOTO  3525
3521    LET A2=U[4]/U[1]* FNF(Z[J])
3522    LET A4=U[2]/U[1]* FNF(Z[J])
3523    LET A5=U[3]/U[1]* FNF(Z[J])
3524    GOTO  3533
3525    LET A1=U[1]/U[4]/ FNF(Z[J])
3526    LET A3= FNM(X2)
3527    LET A4=U[2]/U[4]
3528    LET A5=U[3]/U[4]
3529    GOTO  3533
3530    LET A2=1/ FNM(X2)
3531    LET A4=U[2]/U[4]/ FNM(X2)
3532    LET A5=U[3]/U[4]/ FNM(X2)
3533    LET S[ 0,J]=A1
3534    IF Z[J]>50 GOTO   3540
3535    LET R1=B[Z[J]]
3536    IF Z[J]<=30 GOTO   3538
3537    LET R1=.115*( LOG (Z[J])-2.3)
3538    LET S[3,J]=R1/(1-R1)*A1
3540    LET S[1,J]=A2
3550    LET S[2,J]=A3
3571    LET S[4,J]=.1*A2
3572    LET S[5,J]=.044*A2
3573    LET S[6,J]=(.2808-.0016*Z[J])*A2
3574    LET S[7,J]=A5
3575    LET S[8,J]=.154*A5
3576    LET S[9,J]=.02*A5
3577    LET S[10,J]=.166*A4
3578    LET S[11,J]=.068*A4
3579    LET S[12,J]=.104*A4
3602    LET S[13,J]=.06*A3
```

```
3603    LET S[14,J]=.5*A3*U[8]/U[9]
3604    LET S[15,J]=.05*A3*U[7]/U[9]
3605    LET S[16,J]=.01*A3*U[6]/U[9]
3625    IF I1=J GOTO  3730
3630    LET E7= FNG(J)
3640    LET S6= FNS(E7)
3642    FOR I2= 0 TO 16
3643      IF S[I2,J]> 0 GOTO  3645
3644      LET S[I2,J]= 0
3645    NEXT I2
3730    FOR I2= 0 TO 16
3740      LET E7=G[I2,J]
3742      IF T5=E7 GOTO  3840
3744      IF E7<1 GOTO   3840
3746      IF E7>E0 GOTO   3840
3750      LET S6= FNS(E7)
3760      IF E7<T5-D3 GOTO   3840
3770      IF E7>T5+D3 GOTO   3820
3780      GOSUB  4000
3805      IF K1= 0 GOTO  3815
3810      LET O2=O1/W[J]*S[I2,J]
3812      GOSUB  3855
3814      GOTO  3840
3815      IF I2=L[J]-1 GOTO  3840
3816      LET W[J]=W[J]+O1*S[I2,J]
3819      GOTO  3840
3820      LET S8= 0
3825      GOSUB  3900
3830      LET O2=O1/W[J]*S8*S[I2,J]
3835      GOSUB  3855
3840    NEXT I2
3850    RETURN
3855    LET O2= INT (O2*100000)
3860    IF O2= 0 GOTO  3886
3861    LET E9= 0
3862    LET X2=J
3864    GOTO  3876
3866    LET E9=1
3868    LET X2=I2
3870    GOTO  3876
3872    LET E9=2
3874    LET X2=O2
3876    LET L1= FNC(I1*40+300+E9+J1)
3878    CALL 3,L1,X2
3880    IF E9= 0 GOTO  3866
3882    IF E9=1 GOTO   3872
3884    LET J1=J1+3
3886    RETURN
3890    REM      COMPUTE ESCAPE PEAKS
3900    IF E7<1.838 GOTO  3990
```

```
3903    LET E1=E7
3905    LET E7=E7-1.74
3910    IF T5<E7-D3 GOTO   3990
3920    IF T5>E7+D3 GOTO   3990
3940    GOSUB   1700
3950    LET S7=.5*(1-327.9/A1* LOG (1+A1/327.9))
3960    LET S8=.038*S7/(1-.038*S7)
3970    LET S6= FNS(E7)
3980    GOSUB   4000
3990    RETURN
4000    REM         THIS FUNCTION COMPUTES SPECIFIC OVERLAPS
4010    LET X2=(E3-E7)/S6/1.4142
4020    GOSUB   4500
4025    GOSUB   4200
4030    LET E2= ABS (E8)/2
4040    LET X2=(E4-E7)/S6/1.4142
4050    GOSUB   4500
4055    LET E8= ABS (E8)/2
4060    IF E3>=E7 GOTO   4100
4070    IF E4<=E7 GOTO   4120
4080    LET O1=E2+E8+G4
4090    RETURN
4100    LET O1=E8-E2
4110    RETURN
4120    LET O1=E2-E8+G4
4130    RETURN
4200    REM            THIS FUNCTION COMPUTES AN INCOMPLETE CHARGE
4201    REM            CORRECTION FOR ALL PEAKS.
4210    LET G4= 0
4220    LET X1=6
4230    LET X3=.1
4240    IF E7>=6.4 GOTO   4300
4250    LET X1=.86166*E7*E7-7.4431*E7+18.342
4260    LET X3=-.01683*E7*E7+.14129*E7-.11489
4270    IF X3<= 0 GOTO   4400
4300    IF E3>=E7 GOTO   4400
4310    LET X2=(E3-E7)/X3
4320    LET G4=X1*X3*X3*(1- EXP (X2)*(1-X2))
4330    IF E4>=E7 GOTO   4400
4340    LET X2=(E4-E7)/X3
4350    LET G4=G4-X1*X3*X3*(1- EXP (X2)*(1-X2))
4400    RETURN
4500    REM     THIS FUNCTION INTEGRATES AREA UNDER A GAUSSIAN PEAK
4510    LET T1=2^(-27)
4520    IF X2= 0 GOTO   5070
4530    LET Y1= ABS (X2)
4540    LET Y2=Y1*Y1
4550    IF Y1<=1 GOTO   4630
4560    LET C1=2^(3.5)
4570    LET U1=.83*C1
```

```
4580    LET S1=2^(C1*C1-8)
4590    IF Y1<=U1 GOTO  4770
4600    LET E8=1
4610    LET E9= 0
4620    GOTO  4730
4630    LET S2= 0
4640    LET D1=1
4650    LET T2=1
4660    LET P2=2*Y2
4670    LET D1=D1+2
4680    LET T2=P2*T2/D1
4690    LET S2=T2+S2
4700    IF T2>=T1 GOTO  4670
4710    LET E8=(S2+1)*1.12838*Y1* EXP (-Y2)
4720    LET E9=1-E8
4730    IF X2>= 0 GOTO  4760
4740    LET E8=-E8
4750    LET E9=2-E9
4760    RETURN
4770    LET F2= 0
4780    LET G2=1
4790    LET F1=2*Y1
4800    LET G1=2*Y2+1
4810    LET P3=F1/G1
4820    LET W1=1
4830    LET B1=G1+4
4840    LET A5=-W1*(W1+1)
4850    LET F3=B1*F1+A5*F2
4860    LET G3=B1*G1+A5*G2
4870    LET F4=F3/G3
4880    IF  ABS (1-F4/P3)<=T1 GOTO  5040
4890    IF P3>F4 GOTO  5030
4900    IF G3<S1 GOTO  4950
4910    LET F3=F3/S1
4920    LET G3=G3/S1
4930    LET F1=F1/S1
4940    LET G1=G1/S1
4950    LET F2=F1
4960    LET G2=G1
4970    LET F1=F3
4980    LET G1=G3
4990    LET W1=W1+2
5000    LET B1=B1+4
5010    LET P3=F4
5020    GOTO  4840
5030    LET F4=P3
5040    LET E9=F4* EXP (-Y2)*1.12838/2
5050    LET E8=1-E9
5060    GOTO  4730
5070    LET E8= 0
```

```
5080    LET E9=1
5090    RETURN
5100    REM          THIS SUBROUTINE CORRECTS PEAKS FOR OVERLAP USING
5101    REM          PREVIOUSLY COMPUTED OVERLAP FACTORS.
5110    FOR J= 0 TO N-1
5120      IF L[J]= 0 GOTO  5230
5140      LET A2= 0
5146      LET E1= FNG(J)
5147      GOSUB  2000
5148      FOR I= 0 TO N-1
5150        GOSUB  1700
5152        LET A2=A2+C[I]*A1
5154      NEXT I
5156      GOSUB  2100
5158      LET F[3,J]=F1*D2
5220      LET W[J]=M[J]
5230    NEXT J
5240    FOR T1= 0 TO 2
5250      FOR B1= 0 TO N-1
5255        IF L[B1]= 0 GOTO   5370
5260        LET R1= 0
5265        LET J=B1*40+300
5270        FOR D1= 0 TO 26 STEP 3
5275          LET L2= FNA(J+D1)
5285          LET G1= FNA(J+D1+1)
5290          LET Y1= FNA(J+D1+2)/100000
5292          IF Y1= 0 GOTO   5360
5295          LET E1=G[G1,L2]
5300          LET A2= 0
5305          GOSUB  2000
5310          FOR I= 0 TO N-1
5315            GOSUB  1700
5320            LET A2=A2+C[I]*A1
5325          NEXT I
5330          GOSUB  2100
5340          LET R1=R1+F1*D2*W[L2]*Y1/F[3,L2]
5350        NEXT D1
5360        LET W[B1]=M[B1]-R1
5370      NEXT B1
5380    NEXT T1
5390    RETURN
5500    REM     THIS SUBROUTINE COMPUTES THE MATRIX CORRECTIONS FOR
5501    FOR J= 0 TO 12
5502      FOR I= 0 TO 12
5503        LET P[I,J]= 0
5504      NEXT I
5505    NEXT J
5510    FOR J= 0 TO N-1
5520      IF L[J]= 0 GOTO   6400
5530      LET B1=L[J]^2-1
```

```
5540        IF B1<9 GOTO   5560
5550        LET B1= 0
5560        LET U[J]=E0/E[B1,J]
5570        IF U[J]>=1.5 GOTO   5590
5580        PRINT "OVERVOLTAGE TOO LOW"
5590        LET E1= FNG(J)
5600        FOR I= 0 TO N-1
5610          GOSUB   1700
5620          LET H[I,J]=A1
5630        NEXT I
5750        LET A2=H[J,J]
5760        GOSUB   2100
5770        LET F[ 0,J]=F1
5780        IF L[J]>1 GOTO   5820
5790        LET C1=5
5800        LET F3= 0
5810        GOTO   5890
5820        IF L[J]>2 GOTO   5860
5830        LET C1=3.5
5840        LET F3=1
5850        GOTO   5890
5860        IF L[J]>3 GOTO   5790
5870        LET C1=3.5
5880        LET F3=2
5890        FOR I1= 0 TO N-1
5900          IF I1=J GOTO   6160
5910          LET P3= 0
5920          LET L2=(P3+1)^2-1
5930          IF 1.02*E[L2,I1]-E0>= 0 GOTO   6130
5940          IF G[P3,I1]<E[B1,J] GOTO   6160
5950          IF G[P3,I1]>E[B1,J]+C1 GOTO   6130
5960          LET P[J,I1]=P3+1+2*F3
5970          LET O[J,I1]=E0/E[L2,I1]
6030          LET E1=G[P3,I1]
6040          FOR I= 0 TO N-1
6050            GOSUB   1700
6060            LET H[I+13,I1]=A1
6070          NEXT I
6120          GOTO   6160
6130          IF P3=1 GOTO   6160
6140          LET P3=1
6150          GOTO   5920
6160        NEXT I1
6170        FOR I= 0 TO N-1
6180          IF P[J,I]= 0 GOTO   6381
6190          LET Y1=A[Z[J]]/A[Z[I]]*H[J+13,I]/2*((O[J,I]-1)/(U[J]-1))^1.6

6200          LET T1= EXP (2.373* LOG  (Z[I])-8.902)
6210          LET T2= EXP (2.946* LOG  (Z[I])-13.94)
6220          IF P[J,I]>1 GOTO   6250
```

```
6230        LET D1=.88*T1
6240        GOTO   6380
6250        IF P[J,I]>2 GOTO   6280
6260        LET D1=3.696*T2
6270        GOTO   6380
6280        IF P[J,I]>3 GOTO   6310
6290        LET D1=.18*T1
6300        GOTO   6380
6310        IF P[J,I]>4 GOTO   6340
6320        LET D1=.75*T2
6330        GOTO   6380
6340        IF P[J,I]>5 GOTO   6370
6350        LET D1=.01*T1
6360        GOTO   6380
6370        LET D1=.01*T2
6380        LET O[J,I]=D1*Y1
6381     NEXT I
6382     LET U1=U[J]
6383     IF U1<=10 GOTO   6385
6384     LET U1=10
6385     LET G1=.00873*U1^3-.1669*U1*U1+.9662*U1+.4523
6386     LET G2=.002703*U1^3-.05182*U1*U1+.302*U1-.1836
6387     LET P2=.887-3.44/U1+9.33/U1^2-6.43/U1^3
6392     FOR I= 0 TO N-1
6394        LET V[I,J]=G1-G2* LOG (P2*Z[I]+25)
6395        LET S[I,J]=2*Z[I]/(A[Z[I]]*(E0+E[B1,J]))
6396        LET S[I,J]=S[I,J]* LOG (583*(E0+E[B1,J])/ FNJ(Z[I]))
6398     NEXT I
6400   NEXT J
6405   LET G4= 0
6410   IF N3= 0 GOTO   6550
6417   PRINT "NO PLOT ENTER 0"
6418   INPUT G4
6420   LET S1= 0
6425   PRINT
6430   FOR I= 0 TO N-1
6440     IF L[I]= 0 GOTO   6480
6450     LET M[I]= ROI (I+2)
6460     LET M[I]=M[I]/Q[I]
6470     LET S1=S1+M[I]
6480   NEXT I
6490   IF L[N-1]> 0 GOTO   6520
6500   LET C[N-1]=1-S1
6510   LET S1=1
6520   FOR I= 0 TO N-1
6530     LET C[I]=M[I]/S1
6540   NEXT I
6550   FOR N1= 0 TO N3
6560     FOR I1= 0 TO N-1
6570        IF L[I1]= 0 GOTO   6880
```

```
6580          LET S2= 0
6590          LET X2= 0
6600          LET A2= 0
6610          FOR J= 0 TO N-1
6620            LET S2=S2+C[J]*S[J,I1]
6630            LET X2=X2+C[J]*V[J,I1]
6640            LET A2=A2+C[J]*H[J,I1]
6650          NEXT J
6660          LET E1= FNG(I1)
6670          GOSUB  2100
6680          LET W1=(V[I1,I1]*S2)/(S[I1,I1]*X2)
6690          LET F[1,I1]=F1
6700          LET F2= 0
6710          FOR J= 0 TO N-1
6720            IF P[I1,J]= 0 GOTO  6810
6730            LET A3= 0
6740            FOR I= 0 TO N-1
6750              LET A3=A3+C[I]*H[I+13,J]
6760            NEXT I
6770            LET X1=Q1*A2/A3
6780            LET B1=(333000/(E0^1.65-E1^1.65))/A3*Q2
6790            LET F4= LOG (1+X1)/X1+ LOG (1+B1)/B1
6800            LET F2=F2+C[J]*O[I1,J]/A3*F4
6810          NEXT J
6815          IF C[I1]= 0 GOTO  6880
6820          LET G3=C[I1]/W1*(1+F2)*F[1,I1]/F[ 0,I1]
6830          IF N3> 0 GOTO  6870
6835          IF L[I1]= 0 GOTO  6880
6840          LET M[I1]=M[I1]/G3
6850          PRINT "MELS =";G3
6860          GOTO  6880
6870          LET G2=M[I1]*C[I1]
6872          LET C[I1]=G2*(1-G3)/(G2+G3*(1-M[I1]-C[I1]))
6874          IF N1<N3 GOTO  6880
6875          IF G4= 0 GOTO  6880
6876          GOSUB  8200
6880        NEXT I1
6890        IF N3= 0 GOTO  7110
6900        LET S1= 0
6910        FOR I= 0 TO N-1
6915          IF L[I]= 0 GOTO  6930
6916          IF C[I]> 0 GOTO  6920
6917          LET C[I]= 0
6920          LET S1=S1+C[I]
6930        NEXT I
6940        IF L[N-1]> 0 GOTO  6970
6950        GOSUB  8600
6970        IF N1=N3 GOTO  7050
6980        GOSUB  2200
6982        CALL 4,( 0)
```

```
6986      CALL 4,(3)
6990      GOSUB  5100
6992      CALL 4,(3)
6996      CALL 4,( 0)
7000      FOR I= 0 TO N-1
7010        IF L[I]= 0 GOTO  7040
7020        LET M[I]=W[I]/Q[I]
7030        LET C[I]=C[I]/S1
7040      NEXT I
7050     NEXT N1
7060     PRINT "Z","C","F(X)","K"
7070     FOR I= 0 TO N-1
7075       IF L[I]= 0 GOTO  7085
7080       PRINT Z[I],C[I],F[1,I],M[I]
7082       GOTO  7090
7085       PRINT Z[I],C[I]
7090     NEXT I
7100     PRINT "TOTAL =";S1
7105     CALL 4,(2)
7110     FOR I= 0 TO 1
7120       LET T5= ROI (I)
7130       PRINT "ROI";I, FNE( LCN (157)); FNE( LCN (158))
7140     NEXT I
7150     RETURN
8000     REM      SUBROUTINE TO CREATE A ROI FOR EACH MEASURED LINE
8010     LET L1=644
8015     LET K2=1
8020     LET K1=1.1775
8030     FOR I= 0 TO N-1
8040       IF L[I]= 0 GOTO  8130
8045       LET K2=K2+1
8046       LET I1=L[I]-1
8050       LET S1= FNS(G[I1,I])
8060       LET E1= FNN(G[I1,I]-K1*S1)
8070       LET E2= FNN(G[I1,I]+K1*S1)
8075       CALL 1,101,K2
8080       CALL 1,L1,E1
8090       LET L1=L1+1
8100       CALL 1,L1,E2
8110       LET L1=L1+1
8120       CALL 5
8130     NEXT I
8140     RETURN
8200     REM              THIS ROUTINE RECONSTRUCTS PEAKS IN QUADRANT 3
8210     LET T5=G3*Q[I1]/F[3,I1]
8230     CALL 4,(3)
8240     LET K2= FNA(5)/10000
8250     LET E1= FNG(I1)
8260     LET S1= FNS(E1)
8270     LET E3= FNN(E1-K2*S1)
```

```
8280    LET E4= FNN(E1+K2*S1)
8290    LET G1= 0
8300    LET E2=1
8305    LET S2=S1
8310    GOSUB  8500
8315    LET T5=T5/G1*S1
8320    FOR K1= 0 TO 16
8330      LET E1=G[K1,I1]
8340      IF E1<.7 GOTO  8450
8345      IF E1>10 GOTO   8450
8350      LET S2= FNS(E1)
8355      LET E3= FNN(E1-4*S2)
8360      LET E4= FNN(E1+4*S2)
8365      LET S6= FNA(700+20*I1+K1)/100000
8370      IF S6= 0 GOTO  8450
8375      LET E2=T5/S2*S6
8380      LET A2= 0
8385      FOR I= 0 TO N-1
8390        GOSUB  1700
8395        LET A2=A2+C[I]*A1
8400      NEXT I
8405      GOSUB  2000
8410      GOSUB  2100
8415      LET E2=E2*D2*F1
8425      CALL 4,(2)
8430      GOSUB  8500
8435      CALL 5
8440      CALL 4,(2)
8445     .CALL 4,(3)
8450    NEXT K1
8460    CALL 4,( 0)
8470    RETURN
8500    FOR J=E3 TO E4
8505      IF J>1023 GOTO  8590
8510      LET J1= FNE(J)
8520      LET T1=E2* EXP (-.5* ABS ((J1-E1)/S2)^2)
8530      IF E2>1 GOTO  8560
8540      LET G1=G1+T1
8550      GOTO  8590
8560      LET L1= FNC(J)
8570      LET T1=T1+ FNA(J)
8580      CALL 3,L1,T1
8590    NEXT J
8595    RETURN
8600    REM        STOICHIOMETRY CALC
8605    LET C[N-1]= 0
8610    CALL 4,( 0)
8620    CALL 4,(3)
8630    FOR I= 0 TO N-2
8640      FOR J=10 TO N9 STEP 10
```

```
8650       IF   FNA(J)=Z[I]  GOTO    8670
8660     NEXT J
8665     PRINT "ELEMENT ";Z[I];" NOT FOUND"
8667     STOP
8670     LET G3= FNA(J+3)
8675     IF G3= 0 GOTO   8720
8680     LET F3=.5*C[I]*G3*A[Z[N-1]]/A[Z[I]]
8690     LET C[N-1]=C[N-1]+F3
8700   NEXT I
8702   LET S1=S1+C[N-1]
8704   CALL 4,(3)
8705   CALL 4,( 0)
8710   RETURN
8720   LET C[N-1]=1-S1
8730   LET S1=1
8740   RETURN
```

```
100     REM         THIS ROUTINE COMPUTES THE THICKNESS OF THE BE WINDOW
102     REM    AND THE THICKNESS OF THE SI DEAD LAYER
130     GOSUB   1000
135     PRINT "ENTER AT. NO. AND E0"
140     INPUT Z[ 0],E0
141     PRINT
142     LET L[ 0]=10
143     LET N9=1
144     LET N=1
145     LET Z[N]=4
146     LET Z[N+1]=14
147     LET Z[N+2]=79
148     FOR I= 0 TO N+2
149       GOSUB   1500
150     NEXT I
151     LET C[ 0]=1
152     FOR P2= 0 TO 14
154       GOSUB   2200
155       FOR I=2 TO 3
160         LET M[I]= ROI (I)/( LCN (158)- LCN (157))
170         LET W[I]= FNE(( LCN (157)+ LCN (158))/2)
180       NEXT I
181       FOR J=2 TO 3
185         LET I= 0
190         LET E1=W[J]
200         GOSUB   1700
210         LET A2=A1
220         GOSUB   2100
230         LET T1= LOG (F1/E1)
240         LET G1= LOG (M[J])
250         LET X1=E0-E1
260         LET I=N
270         GOSUB   1700
274         LET X[J-2]=A1*1.82
275         LET I=N+1
276         GOSUB   1700
280         LET Y[J-2]=A1*2.33
285         LET I=N+2
290         GOSUB   1700
291         LET A3=A1*19.3*8E-7
292         LET U[J-2]= LOG (K1*X1*X1+K2*X1)-G1+T1-A3
293       NEXT J
294       LET D1=X[ 0]*Y[1]-Y[ 0]*X[1]
295       LET P6=(U[ 0]*Y[1]-U[1]*Y[ 0])/D1
296       LET P7=(X[ 0]*U[1]-X[1]*U[ 0])/D1
300       PRINT "T BE=";P6;"T SI=";P7
310     NEXT P2
312     PRINT "INSERT THESE VALUES INTO LINES 1454 AND 1455"
320     STOP
390     END
```

NBS-114A (REV. 9-78)

| U.S. DEPT. OF COMM.<br>BIBLIOGRAPHIC DATA<br>SHEET | 1. PUBLICATION OR REPORT NO.<br>NBS TN-1106 | 2. Gov't Accession No. | 3. Recipient's Accession No. |
|---|---|---|---|

| 4. TITLE AND SUBTITLE | | 5. Publication Date |
|---|---|---|
| FRAME C: A Compact Procedure for Quantitative Energy-Dispersive Electron Probe X-ray Analysis | | September 1979 |
| | | 6. Performing Organization Code |

| 7. AUTHOR(S)<br>R. L. Myklebust, C. E. Fiori, and K. F. J. Heinrich | 8. Performing Organ. Report No. |
|---|---|

| 9. PERFORMING ORGANIZATION NAME AND ADDRESS | 10. Project/Task/Work Unit No. |
|---|---|
| NATIONAL BUREAU OF STANDARDS<br>DEPARTMENT OF COMMERCE<br>WASHINGTON, DC 20234 | 11. Contract/Grant No. |

| 12. SPONSORING ORGANIZATION NAME AND COMPLETE ADDRESS (Street, City, State, ZIP) | 13. Type of Report & Period Covered |
|---|---|
| Same as above. | Final |
| | 14. Sponsoring Agency Code |

**15. SUPPLEMENTARY NOTES**

☐ Document describes a computer program; SF-185, FIPS Software Summary, is attached.

**16. ABSTRACT** *(A 200-word or less factual summary of most significant information. If document includes a significant bibliography or literature survey, mention it here.)*

A data evaluation procedure (FRAME C) for carrying out quantitative electron probe microanalysis with a lithium-drifted silicon detector was developed for use with a small computer. The procedure consists of a background correction calculated from two selected background regions of interest, a simple method of resolving overlapping peaks, and the matrix corrections for characteristic radiation (ZAF). To save computation time, small groups of adjacent channels (regions of interest) in the multi-channel analyzer rather than individual channels are used for the calculations. The method for computing the overlap factors is described. Examples of several types of analyses are presented.

**17. KEY WORDS** *(six to twelve entries; alphabetical order; capitalize only the first letter of the first key word unless a proper name; separated by semicolons)* Computer program; energy dispersive detector; multichannel analyzer; peak overlap; quantitative electron probe microanalysis; x-ray continuum; x-ray spectrum

| 18. AVAILABILITY ☒ Unlimited | 19. SECURITY CLASS (THIS REPORT) | 21. NO. OF PRINTED PAGES |
|---|---|---|
| ☐ For Official Distribution. Do Not Release to NTIS | UNCLASSIFIED | 111 |
| ☒ Order From Sup. of Doc., U.S. Government Printing Office, Washington, DC 20402, SD Stock No. SN003-003- 02113-4 | 20. SECURITY CLASS (THIS PAGE) | 22. Price |
| ☐ Order From National Technical Information Service (NTIS), Springfield, VA, 22161 | UNCLASSIFIED | $4.00 |

# NBS TECHNICAL PUBLICATIONS

## PERIODICALS

**JOURNAL OF RESEARCH**—The Journal of Research of the National Bureau of Standards reports NBS research and development in those disciplines of the physical and engineering sciences in which the Bureau is active. These include physics, chemistry, engineering, mathematics, and computer sciences. Papers cover a broad range of subjects, with major emphasis on measurement methodology, and the basic technology underlying standardization. Also included from time to time are survey articles on topics closely related to the Bureau's technical and scientific programs. As a special service to subscribers each issue contains complete citations to all recent NBS publications in NBS and non-NBS media. Issued six times a year. Annual subscription: domestic $17.00; foreign $21.25. Single copy, $3.00 domestic; $3.75 foreign.

Note: The Journal was formerly published in two sections: Section A "Physics and Chemistry" and Section B "Mathematical Sciences."

**DIMENSIONS/NBS**

This monthly magazine is published to inform scientists, engineers, businessmen, industry, teachers, students, and consumers of the latest advances in science and technology, with primary emphasis on the work at NBS. The magazine highlights and reviews such issues as energy research, fire protection, building technology, metric conversion, pollution abatement, health and safety, and consumer product performance. In addition, it reports the results of Bureau programs in measurement standards and techniques, properties of matter and materials, engineering standards and services, instrumentation, and automatic data processing.

Annual subscription: Domestic, $11.00; Foreign $13.75

## NONPERIODICALS

**Monographs**—Major contributions to the technical literature on various subjects related to the Bureau's scientific and technical activities.

**Handbooks**—Recommended codes of engineering and industrial practice (including safety codes) developed in cooperation with interested industries, professional organizations, and regulatory bodies.

**Special Publications**—Include proceedings of conferences sponsored by NBS, NBS annual reports, and other special publications appropriate to this grouping such as wall charts, pocket cards, and bibliographies.

**Applied Mathematics Series**—Mathematical tables, manuals, and studies of special interest to physicists, engineers, chemists, biologists, mathematicians, computer programmers, and others engaged in scientific and technical work.

**National Standard Reference Data Series**—Provides quantitative data on the physical and chemical properties of materials, compiled from the world's literature and critically evaluated. Developed under a world-wide program coordinated by NBS. Program under authority of National Standard Data Act (Public Law 90-396).

NOTE: At present the principal publication outlet for these data is the Journal of Physical and Chemical Reference Data (JPCRD) published quarterly for NBS by the American Chemical Society (ACS) and the American Institute of Physics (AIP). Subscriptions, reprints, and supplements available from ACS, 1155 Sixteenth St. N.W., Wash., D.C. 20056.

**Building Science Series**—Disseminates technical information developed at the Bureau on building materials, components, systems, and whole structures. The series presents research results, test methods, and performance criteria related to the structural and environmental functions and the durability and safety characteristics of building elements and systems.

**Technical Notes**—Studies or reports which are complete in themselves but restrictive in their treatment of a subject. Analogous to monographs but not so comprehensive in scope or definitive in treatment of the subject area. Often serve as a vehicle for final reports of work performed at NBS under the sponsorship of other government agencies.

**Voluntary Product Standards**—Developed under procedures published by the Department of Commerce in Part 10, Title 15, of the Code of Federal Regulations. The purpose of the standards is to establish nationally recognized requirements for products, and to provide all concerned interests with a basis for common understanding of the characteristics of the products. NBS administers this program as a supplement to the activities of the private sector standardizing organizations.

**Consumer Information Series**—Practical information, based on NBS research and experience, covering areas of interest to the consumer. Easily understandable language and illustrations provide useful background knowledge for shopping in today's technological marketplace.

*Order above NBS publications from: Superintendent of Documents, Government Printing Office, Washington, D.C. 20402.*

*Order following NBS publications—NBSIR's and FIPS from the National Technical Information Services, Springfield, Va. 22161.*

**Federal Information Processing Standards Publications (FIPS PUB)**—Publications in this series collectively constitute the Federal Information Processing Standards Register. Register serves as the official source of information in the Federal Government regarding standards issued by NBS pursuant to the Federal Property and Administrative Services Act of 1949 as amended, Public Law 89-306 (79 Stat. 1127), and as implemented by Executive Order 11717 (38 FR 12315, dated May 11, 1973) and Part 6 of Title 15 CFR (Code of Federal Regulations).

**NBS Interagency Reports (NBSIR)**—A special series of interim or final reports on work performed by NBS for outside sponsors (both government and non-government). In general, initial distribution is handled by the sponsor; public distribution is by the National Technical Information Services (Springfield, Va. 22161) in paper copy or microfiche form.

## BIBLIOGRAPHIC SUBSCRIPTION SERVICES

The following current-awareness and literature-survey bibliographies are issued periodically by the Bureau:

**Cryogenic Data Center Current Awareness Service.** A literature survey issued biweekly. Annual subscription: Domestic, $25.00; Foreign, $30.00.

**Liquefied Natural Gas.** A literature survey issued quarterly. Annual subscription: $20.00.

**Superconducting Devices and Materials.** A literature survey issued quarterly. Annual subscription: $30.00. Send subscription orders and remittances for the preceding bibliographic services to National Bureau of Standards, Cryogenic Data Center (736.00) Boulder, Colorado 80303.

SPECIAL FOURTH-CLASS RATE
BOOK